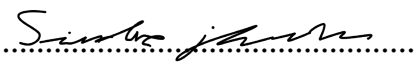




**FACULTY OF SCIENCE AND TECHNOLOGY**

## **MASTER THESIS**

Study programme / specialisation: Engineering Structures and Materials, Specialization Civil Engineering Structures	The spring semester, 2022  Open / Confidential
Author: Sindre Aleksander Mo Jakobsen	
Course coordinator: Guillermo Rojas Orts  Supervisor(s): Guillermo Rojas Orts	
Thesis title: Design and installation of a self-raising roof structure on a circular existing structure	
Credits (ECTS): 30	
Keywords: Self-raising, Pantadome System, Steel structure, Steel design, Frame structure, Truss, Roof, Post-tension, Xàtiva bullring, Alicante bullring	Pages: 90 pages  + appendix: 33 pages  Stavanger, 14.06.2022 date/year

# Abstract

This thesis looks at the self-raising roof built on a bullring in Xàtiva [1] and tries to apply the same construction method and procedure used, on a different structure, under Norwegian conditions. A new structure is designed, with some similarities to the Xàtiva roof. Multiple analyses of the new structure is done, as to assure that the design can withstand the different positions. SAP2000 is the software used to do the analyses, which encompasses examining the element forces in the truss structure and running a steel capacity check for the structure. Using these results a steel design is proposed. The method that allows the structure to self-raise is a version of the Pantadome System that applies a clever use of post-tension jacks. The forces that the jacks need to produce is found for the new structure. As the new roof is in a vulnerable position while lifting, a high safety factor is used, which the design passed. Design of details thought to be critical are suggested and drawings of the final design are presented.



# Thanks

This master thesis concludes my five years of studying structural engineering at the University of Stavanger, where I also did my bachelor's degree. The department of Mechanical and Structural Engineering and Materials Science have been excellent in providing educational and inspiring courses and assistance through these last five years. I want to especially thank Sudath C. Siriwardane for going beyond in his work for the department, and as a professor and teacher.

Then I want to thank my supervisor Guillem Rojas Orts for the thesis topic and guidance throughout the thesis. The thesis would not be at the level it is without his expertise or eye for details.

Lastly, I want to thank my fellow students for and support and encouragement through five challenging years, especially Marcus Bautz for comments and input on this thesis.

- Sindre Jakobsen, Stavanger, 14.06.2022

# Contents

<b>1</b>	<b>Introduction</b>	<b>6</b>
1.1	Research question . . . . .	6
1.2	Existing structures . . . . .	7
1.3	Existing literature . . . . .	8
<b>2</b>	<b>Method</b>	<b>10</b>
2.1	Pantadome system . . . . .	10
2.2	Choosing a geometry . . . . .	12
2.2.1	Old drawings . . . . .	12
2.2.2	Truss . . . . .	15
2.2.3	3D drawing . . . . .	16
2.2.4	The ring . . . . .	18
2.2.5	Lifting model . . . . .	19
2.3	Loads on structure . . . . .	22
2.3.1	Snow load . . . . .	22
2.3.2	Wind load . . . . .	24
2.3.3	Live load . . . . .	26
2.3.4	Dead load . . . . .	26
2.3.5	Load combinations . . . . .	27
2.4	SAP2000 . . . . .	28
2.5	Simulate lifting in SAP2000 . . . . .	31
<b>3</b>	<b>Analysis</b>	<b>33</b>
3.1	Analysis of final structure . . . . .	33
3.1.1	Element forces . . . . .	33
3.2	Structure in the final position . . . . .	36
3.2.1	Design of tension members . . . . .	37
3.2.2	Design of compression members . . . . .	38
3.2.3	Design of beam members . . . . .	40
3.2.4	Design of ring elements . . . . .	47
3.2.5	Steel design in SAP2000 . . . . .	49
3.2.6	Summary of design for final position . . . . .	52
3.3	Structure in starting position . . . . .	52
3.4	Lifting of the structure . . . . .	56

3.4.1	New members . . . . .	58
3.4.2	Temperature loading - equation to post-tension . . . . .	62
3.4.3	Jacking system . . . . .	64
3.4.4	Animation of the lifting . . . . .	66
3.4.5	Summary . . . . .	68
3.5	Design of connections . . . . .	70
3.5.1	Joint 5 . . . . .	70
3.5.2	Joint 11/12 . . . . .	76
3.5.3	Joint 7 . . . . .	79
3.5.4	Joint 1 . . . . .	83
<b>4</b>	<b>Discussion</b>	<b>85</b>
4.1	Geometry . . . . .	85
4.2	Anaysis . . . . .	85
4.3	Xàtiva roof . . . . .	86
4.4	Conclusion . . . . .	87
4.4.1	Forward research . . . . .	88
<b>A</b>	<b>Drawings</b>	<b>92</b>
<b>B</b>	<b>Design of steel members</b>	<b>108</b>
B.1	Tension members . . . . .	108
B.2	Compression members . . . . .	109
B.2.1	Class classification . . . . .	109
B.2.2	Buckling capacity . . . . .	110
B.3	Beam members . . . . .	111
B.3.1	Trial design . . . . .	111
B.3.2	Class classification . . . . .	111
B.3.3	Bending moment resistance - Yield capacity . . . . .	114
B.3.4	Bending moment resistance - Local buckling of flange . . . . .	115
B.3.5	Bending moment resistance - Lateral (flexural) torsional buckling of beam . . . . .	115
B.3.6	Reduced moment capacity due to axial load . . . . .	116
B.3.7	Members subjected to compression and bending moment . . . . .	116
B.3.8	Shear resistance - Yielding of web . . . . .	117
B.3.9	Shear resistance - Shear buckling . . . . .	117
<b>C</b>	<b>Data sheets</b>	<b>119</b>

# Chapter 1

## Introduction

This thesis will be a case study of the construction method used in the renovation of the Xàtiva[1] bullring and will attempt to replicate the roof system used. The construction method used is a self-raising method, where the structure will be constructed without the use of large cranes or temporary structures. Instead take advantage of the geometry of the structure and a method called the "Pantadome system" to move the roof into the desired position [2]. By the means of post-tension, a force is applied to the structure to make the mechanism lift.

This construction system requires a specific geometry, the circular geometry is what allows the method to work. A bullring is one of the types of structure that suits this method quite well. The geometry is crucial for this method to work.

### 1.1 Research question

The scope of the thesis will include choosing the geometry of all the parts of the new roof structure, and making the required models and drawings. Multiple structural analyses will be needed to choose an appropriate design for the steel members. The analysis will be part manual and part software assisted. While the analysis and designing are important, the scope also includes learning more about the self-raising system, as it is the key motivation behind choosing this thesis.

The topic of a structure of this nature and the self-raising/pantadome system is chosen for a couple of reasons: the challenges of not only working on a structure of this type but, also the knowledge gained on the self-raising system.

The problem to be addressed in this thesis is:

How can the Pantadome system used in Xàtiva be applied to a Norwegian location?

## 1.2 Existing structures

A new roof structure is to be designed that is similar to the roof built in Xàtiva, it is imagined that Kuppelhallen in Stavanger, Bjerghallen needs a new roof, so that will be the location for this roof structure. The roof will need to be renovated, be able to accommodate a larger seating area, be lightweight and mainly be a self-raising structure. Self-raising is important to avoid large cranes and scaffolding. Comparing different alternatives shows that the system used in Xàtiva is suitable. This system would be suitable to be used in Alicante, therefore this study will be based on the bullrings in these two cities. The analysis will be done with the Alicante bullrings dimensions as these are easily available and similar to the Xàtiva bullring. The system is equivalent and can be adjusted to the geometry of the building in Stavanger and the knowledge acquired can be applied there. Nevertheless, the existing structure is of second interest, as the roof and the self-raising system is the main focus of the thesis.

The Alicante bullring was constructed in 1847 and has a seating capacity of 15234 people [3]. The arena has a diameter of 43.4 meters and the seating area without a roof extends 13.74 meters [4], then there is some seating at the outer edge which already has a roof. It's larger than the bullring in Xàtiva and there is no need for an increase in seating or any additional lower structure, but a roof covering the seating would be important, as was done in Xàtiva. The new roof will cover the seating without a roof but will leave a hole in the middle of the ring where the seating ends. It is desired to not cover or hide any parts of the old structure as it represents historic value, so the new roof will end as the roof at the outer edge begins.



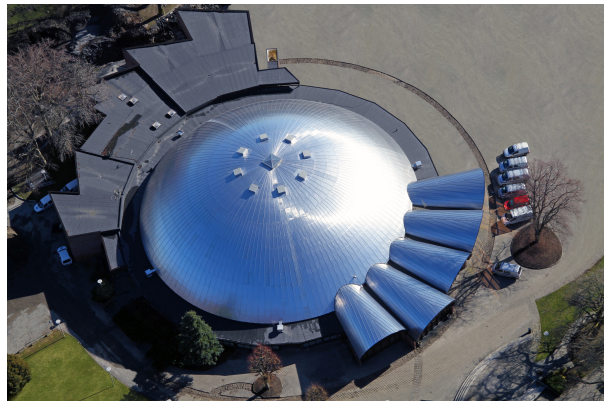
(a) Bullring in Alicante[3]



(b) Bullring in Alicante, with a theater setup [5]



(c) Bullring in Xàtiva, with the new dome roof [6]



(d) Kuppelhallen in Stavanger [7]

Figure 1.1: Existing structures

### 1.3 Existing literature

The main inspiration for this thesis is the 2015 paper: *Renovation of the bullring arena Xàtiva (Spain)*[1], with the main authors being C.Lázaro and Alberto Domingo. It's a short paper of nine pages but does highlight the decisions made when restoring the Xàtiva bullring, such as various dimensions, steel sections, and a brief description of the construction process. The most interesting element of the restoration is the design and system used to lift the roof. The construction of the roof started at the end of December 2006 and was finished February 2007, where the roof was constructed a small distance over the arena floor, then lifted by a version of the Pantadome System over a duration of under two days. The paper provided good pictures and information that guided the design of the roof in this thesis.

There is another paper about the renovation in Xàtiva: *Detailing and Construction of the Pantadome Roof Structure for a Bullring in Xàtiva(Spain)*, published in 2010 [8]. This paper explains the design, dimensions, and mechanics of the structure and the roof/lifting of the roof more thoroughly than the previous paper. It also presents

equations that relate the angle of some members to the shortening of strands, and an equation that predicts the force needed to jack the cable.

Another great paper is the 2016 paper: *Advancement on Self-Ascending Pantadome System Using Plastic Board Model with Electric Motor*, by Hiroyuki Tagawa, Yusei Tazaki, Kazuhiko Yanagisawa, Shigeyuki Okazaki, and Mamoru Kawaguchi [9]. In this smaller paper, models were made to test the pantadome system, with different methods to provide lift. The paper provides a great explanation of how the system works and also explains how the system was used in Xàtiva.

Then there is the paper by Kawaguchi, Mamoru published in 1994 titled: *Application of Pantadome system to long-span roof structures* [2], which is the original paper that presents the Pantadome system. The paper explains the struggle with the construction of long-span roofs, as it is time-intensive, requires massive temporary structures, and is laborious. The roof type discussed in the paper, domical space frame, is according to the paper especially difficult to erect. This is most likely the motivation for the author to develop the Pantadome System, as he quotes: "a more rational construction of domical space frame". The paper then explains the theory behind the lifting method, which will be discussed in chapter 2.1. Then examples of the method in action are shown, again with domical space frames.

# Chapter 2

## Method

### 2.1 Pantadome system

The key feature of this structure is the usage of the Pantadome system or a variation of the system Kawaguchi, Mamoru, described in the 1994 paper: *Application of Pantadome system to long-span roof structures* [2]. The author expresses the advantages of a spatial roof structure, stating the efficiency of the roof to cover a large area, but also the difficulties with constructing such a roof. Kawaguchi then developed this system for the construction of space frame structures, which was applied to the World Memorial Hall in Kobe in 1984.

The system works by removing members from a space frame structure in the planning phase to make a mechanic/hinge at key points. The system needs three hinges to work, often two at the edge of the structure, near the ground support. The last hinge is then somewhere in the middle of the other edge and centre. This structure with removed members can be constructed close to the ground in folded-out state, which is faster, easier, safer, and can be constructed with more accuracy.

The geometry that is left after removing members will only inhibit hinge no.1 (the hinge closes to the centre) to have a single freedom of movement, that is vertical. This point on the structure should not drift from the straight vertical path under any circumstances, and should not require any external cables or bracing to do so. To lift the entire structure in place one should simply apply a vertical force to this point with an appropriate force. The required force to lift the structure will in most cases start off higher, and then gradually reduced. As the structure is raised more of the weight is transferred to the ground and less to the force-applying device (e.i hydraulic jacks can produce a lower force).

As seen in figure 2.1a hydraulic jacks are used to lift the structure, by providing a vertical force at hinge no.1. Here the lifting can stop when the hydraulic jacks have travelled the desired distance, then the removed members can be installed, and the structure will carry itself.

This is the same system used in Xàtiva and to be used in this thesis, but the system is changed a bit. As is explained in the 2016 paper: *Advancement on Self-Ascending*



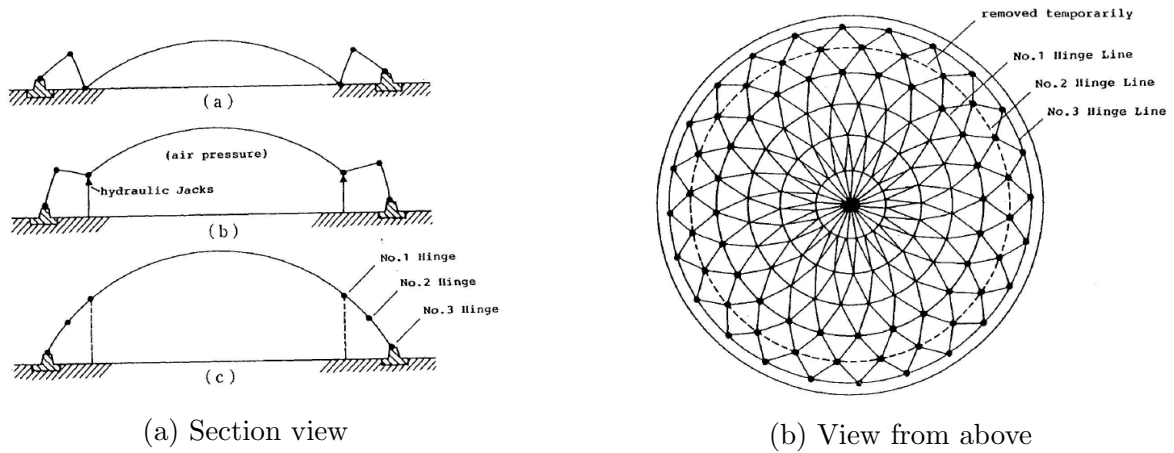


Figure 2.1: Pantadome system applied on a generic space frame structure [2]

*Pantadome System Using Plastic Board Model With Electric Motor [9],*

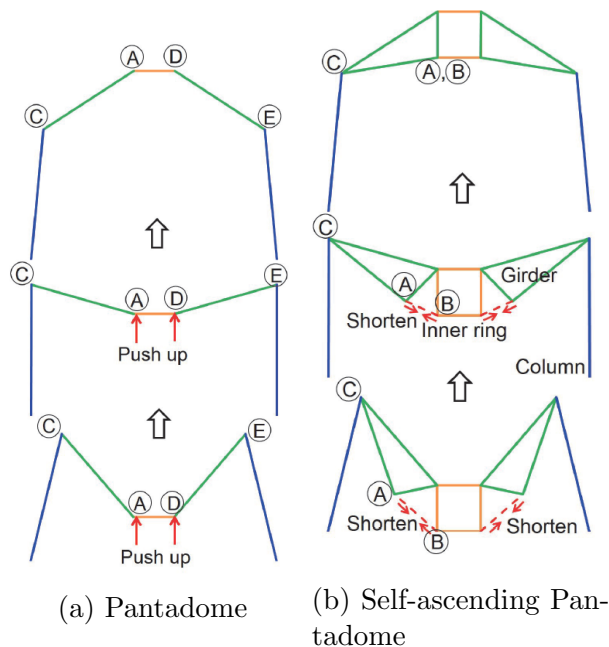


Figure 2.2: Two different Pantadome systems[9]

instead of hydraulic jacks or other external ways to directly lift the structure, the characteristics of the structure can be exploited to provide vertical movement. In Xàtiva and as figure 2.2b show, there is an inner ring and truss/girder structure instead of a space frame. When the structure is on the ground the distance between the bottom of the inner ring and the girder is further than when the structure is in the desired position. As figure 2.2 show this distance is zero at the end. This lifting mechanism in this system boils down to reducing the length of this wire. By reducing the length of

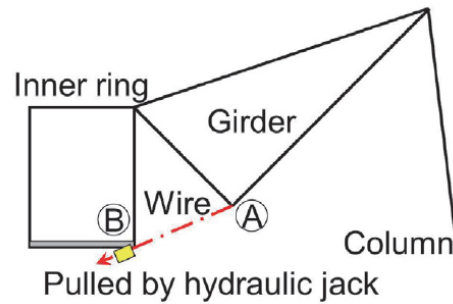


Figure 2.3: The self-ascending method used in Xàtiva [9]

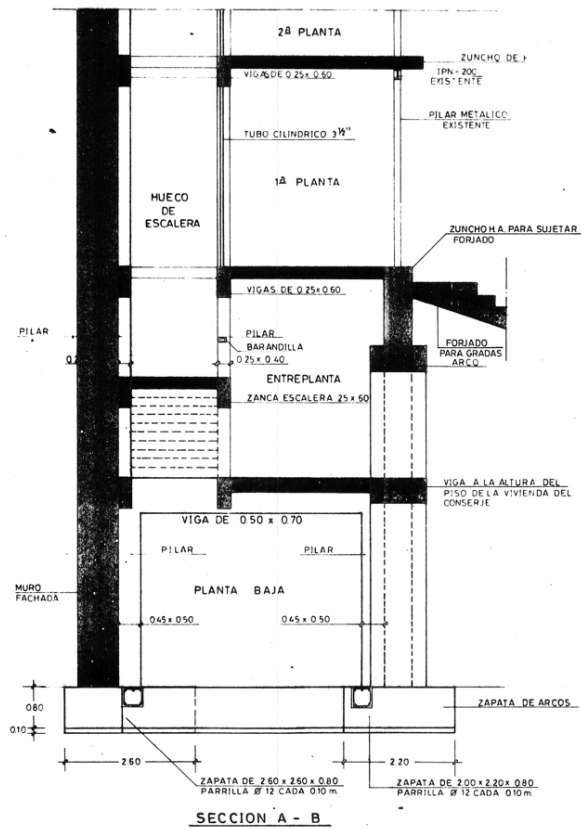
this wire the girder is rotated towards the inner ring: this change in geometry results in a higher position of the ring. The 2016 paper proposes three different ways to reduce the length of the wire: pulling by a hydraulic jack, pulling by human power, or rolling with an electric motor, with the two latter being more realistic for smaller structures. The first method mentioned, the pulling by a hydraulic jack, was the method used in Xàtiva and is the most suitable for the structure in this thesis.

The type of jacks used are jacks meant for pulling steel strands in post-tensions concrete members and the wire used can also be the same as the post-tension wires. Mounting a jack of this type to each truss is not a significant increase in dead load but can provide a high pulling force. The jacks will need to be connected together in a way that ensured that the jacks will deliver the force simultaneously.

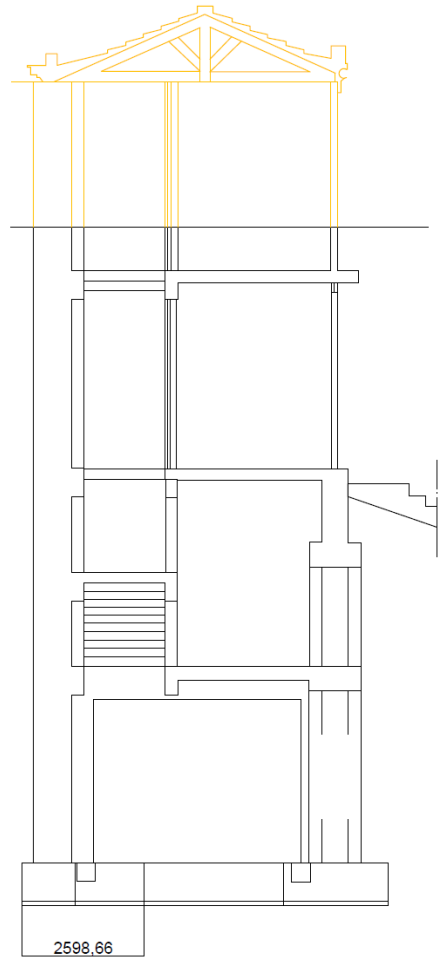
## 2.2 Choosing a geometry

### 2.2.1 Old drawings

Before a structural analysis could proceed, a geometry had to be chosen. This started by looking at drawings and pictures of the old bullring in Alicante. Drawings from 1987 with different plan views and sections were provided by the university. Then the challenge was to determine the dimensions of the structure, as only some dimensions on the drawing had been annotated. This was solved by importing the drawings of interest to Autocad, lining up one of the annotated dimensions; tracing (drawing lines) the on top of the old drawing. The old section drawings did not show the entire building, the top floor and roof were missing, as well as most of the seating area. Looking at similar bullrings a section sketch of the Alicante bullring was made (figure 2.4b). The seating was completed by the use of another drawing and combined with figure 2.4a to make a section for one side of the structure. The diameter of the seating area and the diameter of the arena was roughly measured with the measurement tool in google maps (figure 2.5). With the measured dimension of the seating area, it could then be extended to this dimension. Drawing a line with the diameter of the arena and mirroring the section makes a complete section of the old structure. The drawing, figure 2.6, can be used to measure all the dimensions needed from the old structure when designing the dome roof.

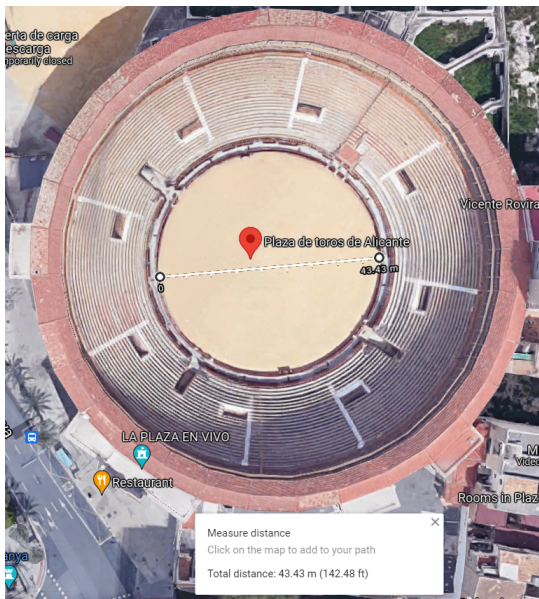


(a) Old section drawing

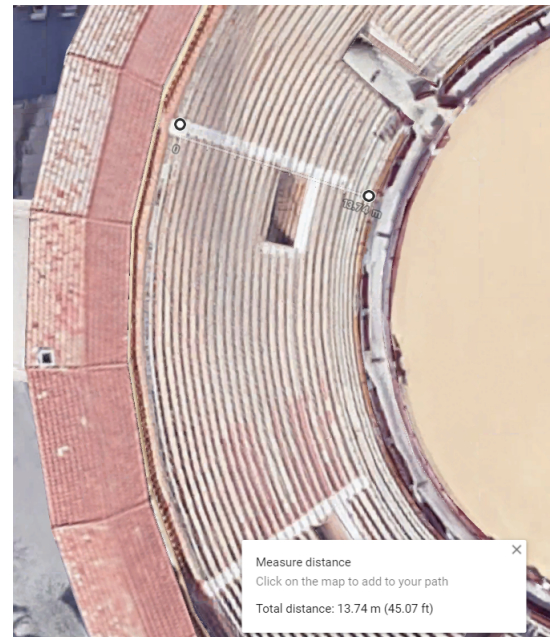


(b) Tracing of the old section drawing

Figure 2.4: Section of bullring in Alicante



(a) Measurement of arena



(b) Measurement of seating

Figure 2.5: Measurements in google maps [4]

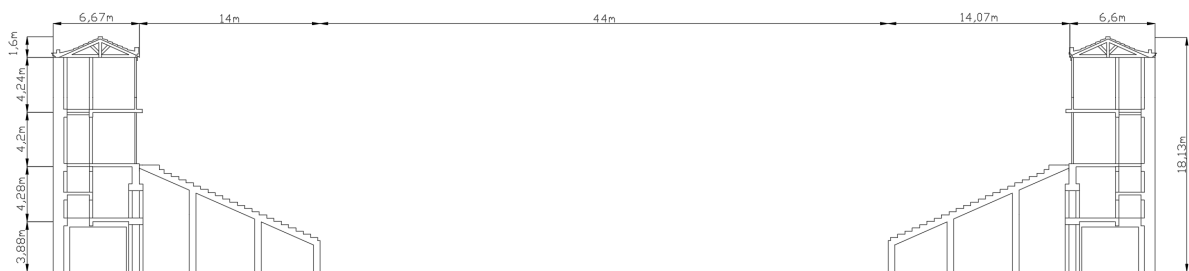


Figure 2.6: Full section drawing of old structure

### 2.2.2 Truss

The first task when choosing a geometry for the roof was to choose a shape for the truss and the accompanying beam. The roof had some criteria that would need to be met: firstly have a dome shape with an opening in the centre, secondly, start at the outer edge of the seating area/edge of the old roof. An important feature was also that the truss would need to have a member that could be replaced by a cable, which then would be used to lift the structure.

Because of the nature of the lifting system, not every truss shape can complete the lifting process, regardless of the selection of steel section and the number of supporting members. There was a possibility that a shape could be chosen that appeared suitable, but would further in the analysis reveal itself to be impossible to lift. As the self-weight is critical in a structure like this, simply increasing the dimension of a member could lead to the failure of other members, there might be members where there is no suitable cross-section.

A decision was made to use a truss shape similar to the truss in the Xàtiva paper [1]. That truss is Waddell "A" truss [10], that is turned upside down. The bottom of such a truss is usually a straight beam, in this case, that is replaced with a curved beam, that is shaped to the desired shape of the dome.

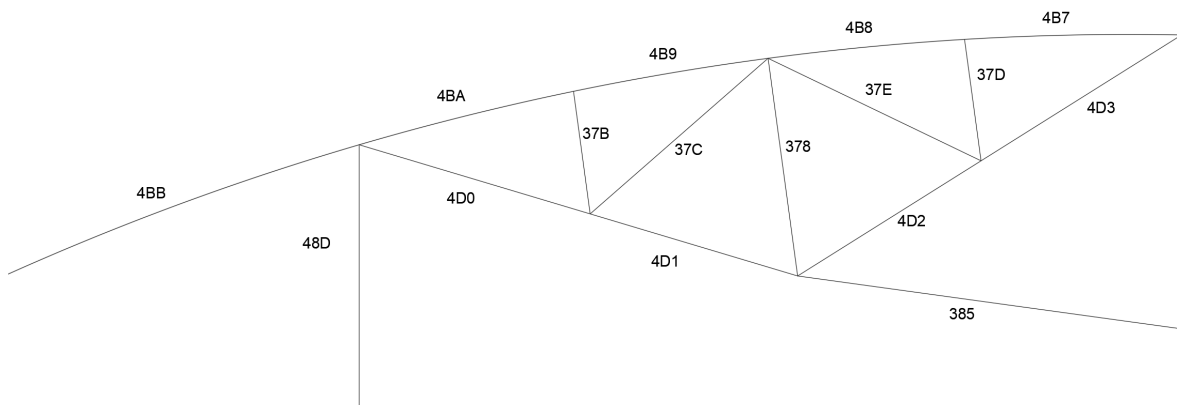


Figure 2.7: Shape of truss, with element names

Figure 2.18 is a proposed shape of the truss (the names of the members were assigned when the first analysis was run, it is recommended to have this figure nearby when reading the thesis). The members 4BB, 4BA, 4B9, 4B8 and 4B7 are depicted as a curved beam here but might be separate straight members in some drawings/models, for simplicity. Member 4BB ends at the edge of the old roof and member 4B7 ends at the edge of the seating area. Member 48D is a column that extends to a concrete support.

There were boundary conditions that the truss shape had to conform to, when choosing the shape, there were in reality only a few dimensions to decide upon: where on the curved beam member 48D connects, the length of member 378 and the height of the vertical member to the right of member 385 (this member is what will be the column in

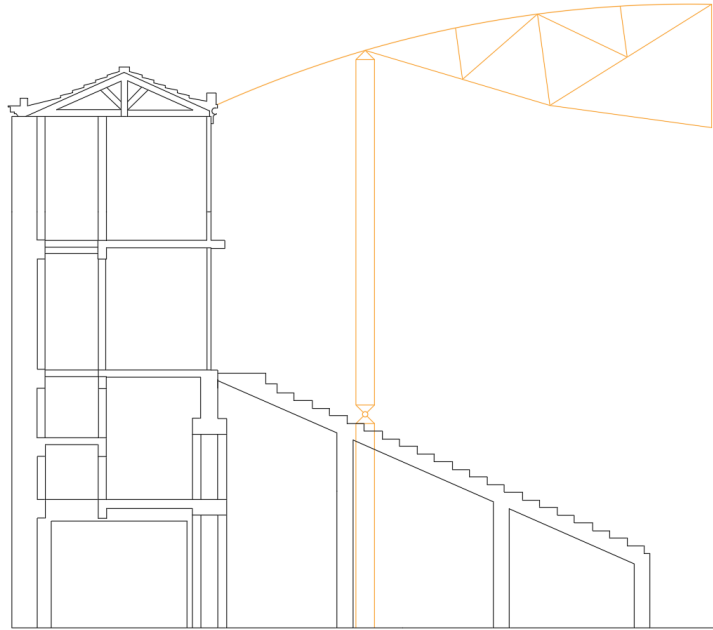


Figure 2.8: New structure and old structure

the ring later). The rest of the dimensions depend on the dimension of these members, 37B, 378 and 37D are perpendicular to the beam. 4D0 and 4D1 are two members that form a straight line between 48D and 378, likewise with members 4D2 and 4D3 except from 378 to 4B7. Members 37B and 37C have to connect at the joint between 4D0 and 4D1, same with 37E and 37D which connects between 4D2 and 4D3.

The process to obtain this design involved drawing member 378 with different lengths. This member has a length of  $3m$  in the proposed design, the drawings where this member was  $2m$  and  $5m$  both looked strange and unrealistic, although any length somewhere between  $3m$  and  $4m$  would have been equally visually passing, and might be more suitable. The mentioned member to the right of 385 is the ring column and here a height of  $4m$  was chosen.

### 2.2.3 3D drawing

A brilliant characteristic of a circular shape is that the same truss will repeat itself in intervals around the centre of the arena. Next was to decide how many of these trusses were needed around the circle, the number would have to be an even number as the trusses would be split into pairs later. A number of 40 trusses was decided upon, which did prove itself to be a quite good choice, as the distance between each truss was exactly  $9^\circ$  ( $40 \cdot 9^\circ = 360^\circ$ ). Having a simple number for the degrees between the trusses made drawing and modelling much swifter as many elements would need to be rotated this amount.

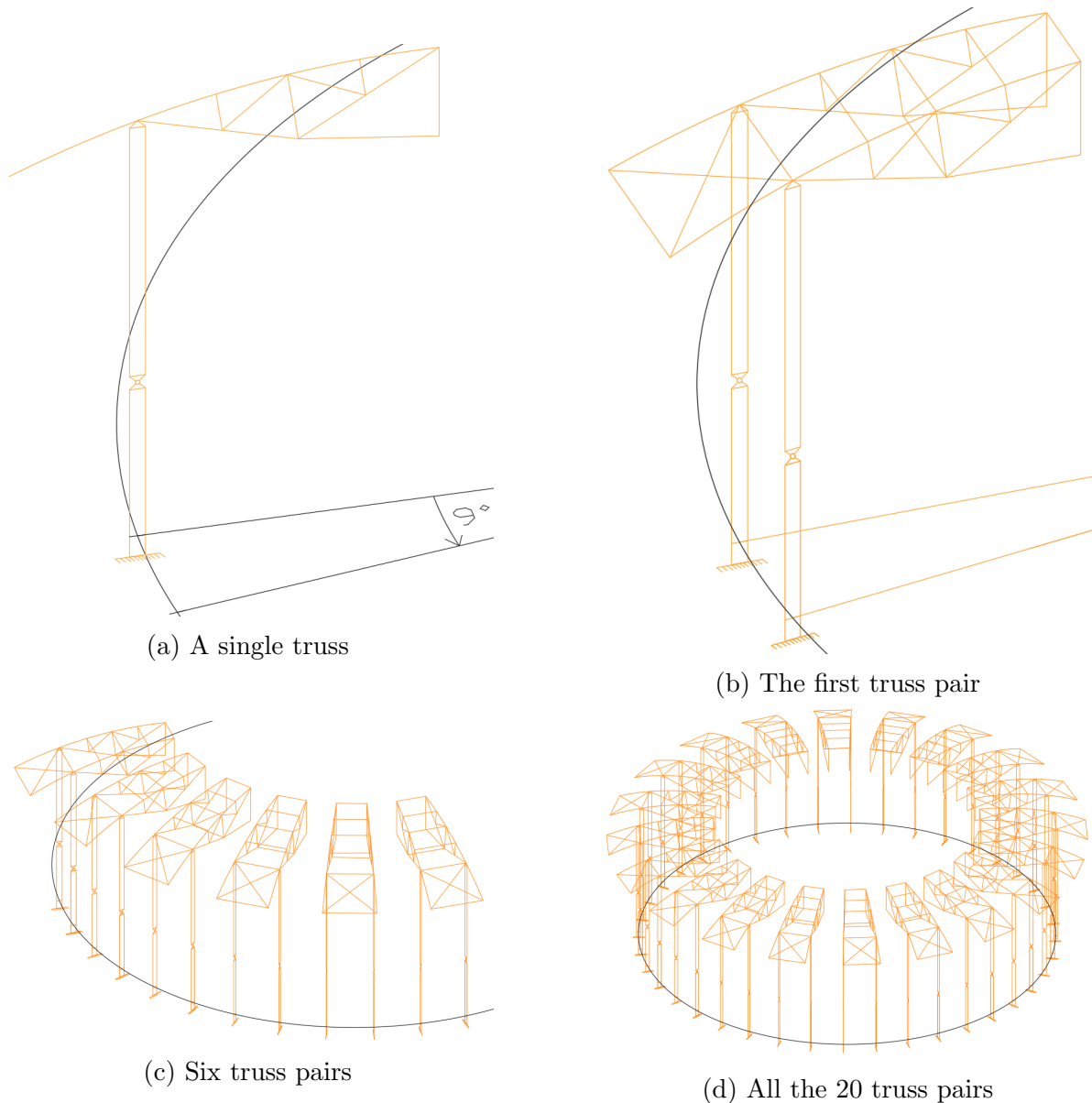


Figure 2.9: Process of making the first 3D model

The First step in the making of the 3D model in Autocad was to rotate the truss around the x-axis 90 degrees so it was standing upright. Then a circle was made with a diameter of 44 m going through element 48D (figure 2.9a), the truss could then be rotated around the centre of this circle. Using the rotate-copy function a copy of the truss could be made and rotated. Figure 2.9b shows the first truss pair with bracing and stiffeners between the two trusses, the trusses are paired like this to accommodate the lifting process. Rotating and copying the truss pair produces the models in figure 2.9c and 2.9d.



### 2.2.4 The ring

The ring is a key component of this structure, it acts as a second 'support' to the trusses. All the trusses are leaning on the truss on the opposite side, with the ring acting as an intermediate. The ring is made of two beams curved in a circle, one upper beam and a bottom beam. Where the ring connects to a truss there is a vertical member between the upper ring and lower ring, called the ring column. Between these columns are stiffeners which join the upper beam and bottom beam, forming an 'x'.

All the dimensions for the ring have already been defined by the truss, the height of the ring is  $4\text{ m}$ , and since the ring has to be connected to the end of each truss. The distance between two trusses on opposite sides is  $40\text{ m}$ , which will be the diameter of the ring.

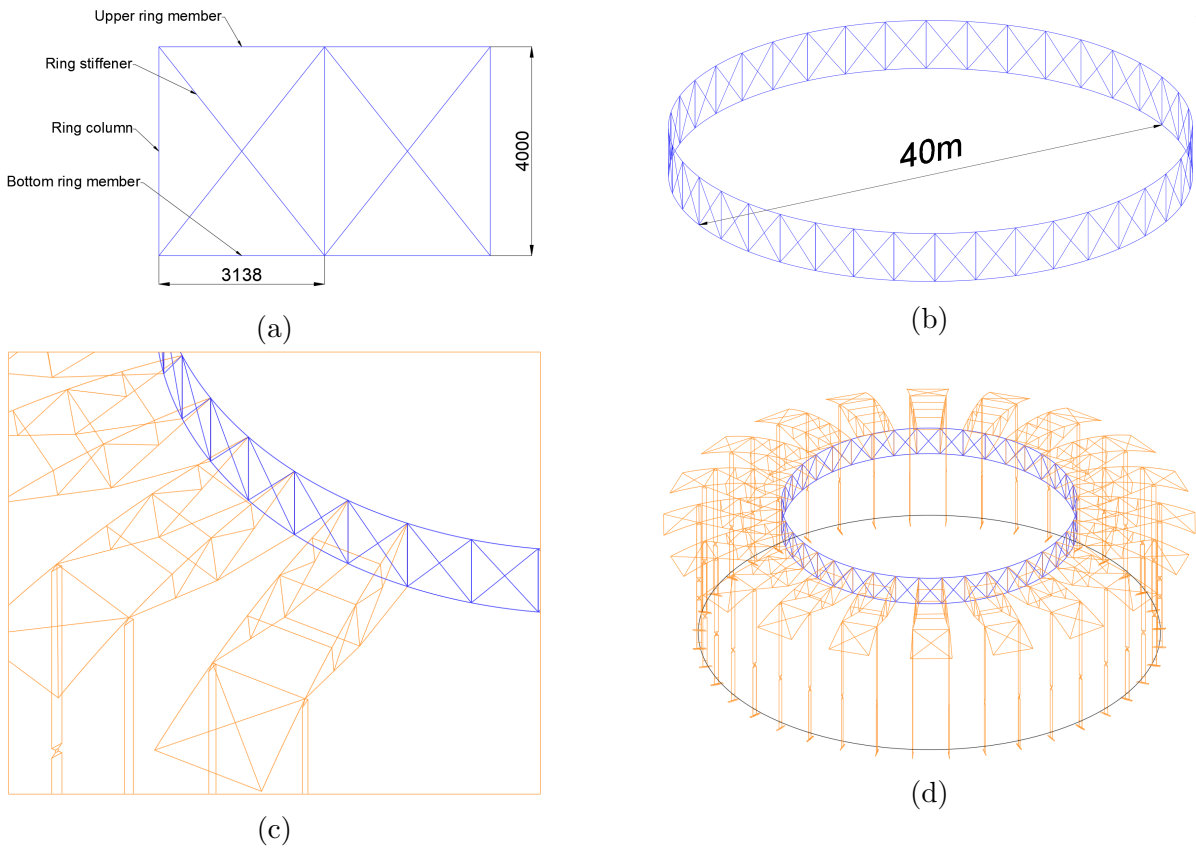


Figure 2.10: Models of the ring

The ring was drawn by making drawing a circle with  $40\text{ m}$  diameter, then copying and pasting the circle 4 meters up in the  $z$ -direction. Then the two circles were moved so that they aligned with the ring of trusses. The ring columns were already drawn on the truss, so the only part left was to draw the stiffeners between the ring columns once and rotate-copy them around the structure.



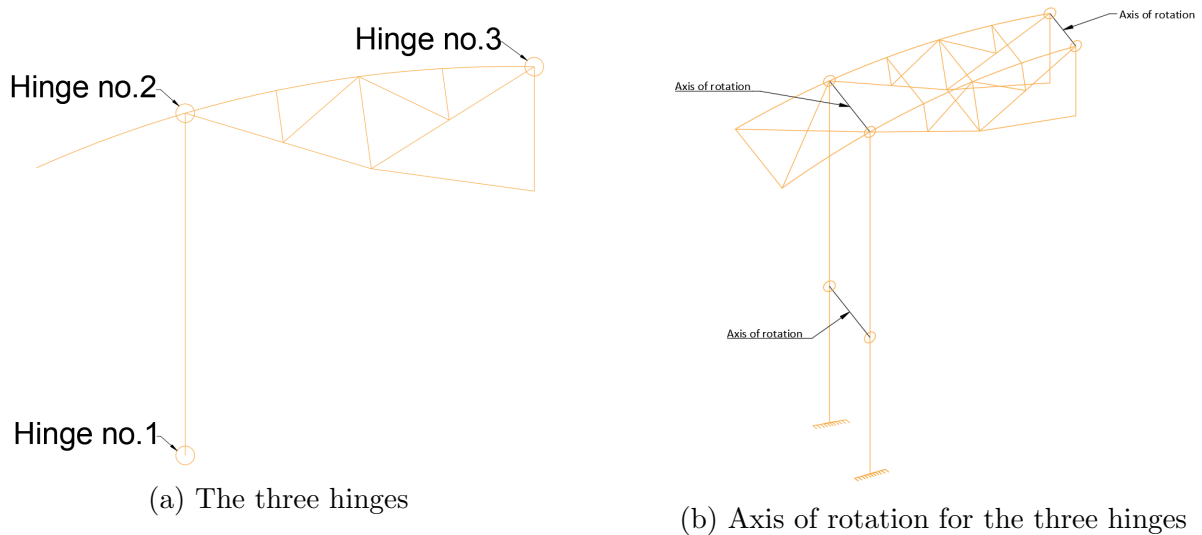


Figure 2.11: Hinges for rotation the truss

### 2.2.5 Lifting model

As the Pantadome system was to be used on this structure and not constructed in the position shown in 2.9d, another model was required: the model at the start of the lifting phase.

Some parameters were required before such a model could be made, mainly the distance from the ground up to the ring, as the ring is to be constructed closer to the ground and lifted up. In the starting position model, this distance is  $1.5\text{ m}$  and in the final position, this distance is  $16.2\text{ m}$ , with a distance of  $9.5\text{ m}$  between the two positions. Before a 3D model or 2D model could be made the geometry had to be figured out. For the system to work three hinges on each truss are needed, the first hinge is at the bottom of member 48D, the second hinge is at the top of member 48D where the member meets the curved beam, and the third hinge is at the end of the curved beam (member 4B7) where the beam meets the ring, see figure 2.11a. To make a 2D model of the truss in different lifting positions requires no calculation of angles. First, the truss without member 48D is moved down to the desired height. Then two circles are needed, one with a centre at hinge no.1 with a radius of the distance between hinge no.1 and hinge no.2. The second circle has a centre at hinge no.3 and a radius of the distance between hinge no.3 and hinge no.2. The two circles will intersect at two points, one of these points will have to be the point where the truss and member 48D connects (hinge no.2).

Figure 2.12 shows the truss in two different positions. There are two important details to notice: the different length of member 385 between the two figures and that hinge no.1 and the ring column underneath move straight up in a vertical line. The horizontal position of hinge no.1 is a boundary condition that the structure has to adhere to, and as long as the length of member 385 is as expected it always will.

Making the 3D model for the structure in different lifting positions was not as simple as rotating the lowered 2D truss around in a circle. It was discovered that the distances

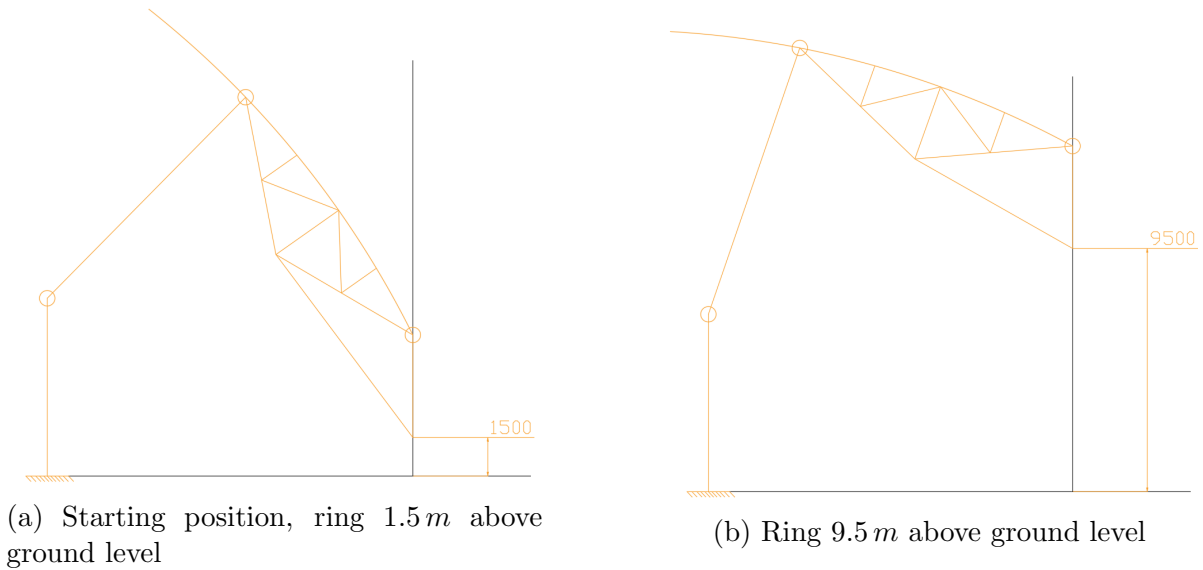


Figure 2.12: Truss in different positions

between the trusses changes in the different positions when just rotating and copying. So, stiffeners that would fit in the finished position would not fit in a lower position. Here a crucial detail was discovered: **all the three hinges in a truss pair would need to be parallel with each other, otherwise the lifting would not be possible.** If the structure was constructed on the ground with all the hinges perpendicular to the ring, it would not be possible to lift the structure as the distance between the trusses would be reduced significantly, as it travelled upwards, and compressed the stiffeners.

The solution was to not use the 2D truss in the lower position and rotate-copy it but to use one of the 3D truss pairs, and rotate the two trusses into the bottom position simultaneous around a shared axis, and not the axis perpendicular to a single truss (as there is a  $9^\circ$  difference). This shared axis would not be perpendicular to either trusses, it would be the axis one got if a straight line was drawn between to two of the same hinge, as seen in figure 2.11. Rotating the truss pairs results in the two models shown in figure 2.13 and figure 2.14.

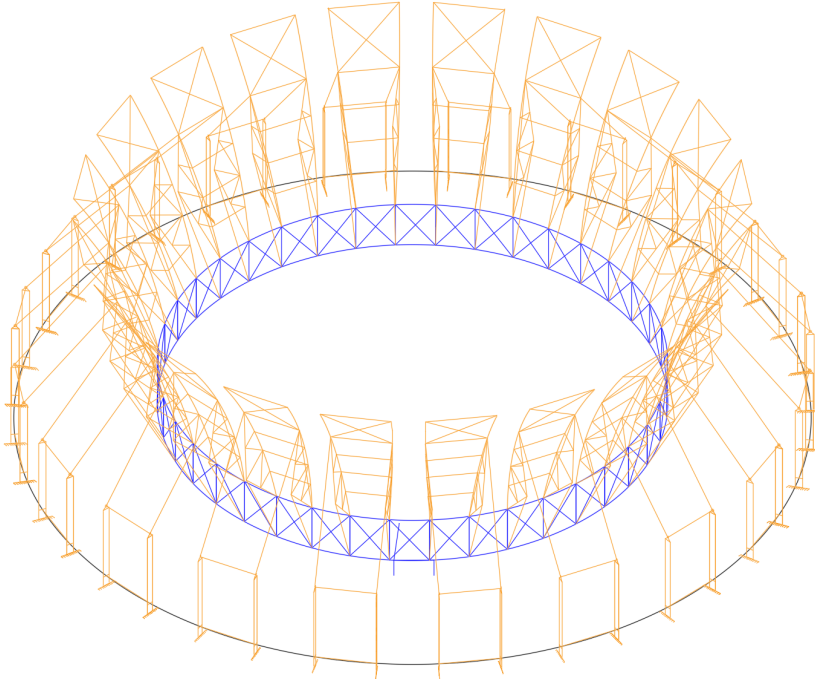


Figure 2.13: 3D model of structure in starting position

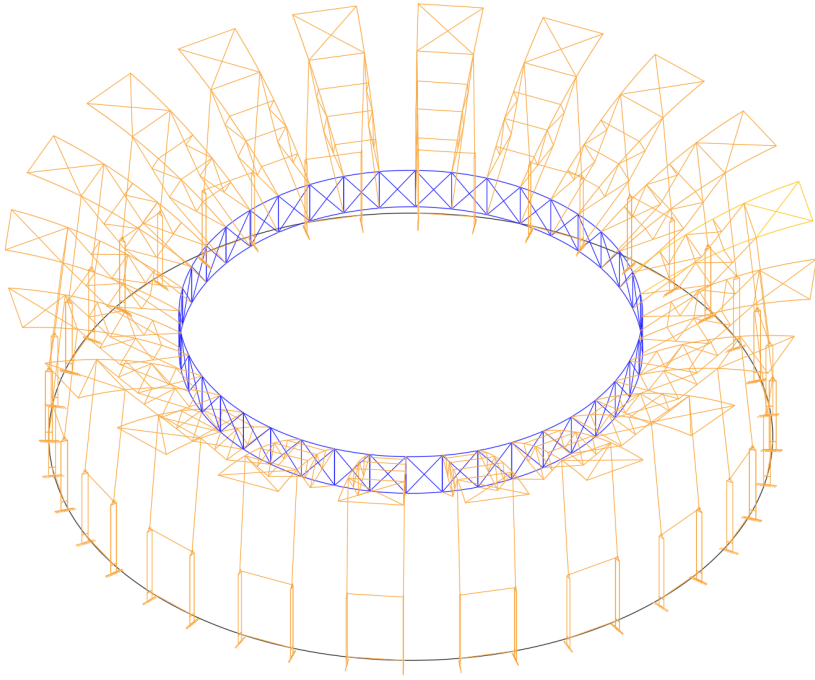


Figure 2.14: 3D model of structure in middle position

## 2.3 Loads on structure

The structure is subjected to different types of loads: dead, live, snow and wind. The dead load consists of the weight of the truss members, which is critical in the lifting phase, but also the weight of the roofing sheets. Since the roof is only accessible for maintenance and repairs there is not a usual live load, but a smaller live load to accommodate maintenance work. The area of the roof is quite large so the roof may be experiencing a large snow load, especially on the outer edge where snow may accumulate. Calculating the different loads will be done in accordance with the respective Eurocode.

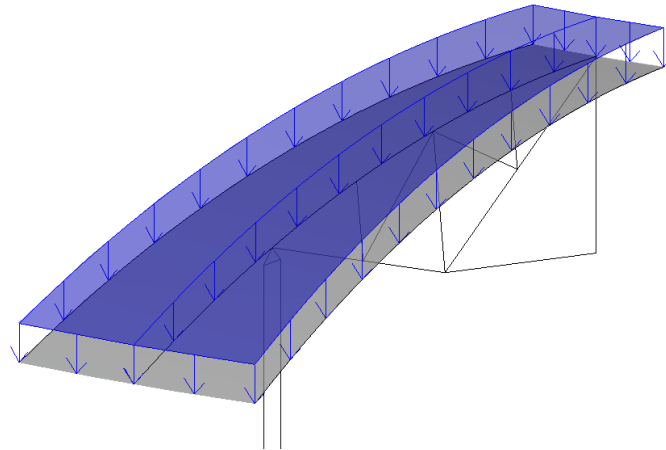


Figure 2.15: Influence area of all imposed load on a truss

The load on the roof will be carried by the trusses, who splits the loading between them. Figure 2.15 is a visualization of the influence area on a single truss.

### 2.3.1 Snow load

To calculate the required snow load, NS-EN 1991-1-3 (2003) (English): Eurocode 1: Actions on structures - Part 1-3: General actions - Snow loads [11], was used:

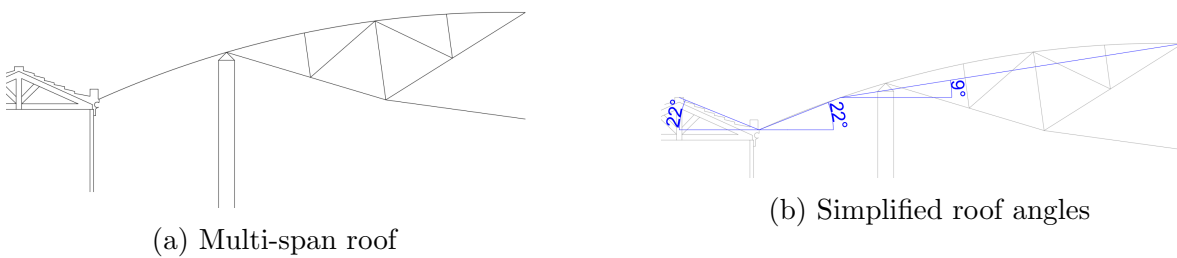


Figure 2.16: Roof illustration for snow load

$$S = \mu_i \cdot C_e \cdot C_t \cdot S_k + M_{Ed}^2 \quad (\text{EN 1991-1-3: eq: 5.1})$$

where the characteristic snow load,  $S_k$ , is given by the national annex: NA.4.1 in EN 1991-1-3 [11]:

$$S_k = S_{k,0} + n\Delta S_k$$

$$n = \frac{(H - H_g)}{100}$$

where:

- $C_e$  = Exposure coefficient
- $C_t$  = Thermal coefficient
- $H$  = Heigh of area over sea level
- $H_g$  = Critical height limit
- $\mu_i$  = snow load shape coefficient

Values for a building in Stavanger, Rogaland:

- $S_{k,0} = 1.5 \text{ kN/m}^2$
- $C_e = 1$
- $C_t = 1$

Since  $H < H_g$ :

$$S_k = S_{k,0} + n\Delta S_k = S_{k,0} = 1.5 \text{ kN/m}^2$$

### Loading on element 4BB

The snow load on this part of the roof will be higher because of the accumulation of snow in between the new and old roof. The two roof angles will be the same:

- $\alpha_1 = 22^\circ$
- $\alpha_2 = 22^\circ$

From table 5.2 in NS-EN 1991-1-3:

$$\mu_1 = \mu_1(\alpha_1) = \mu_1(22^\circ) = 0.8$$

$$\alpha = \frac{\alpha_1 + \alpha_2}{2} = \frac{22^\circ + 22^\circ}{2} = 22^\circ$$

$$\mu_2 = 0.8 + 0.8 \cdot \frac{\alpha}{30} = 0.8 + 0.8 \cdot \frac{22^\circ}{30} = 1.38$$

Further we get:

$$S_1 = \mu_2 \cdot C_e \cdot C_t \cdot S_k = 1.38 \cdot 1 \cdot 1 \cdot 1.5 \text{ kN/m}^2 = \underline{\underline{2.07 \text{ kN/m}^2}}$$

### Loading on element 4BA, 4B9, 4B8 and 4B7

The rest of the roof is not subjected to the same snow accumulation, the angle of the roof is also lower:

- $\alpha_2 = 9^\circ$
- Table 5.2:  $\mu_1 = 0.8$

$$S_2 = \mu_2 \cdot C_e \cdot C_t \cdot S_k = 0.8 \cdot 1 \cdot 1 \cdot 1.5 \text{ kN/m}^2 = \underline{1.2 \text{ kN/m}^2}$$

### 2.3.2 Wind load

NS-EN 1991-1-4:2005+NA:2009 [12] is the standard used to calculate wind loading. The following parameters depend on the position of the structure:

- Reference height:  $Z_e = 20.27 \text{ m}$  (highest height of the roof structure)
- Basic wind velocity:  $V_b = 26 \text{ m/s}$  (For the Stavanger area)
- Roughness length:  $Z_0 = 0.3 \text{ m}$
- Minimum height:  $Z_{min} = 5 \text{ m}$
- Orography factor:  $C_o(Z_e) = 1.0$

The terrain category is III, terrain roughness is given by ( $Z_{0,||}$  is  $0.5 \text{ m}$ ):

$$k_r = 0.19 \cdot \left( \frac{Z_0}{Z_{0,||}} \right)^{0.07} = \underline{0.215} \quad (\text{EN 1991-1-4: eq: 4.5})$$

The roughness factor  $C_r(Z_e)$ , for  $Z_e \geq Z_{min}$ , is given by:

$$C_r(Z_e) = k_r \cdot \ln \left( \frac{Z_e}{Z_0} \right) = \underline{0.9075} \quad (\text{EN 1991-1-4: eq: 4.4})$$

The mean wind velocity can then be calculated:

$$V_m(Z_e) = C_r(Z_e) \cdot C_o(Z_e) \cdot V_b = 23.59 \text{ m/s} \quad (\text{EN 1991-1-4: eq: 4.3})$$

Peak velocity is then given by:

$$q_p(Z) = [1 + 7 \cdot I_v(Z)] \cdot \frac{1}{2} \cdot \rho \cdot V_m^2(Z) = 0.926 \text{ kN/m}^2 \quad (2.1)$$

Where  $\rho$  is the air density, which is  $\rho = 1.25 \text{ kg/m}^3$ .

In some areas of the roof, the wind will cause a down-force, but on most of the roof, the wind will cause an uplifting effect. The clause in the Eurocode which closets resemble the building in this thesis is the clause 7.2.8. Here figure 7.12 can be used to

read the form factor,  $C_{pe,10}$  for the three zones on the roof: A, B and C. Zone A is the place on the structure where the wind first meets the structure, zone C is the opposite side of A, and zone B is the zone between A and C.

To read the graph two ratios are required: the ratio  $h/d$  and the ratio  $f/d$ . For the structure the dimensions are:

- $h = 16.9\text{ m}$
- $f = 3.25\text{ m}$
- $d = 6.2\text{ m}$

The ratios will then be:

- $h/d = 2.72$
- $f/d = 0.52$

Looking at figure 7.12 shows that for a  $f/d$  ratio higher than 0.5 gives constant values of A, B and C. The form factor are:

- A:  $C_{pe,10} = +0.8$
- B:  $C_{pe,10} = -1.2$
- A:  $C_{pe,10} = -0.5$

The sign on the form factor indicates if that area experiences a wind-load that pushed down or a wind load that lifts up. Using these form factors (A,B and C) the wind load of the different zones can be calculated. Since the roof is larger than  $10\text{ m}^2$ ,  $C_{pe,10} = C_{pe}$ . The wind pressure on the three zones are given by the equation:

$$W_e = q_p(b) \cdot C_{pe} \quad (2.2)$$

For the different zones this is:

- $W_{e,A} = 0.8 \cdot 0.926 = 0.74\text{ kN/m}^2$
- $W_{e,B} = -1.2 \cdot 0.926 = -1.11\text{ kN/m}^2$
- $W_{e,C} = -0.5 \cdot 0.926 = -0.46\text{ kN/m}^2$

The negative pressure will try to lift the top of the structure and the positive will press down on the structure. The pressure with the highest magnitude is a negative pressure, adding this to a load combination would only result in a lower load, and less critical. The wind load is therefore not added in the load combination here but is added in the software and taken into account in the software's capacity check. The wind load on different members is:

Table 2.1: Distributed wind-load along the beam members

Element Name	Width of influence area	A	B	C
4BB	5.2 m	3.84 kN/m	-5.77 kN/m	-2.39 kN/m
4BA	4.7 m	3.47 kN/m	-5.21 kN/m	-2.16 kN/m
4B9	4.2 m	3.10 kN/m	-4.66 kN/m	-1.93 kN/m
4B8	3.8 m	2.81 kN/m	-4.21 kN/m	-1.74 kN/m
4B7	3.8 m	2.81 kN/m	-4.21 kN/m	-1.74 kN/m

### 2.3.3 Live load

The recommended live load is given by the standard NS-EN 1991-1:2002 [13]. The roof is a category H - roof that is not accessible except for maintenance and repairs. Table NA.6.10 in the national annex recommends  $0.75 \text{ kN/m}^2$  for roofs with a pitch less than  $20^\circ$  angle and  $0 \text{ kN/m}^2$  for roofs with a pitch greater than  $40^\circ$  angle, interpolation the load for roofs between  $20^\circ$  and  $40^\circ$  pitch. The roof has a max pitch of  $22^\circ$  at the outer edge and flattens out to approximately  $0^\circ$  at the inner edge. The max live load was therefore used for the entire roof:

$$q_k = \underline{0.75 \text{ kN/m}^2} \quad (2.3)$$

### 2.3.4 Dead load

The dead load consists of two components: the weight of the roofing sheets and the weight of the structural components: the truss and the ring. The weight of the structural components is automatically accounted for by the analysis software, as sections are defined with weight/m.

#### Roof sheets

The roofing sheet are not modelled in SAP2000 but added as a load on the beam members (Element 4BB, 4BA, 4B9, 4B8 and 4B7). The roof sheets chosen are the *Plannja 70* [14], see appendix C for the data sheet for the roof sheets.

**Element 4BB** The longest span is at the outer edge of the ring, between the 4BB beams, with a span of  $5100 \text{ mm}$ . This area of the roof has the highest snow load from  $2.07 \text{ kN/m}^2$  decreasing to  $1.2 \text{ kN/m}^2$ , and a live load of  $0.75 \text{ kN/m}^2$ . As both maintenance and maximum snow load won't be possible simultaneously, only the snow load will be accounted for when choosing the roofing sheet. A thickness of  $0.85 \text{ mm}$  will provide a dimensioning load-bearing capacity of  $2.67 \text{ kN/m}^2$ , which is not enough if a safety factor of 1.5 is used on the maximum snow-load, but the snow-load is not uniform. This



capacity should suffice:

$$\frac{2.07 \text{ kN/m}^2 + 1.2 \text{ kN/m}^2}{2} = 1.635 \text{ kN/m}^2$$

$$1.635 \text{ kN/m}^2 \cdot 1.5 = 2.45 \text{ kN/m}^2 < 2.67 \text{ kN/m}^2$$

**Element 4BA, 4B9, 4B8 and 4B7** The rest of the beams have a span decreasing from 4.9 m to 3.1 m, and a lower snow-load of 1.2 kN/m<sup>2</sup>. The *Plannja 70* with a thickness of 0.85 mm has a capacity of 2.67 kN/m<sup>2</sup> at span length 5.1 m, and 6.37 kN/m<sup>2</sup> at span length 3.3 m, which is more than enough. A different - and/or lighter - sheet section could arguably be chosen for these spans, but for simplicity when calculating and constructing the same sheets are used.

This sheet has a self-weight of:

$$g_k = \underline{0.109 \text{ kN/m}^2} \quad (2.4)$$

### 2.3.5 Load combinations

To obtain the ULS design load the NS-EN 1990:2002+A1:2005+NA:2016 [15] was used. According to the code, the least favourable of equation 6.10a and 6.10b should be used to calculate the load combination. The equations are written as such:

$$\sum_{j \geq 1} \gamma_{G,j} G_{k,j} + \gamma_p P + \gamma_{Q,1} \psi_{0,1} Q_{k,1} + \sum_{i > 1} \gamma_{Q,1} \psi_{0,i} Q_{k,i} \quad (6.10a)$$

$$\sum_{j \geq 1} \zeta_j \gamma_{G,j} G_{k,j} + \gamma_p P + \gamma_{Q,1} Q_{k,1} + \sum_{i > 1} \gamma_{Q,1} \psi_{0,i} Q_{k,i} \quad (6.10b)$$

The two equations can be simplified:

$$1.35 G_k + 1.5 \psi_0 S_k + 1.5 \psi_0 Q_k \quad (6.10a)$$

$$1.2 G_k + 1.5 S_k + 1.5 \psi_0 Q_k \quad (6.10b)$$

where  $\psi_0 = 0.7$  for this structure.

Table 2.2: Loads, in kN/m<sup>2</sup>

Element name	Snow-load	Live-load	Dead-load	6.10a	6.10b
4BB	2.07	0.75	0.109	3.44	4.36
4BA	1.2	0.75	0.109	2.53	3.05
4B9	1.2	0.75	0.109	2.53	3.05
4B8	1.2	0.75	0.109	2.53	3.05
4B7	1.2	0.75	0.109	2.53	3.05

Choosing the highest value of 6.10a and 6.10b or as it is written in the Eurocode "least favourable" value, and multiplying that value with the width of the influence area (to go from  $kN/m^2$  to  $kN/m$ ) to get the distributed load:

Table 2.3: Distributed load along the beam members

Element name	Width of influence area	Distributed-load
4BB	5.2 m	22.67 kN/m
4BA	4.7 m	14.33 kN/m
4B9	4.2 m	12.81 kN/m
4B8	3.8 m	11.59 kN/m
4B7	3.8 m	11.59 kN/m

## 2.4 SAP2000

For the structural analysis, the software used was SAP2000, made by *Computers and Structures, Inc.* The software can provide all the tools needed for this analysis, most importantly calculating element forces, and assigning accurate loads and steel sections to members. A feature that also proved itself useful was the steel check tool. The software has some quality of life functions and is overall easy to use. SAP2000 is a software the University of Stavanger had access to and is familiar to the author.

Now three 3D models were made in Autocad: structure in final position, bottom position and middle position. Drawing these models again in SAP2000 or any analysis tool would have taken quite some time (the drawing tools in most analysis software are not as polished as in Autocad), so exporting the models from Autocad to SAP2000 was preferred.

It was first tried to import smaller parts of the structure. This was done with import the Autocad file (DWG format) directly into SAP2000, which was not always optimal, as the SAP2000 often crashed, and the imported structure was sometimes missing elements. Importing the 3D model of the entire structure would almost always crash the software. Another method was tried: saving the Autocad file in the IGES (Initial Graphics Exchange Specification) format and importing that format, this worked surprisingly well except that the software would not connect members to the curved members: the ring and the curved beam at the top of the truss. So the ring and the curved beam were replaced by straight members between connecting members, which provides a similar geometry (at a distance they still looked curved, only at closer inspection can one see that they are not).

The most important models were the model for the structure in the final position and the structure in the bottom positions, so the preparation of these models was made first. The model of the structure in the middle position was left to be used only if time permitted it.

In SAP2000 two models were made from the import of the structure in the bottom

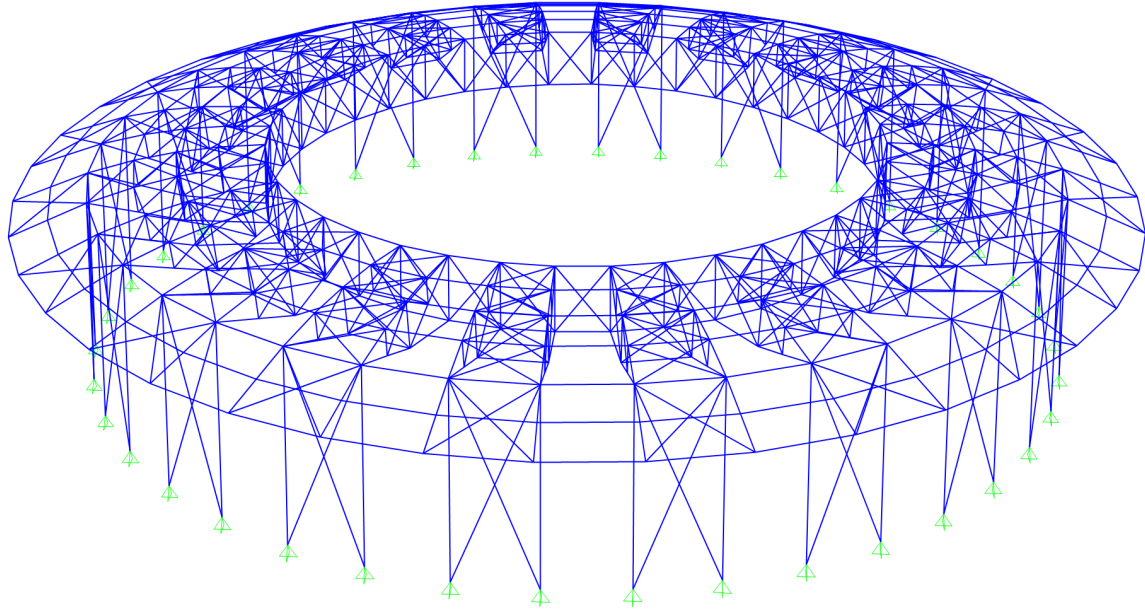


Figure 2.17: Sap2000 model of the structure in the finished position

positions: One before the lifting started and one after. The difference here is that the ring is resting on supports before the lifting, and after lifting the reaction from the supports is replaced by the jacking force from the jacks.

The first iteration of the SAP2000 model was in the finished position without any bracing or stiffeners, but this model was not stable when running an analysis. When looking at the deformation of the structure, without any significant loading, the ring would begin to rotate clockwise. To stop this rotation the stiffeners between the 48D members were added, which stopped the rotation. Another problem was that on some trusses the lower part of the truss (member 4D1/385) would displace out of the plane of the truss, to stop this a bracing at the joint where 4D1 and 385 meet was added between the trusses in the truss pair. Additional bracing was added at the beam connections between the trusses in a pair, and stiffeners was added on as a cross between the beams. The model now acted more predictable. Adding these was done in SAP2000 but could have been done faster in Autocad.

Throughout the analysis, there was a lot of trial and error, and different aspects of the analysis model would be changed constantly. Not all the shortcomings of the analysis model were discovered early in the analysis process. The analysis was done several times before the model produced a satisfying result. To smooth this process groups were made for all the identical members. Groups make it possible to quickly select every element that is a member of the respective group and making changes to the elements of the selected group. This initially was a tedious process but saved a great amount of time in the long run. Selecting every instance of the member 4B7 to assign a steel section or a load would have consumed so much time that the analysis would not be feasible in the given time frame. Other groups were also made: a group for selecting a single truss, a

group for selecting the ring and also different parts of the ring, and a group for selecting all the stiffeners and bracing for the purpose of hiding them (these often just cluttered the model).

To assign the loading on the structure, first, a load pattern for each type of load was needed to be defined: Dead, snow, live and wind load. A type can be assigned to the load that matches the nature of the load. Choosing some types opens up additional options relevant to that load type. When the load patterns have been defined the next step was to define the load cases. When the load pattern was defined an association load case is automatically defined with the same name and with a standard set of options, which is fine for this analysis. Each load case is defined with a scale factor of 1 and the type is linear static. Lastly, a load combination can be defined, with the safety factor from the Eurocode. The critical load combination was 6.10b, which was defined. This is the combination that will be used to design the members of the structure, but the steel check takes every combination into account. Once the load combination has been defined, a frame load could be assigned. All the instances of a member are selected, and then a distributed load is assigned to the member with one of the load patterns selected with the accompanying magnitude. This was repeated for all the beam members, as these are the only members subjected to external loading.

Next restraints (supports) were assigned. These are pin support at the end of the 4D8 members which restrain the translation in all the three directions but do not restrain any rotation.

When importing the model into SAP2000 the software assumes that every member is a frame element with rigid connections between the members, as this is a bar truss this is not the case. All the truss members would need to be released to allow for rotation. This is done by assigning a frame release at the ends of the members which should allow for rotation, where Moment 33 (major) is released.

Another release needed but was not immediately clear, was the release of the axial load on some members. The design is made so that the ring in the middle stops the trusses from falling inwards, so the ring is absorbing a high axial load this way. What happened was that some of the bracing begin absorbing axial load away from the ring, which was not the purpose of the bracing. Releasing axial load on one end of the members fixed this issue (SAP2000 did not allow to release of the axial on both ends).

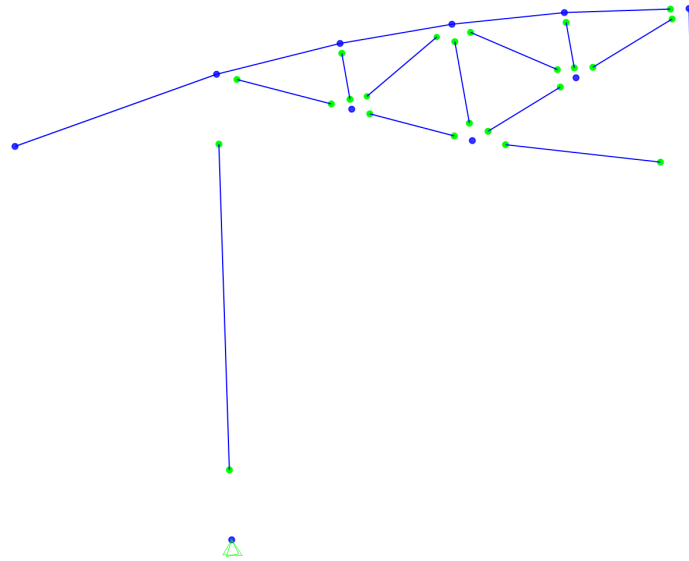


Figure 2.18: Moment 33 releases in green

The model was now ready to run the analysis, where the goal was to obtain the max axial, shear and moment in the members of a truss and the ring. As the trusses are all similar there is no need to examine more than one. Suitable members could then be designed with the guidance of the relevant Eurocode. Now when designing the steel section to use for the different members SAP2000 could assist with a useful tool, the steel design/check for structure tool.

The steel design preferences presented itself with a large number of options to choose from. Here the design code used for the checks could be selected, there was an option for Eurocode 3-2005 which was selected. The country could also be selected, so the correct national annex could be used and the Norwegian annex was selected. The other options were mostly left untouched, but the tool could be tailored even more to the analysis. The tool automatically makes all the load combinations it needs, running the tool then shows the capacity ratio for the most critical load combination. The tool colours the members according to how much of the capacity is used, with red colour if the ratio is over one (failure) and blue if the ratio is under 0.5 with green, yellow and orange between them. As long as a member has a capacity ratio under 1 it is good (red in SAP2000). All the calculated parameters and the critical check can be viewed in a data-sheet in SAP2000, which will be compared to the manual calculation to ensure a proper design. Some of the calculations may differ at times due to different calculation choices.

## 2.5 Simulate lifting in SAP2000

To simulate the jacking of the cable in SAP2000 a temperature loading can be used. A temperature loading will inflict a deformation on the cable - extending the cable with positive temperature and shortening the cable with a negative temperature. In this case a reduction of length is desired, as this will move the ring upwards. The jacks will pull

the cable (element 385), pulling the structure upwards and reducing the length of the cable. This jacking force and reduction of length is what the temperature loading will try to emulate. Simply applying a point load or a distributed load to the cable will not result in the desired deformation or tension force in the cable.

To calculate the needed temperate loading the following formulas from Advanced Mechanics of Materials, Boresi, Arthur P. [16] was used:

$$N = A \cdot \sigma \quad (2.5)$$

$$\sigma = \varepsilon \cdot E \quad (2.6)$$

$$\varepsilon = \Delta T \cdot \alpha \quad (2.7)$$

Rearranging the equations:

$$N = A \cdot E \cdot \alpha \cdot \Delta T \quad (2.8)$$

Solving for  $\Delta T$ :

$$\Delta T = \frac{N}{A \cdot E \cdot \alpha} \quad (2.9)$$

where

- $\Delta T$  = change from reference temperature  $T$ (room temperature)
- $A$  = Cross section of cable
- $E$  = Modulus of elasticity (Young's modulus)
- $N$  = Axial force on cable (tension)
- $\alpha$  = temperature coefficient

The temperature coefficient of the material  $\alpha$  is very low for normal S355 steel or for Y1860/Y1775 strand steel, which would require high temperature differences for a noticeable deformation. A fictive material will be defined with a higher  $\alpha$  value such that more manageable temperatures can be applied.

# Chapter 3

## Analysis

### 3.1 Analysis of final structure

The final structure is the structure that is going to be standing when the lifting of the structure is completed. This structure is subjected to snow and live-load and has additional elements that are installed after the raising is done. Designing this first produces a structure that can be used as a trial structure for the raising procedure, with most importantly cross-sections for the different elements, which will provide the structure with an appropriate self-weight.

As the structure is raised, different loads will be applied to the elements than in the final position. They will have a different orientation, and as such will distribute forces differently, some elements will also change between being in compression and tension. There can be elements that have a suitable design for the structure in the final position, but in the lifting phase, the member can be subjected to failure.

#### 3.1.1 Element forces

Applying the snow, live and dead-load as distributed to the beam elements, defining the load combination 6.10b, and running a linear static analysis will produce the element forces in each element.

Figure 3.1 shows the element forces in the truss. The beams that make up the top of the truss are subjected to a compression force and the bars at the bottom are subjected to a tension force. The members in between are some compression members and some tension members, but they are all relatively low load members, and two members carry such a low axial force that they can be called zero-force members. The shear force and bending moment are exclusively carried by the beam at the top, as expected.

The top part of the ring members is in compression and the bottom members in tension. There is a low shear force and bending moment, but the ring is predominantly subjected to axial forces. The forces are read of the elements and is summarised in table 3.1. With these values the first design can be made.

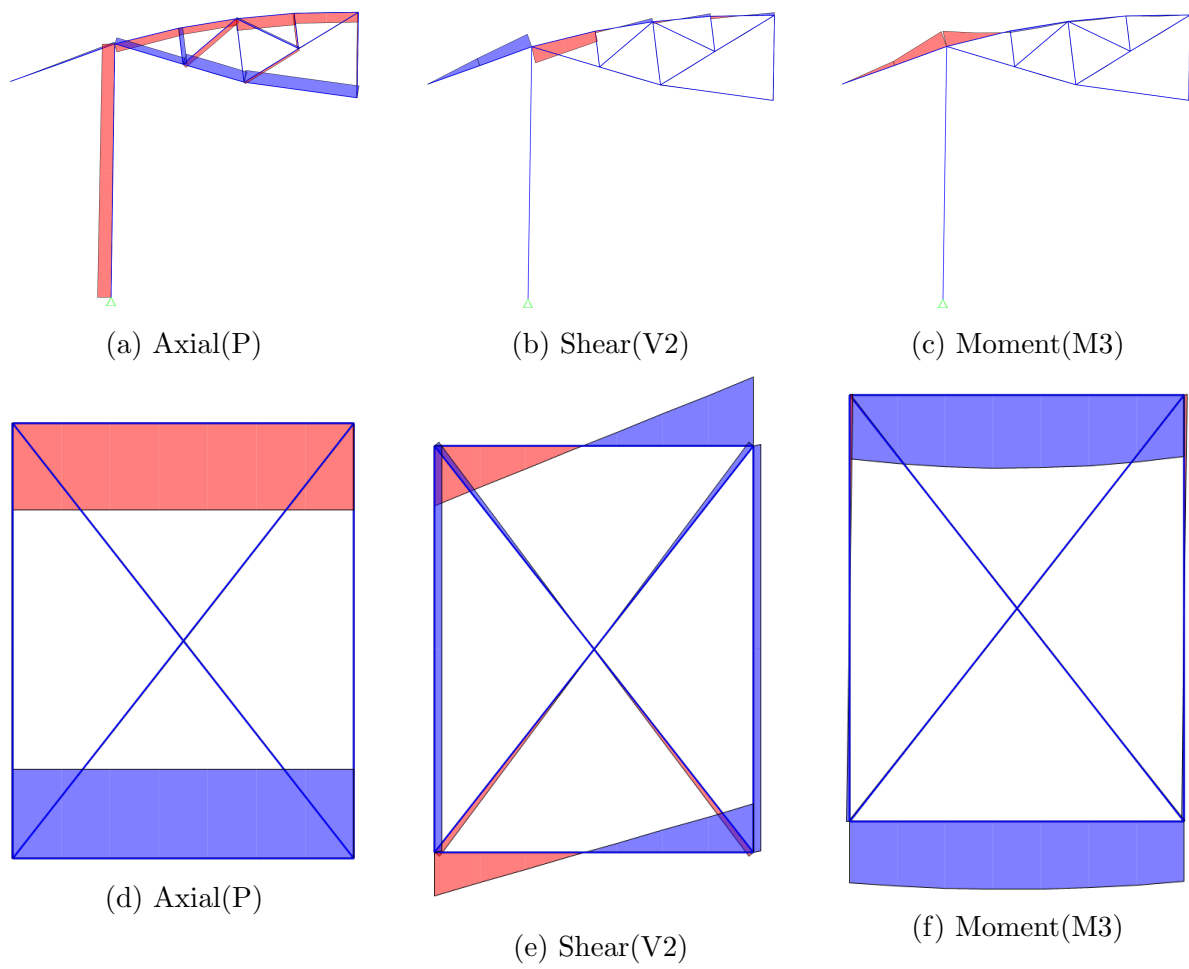


Figure 3.1: Element forces, axial: compression in red and tension in blue



Table 3.1: Forces in the final position

Element	Axial(P)	Shear(V2)	Moment(M3)
Tension bars:			
37B	66.639 <i>kN</i>	0 <i>kN</i>	0 <i>kN-m</i>
37E	26.731 <i>kN</i>	0 <i>kN</i>	0 <i>kN-m</i>
385	184.829 <i>kN</i>	0 <i>kN</i>	0 <i>kN-m</i>
4D0	99.754 <i>kN</i>	0 <i>kN</i>	0 <i>kN-m</i>
4D1	164.652 <i>kN</i>	0 <i>kN</i>	0 <i>kN-m</i>
Compression bars:			
378	3.112 <i>kN</i>	0 <i>kN</i>	0 <i>kN-m</i>
37C	70.815 <i>kN</i>	0 <i>kN</i>	0 <i>kN-m</i>
37D	24.78 <i>kN</i>	0 <i>kN</i>	0 <i>kN-m</i>
48D	244.867 <i>kN</i>	0 <i>kN</i>	0 <i>kN-m</i>
4D2	30.626 <i>kN</i>	0 <i>kN</i>	0 <i>kN-m</i>
4D3	5.97 <i>kN</i>	0 <i>kN</i>	0 <i>kN-m</i>
Beams:			
4B7	158.201 <i>kN</i> (C)	17.127 <i>kN</i>	12.682 <i>kN-m</i>
4B8	183.783 <i>kN</i> (C)	18.087 <i>kN</i>	13.9116 <i>kN-m</i>
4B9	107.06 <i>kN</i> (C)	23.23 <i>kN</i>	26.665 <i>kN-m</i>
4BA	125.778 <i>kN</i> (C)	110.69 <i>kN</i>	247.665 <i>kN-m</i>
4BB	30.785 <i>kN</i> (T)	90.139 <i>kN</i>	247.625 <i>kN-m</i>
Ring elements:			
Upper ring	1140.55 <i>kN</i> (C)	3.376 <i>kN</i>	17.195 <i>kN-m</i>
Lower ring	1164.48 <i>kN</i> (T)	2.37 <i>kN</i>	15.974 <i>kN-m</i>
Ring column	16.837 <i>kN</i> (C)	0 <i>kN</i>	1.66 <i>kN-m</i>
C = compression, T = tension			

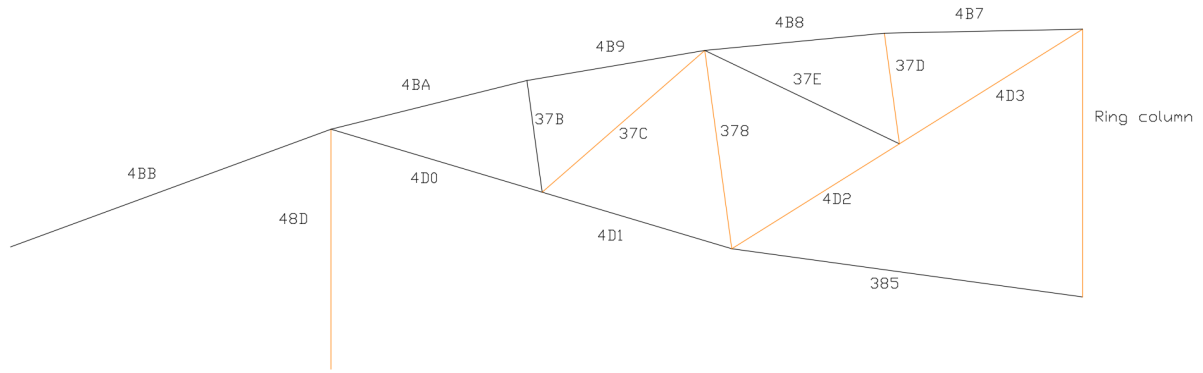
## 3.2 Structure in the final position

The element forces from the SAP2000 analysis model of the finished structure have been identified and noted. Now a suitable steel section can be assigned to each member. The different members serve different purposes which must be considered when choosing a section. The beam members are subjected to shear and moment, some to a high axial load and some to a low axial load. Some truss members are in compression and some in tension, with some members being very low force members. The curved member in the ring is almost exclusively subjected to axial force, with the top member in compression and the bottom member in tension.

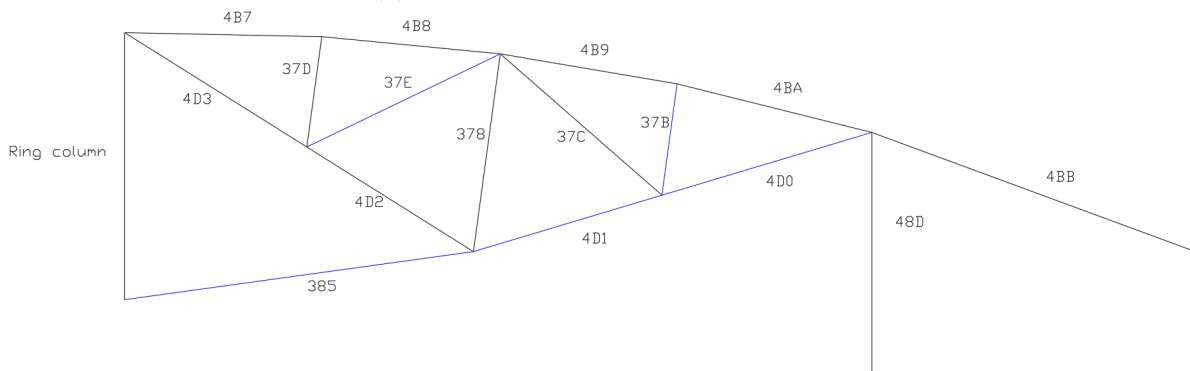
First, a trial section has to be chosen, and then the capacity of that section can be calculated. If a section does not have the desired capacity the trial section has to be replaced by a different section (often a larger cross-section area) and tried again.

As these calculations are repetitive MATLAB will be used, where members are objects and the different elements are classes: tension bars, compression bars and beam/column-beam.

The calculations will follow the Eurocode: NS-EN 1993-1-1:2005 + A1:2014 + 2015 [17] or EC3 for short. The equations used are summarised in appendix B.



(a) Compression members in orange



(b) Tension members in blue

Figure 3.2: Forces in bar members

### 3.2.1 Design of tension members

To choose a section for the members in tension, first,  $A_{min}$  is calculated. Then a section with a higher cross-section area is chosen. For tension members, this section will most likely have enough capacity. The calculations are summarized in table 3.2.

Table 3.2: Tension members design

Element	$N_{Ed}$	$A_{min}$	Section	A	$N_{pl,Rd}$
37B	66.6 kN	197.1 mm <sup>2</sup>	CHS26.9/2.6	198 mm <sup>2</sup>	67.1 kN
37E	26.7 kN	79 mm <sup>2</sup>	CHS21.3/2.3	137 mm <sup>2</sup>	46.4 kN
385	184.8 kN	546.6 mm <sup>2</sup>	HEA100	2124 mm <sup>2</sup>	718.1 kN
4D0	99.7 kN	295 mm <sup>2</sup>	HEA100	2124 mm <sup>2</sup>	718.1 kN
4D1	164.6 kN	487 mm <sup>2</sup>	HEA100	2124 mm <sup>2</sup>	718.1 kN
Element	$N_{pl,Rd} > N_{Ed}$				
37B	OK				
37E	OK				
385	OK				
4D0	OK				
4D1	OK				
CHS = Circular Hollow Section, HEA = "H" section					

### 3.2.2 Design of compression members

Similarly, for tension members, a trial section has to be chosen and tested. The difference here is that now there is also a chance that the member can be subjected to buckling, taking this into account lengthens the calculation.

Table 3.3: Trial sections for compression members

Element	$N_{Ed}$	$A_{min}$	Trial section	A	$N_{pl,Rd}$
378	3.1 kN	29.22 mm <sup>2</sup>	HEA100	2124 mm <sup>2</sup>	718.1 kN
37C	70.8 kN	664.93 mm <sup>2</sup>	HEA100	2124 mm <sup>2</sup>	718.1 kN
37D	24.78 kN	232.86 mm <sup>2</sup>	HEA100	2124 mm <sup>2</sup>	718.1 kN
48D	244.8 kN	2299.2 mm <sup>2</sup>	HEA120	2534 mm <sup>2</sup>	856.6 kN
4D2	30.6 kN	287.57 mm <sup>2</sup>	HEA100	2124 mm <sup>2</sup>	718.1 kN
4D3	5.9 kN	56 mm <sup>2</sup>	HEA100	2124 mm <sup>2</sup>	718.1 kN
HEA = "H" section					

#### Design of elements

**Element 378** The trial section for this member is HEA100; the length is 3 m. The connections at the ends of the bar are as pin supports. Effective length factor,  $k_e$ , is 1.0 and then  $L_{cr} = 3$  m.

Table 3.4: Summary of calculations for element 378

Section	A	$i_{min}$	$\alpha$	$N_{b,Rd}$
HEA100	$2124 \text{ mm}^2$	$25.1 \text{ mm}$	0.49	$211.16 \text{ kN}$
Section	$N_{Ed}$	$N_{pl,Rd}$	$N_{pl,Rd} > N_{Ed}$	$N_{b,Rd} > N_{Ed}$
HEA100	$3.1 \text{ kN}$	$718.1 \text{ kN}$	OK	OK

**Element 37C** The trial section for this member is HEA100; the length is  $3.2 \text{ m}$ . The connections at the ends of the bar are as pin supports. Effective length factor,  $k_e$ , is 1.0 and then  $L_{cr} = 3.2 \text{ m}$ .

Table 3.5: Summary of calculations for element 37C

Section	A	$i_{min}$	$\alpha$	$N_{b,Rd}$
HEA100	$2124 \text{ mm}^2$	$25.1 \text{ mm}$	0.49	$187.3 \text{ kN}$
Section	$N_{Ed}$	$N_{pl,Rd}$	$N_{pl,Rd} > N_{Ed}$	$N_{b,Rd} > N_{Ed}$
HEA100	$70.81 \text{ kN}$	$718.1 \text{ kN}$	OK	OK

**Element 37D** The trial section for this member is HEA100; the length is  $1.6 \text{ m}$ . The connections at the ends of the bar are as pin supports. Effective length factor,  $k_e$ , is 1.0 and then  $L_{cr} = 1.6 \text{ m}$ .

Table 3.6: Summary of calculations for element 37D

Section	A	$i_{min}$	$\alpha$	$N_{b,Rd}$
HEA100	$2124 \text{ mm}^2$	$25.1 \text{ mm}$	0.49	$187.3 \text{ kN}$
Section	$N_{Ed}$	$N_{pl,Rd}$	$N_{pl,Rd} > N_{Ed}$	$N_{b,Rd} > N_{Ed}$
HEA100	$24.78 \text{ kN}$	$718.1 \text{ kN}$	OK	OK

**Element 48D** The trial section for this member is HEA120; the length is  $11.8 \text{ m}$ . The connections at the ends of the column are as pin supports. Effective length factor,  $k_e$ , is 1.0 and then  $L_{cr} = 11.8 \text{ m}$ .

Table 3.7: Summary of calculations for element 48D

Section	A	$i_{min}$	$\alpha$	$N_{b,Rd}$
HEA120	$2534 \text{ mm}^2$	$30.2 \text{ mm}$	0.49	$29.63 \text{ kN}$
HEA240	$7684 \text{ mm}^2$	$60 \text{ mm}$	0.49	$323.63 \text{ kN}$
Section	$N_{Ed}$	$N_{pl,Rd}$	$N_{pl,Rd} > N_{Ed}$	$N_{b,Rd} > N_{Ed}$
HEA120	$244.8 \text{ kN}$	$856.6 \text{ kN}$	OK	NOT OK
HEA240	$244.8 \text{ kN}$	$2727.66 \text{ kN}$	OK	OK

**Element 4D2** The trial section for this member is HEA100; the length is 2.95 m. The connections at the ends of the bar are as pin supports. Effective length factor,  $k_e$ , is 1.0 and then  $L_{cr} = 2.95$  m.

Table 3.8: Summary of calculations for element 4D2

Section	A	$i_{min}$	$\alpha$	$N_{b,Rd}$
HEA100	2124 mm <sup>2</sup>	25.1 mm	0.49	215.27 kN
Section	$N_{Ed}$	$N_{pl,Rd}$	$N_{pl,Rd} > N_{Ed}$	$N_{b,Rd} > N_{Ed}$
HEA100	30.626 kN	718.1 kN	OK	OK

**Element 4D3** The trial section for this member is HEA100; the length is 3.2 m. The connections at the ends of the bar are as pin supports. Effective length factor,  $k_e$ , is 1.0 and then  $L_{cr} = 3.2$  m.

Table 3.9: Summary of calculations for element 4D3

Section	A	$i_{min}$	$\alpha$	$N_{b,Rd}$
HEA100	2124 mm <sup>2</sup>	25.1 mm	0.49	201.53 kN
Section	$N_{Ed}$	$N_{pl,Rd}$	$N_{pl,Rd} > N_{Ed}$	$N_{b,Rd} > N_{Ed}$
HEA100	5.97 kN	718.1 kN	OK	OK

### 3.2.3 Design of beam members

The beam members, in addition to axial load, must resist the shear force and bending moment imposed on the beam. This increase the number of checks to test and combined load checks should also be done. Instead of calculating  $A_{min}$  and using that value to choose a trial section, for beams, the value  $W_{pl,min}$  (plastic section modulus) is calculated and a section with a higher  $W_{pl}$  is chosen as a trial section.

The beam members 4B7, 4B8, 4B9, 4BA and 4BB are in reality a single curved beam and must therefore have the same cross-section, but the parts of the curved beam will be designed individually, and a single section will be chosen that is suitable for all the parts.

Table 3.10: Trial sections for compression members

Element	$M_{y,Ed}$	$W_{pl,min}$	Trial section	$W_{pl}$
4B7	12.68 kN	$75.02 \cdot 10^3 \text{ mm}^3$	IPE140	$88.34 \cdot 10^3 \text{ mm}^3$
4B8	13.91 kN	$82.29 \cdot 10^3 \text{ mm}^3$	IPE140	$88.34 \cdot 10^3 \text{ mm}^3$
4B9	26.89 kN	$159.0 \cdot 10^3 \text{ mm}^3$	IPE180	$166.4 \cdot 10^3 \text{ mm}^3$
4BA	247.66 kN	$1465.0 \cdot 10^3 \text{ mm}^3$	IPE450	$1702 \cdot 10^3 \text{ mm}^3$
4BB	247.62 kN	$1464.8 \cdot 10^3 \text{ mm}^3$	IPE450	$1702 \cdot 10^3 \text{ mm}^3$

IPE = European "I" Beams

Table 3.11:  $\lambda$ (lambda)-check and reduced moment capacity for trial sections

Element	Trial section	$\lambda$ check	$M_{c,Rd}$	$M_{b,Rd}$
4B7	IPE140	Not ok	29.86 kN-m	10.35 kN-m
4B8	IPE140	Not ok	29.86 kN-m	20.18 kN-m
4B9	IPE180	Not ok	56.28 kN-m	46.87 kN-m
4BA	IPE450	Ok	575.43 kN-m	575.43 kN-m
4BB	IPE450	Ok	575.43 kN-m	575.43 kN-m

### Design of elements

A suitable cross-section for the beams will be chosen here. Although members 4B7, 4B8, and 4B9 are beams, the axial load is dominant for these members, so they will perform like a column and the axial capacity will most likely be the deciding design factor.

The beams will be checked without any intermediate transverse web stiffeners, a rigid end post, or load-bearing stiffeners. If the resistance to transverse forces/bearing resistance is too low, stiffeners should be added.

**Element 4B7** This beam element is connected to the ring by a hinge connection and is fixed to element 4B8. The member has a length of 2.9 meters. Effective length factor,  $k_e$ , is 0.7. Effective length is 2.07 meters.

Table 3.12: Design load and critical length of element 4B7

$N_{Ed}$	$V_{Ed}$	$M_{Ed}$	$L_{cr}$
158.2 kN	17.127 kN	12.68 kN-m	2073 mm

**Compression and bending moment check:** Reading  $\chi_{LT}$ ,  $k_{yy}$  and  $k_{yz}$  from SAP2000 provides the values needed to calculate the combined axial and moment requirements (EC3: 6.61 and 6.62)

Table 3.13: Buckling factors for the combined axial and bending moment criterion

Section	$\chi_{LT}$	$k_{yy}$	$k_{yz}$	EC3: 6.61	EC3: 6.62
IPE 140	0.388	1.064	1.802	2.14	2.94
IPE 160	0.413	1.026	1.684	1.42	1.90
IPE 200	0.467	0.967	1.022	0.70	0.72

Table 3.14: Trial sections for compression members

Section	IPE140	IPE160	IPE200
Class	1	1	1
$\lambda$ check	Not ok	Not ok	Ok
$M_{c,Rd}$	29.86 kN-m	41.89 kN-m	74.58 kN-m
$M_{N,y,Rd}$	26.48 kN-m	40.06 kN-m	74.58 kN-m
$M_{b,Rd}$	10.35 kN-m	17.53 kN-m	42.61 kN-m
$V_{c,Rd}$	149.26 kN	188.48 kN	273.2 kN
$N_{b,Rd}$	162.11 kN	237.15 kN	237.15 kN
$M_{c,Rd} > M_{Ed}$	Ok	Ok	Ok
$M_{N,y,Rd} > M_{Ed}$	Ok	Ok	Ok
$M_{b,Rd} > M_{Ed}$	Not ok	Ok	Ok
$V_{c,Rd} > V_{Ed}$	Ok	Ok	Ok
$N_{b,Rd} > N_{Ed}$	Ok	Ok	Ok
$6.61 \leq 1$	Not Ok	Not Ok	Ok
$6.62 \leq 1$	Not Ok	Not Ok	Ok
Suitable:	No	No	Yes

**Element 4B8** This beam element is fixed to beam 4B7 and 4B8 and has a length of 2.7 meters. Effective length factor,  $k_e$ , is 0.5: effective length is 1.34 meters.

Table 3.15: Design load and critical length of element 4B8

$N_{Ed}$	$V_{Ed}$	$M_{Ed}$	$L_{cr}$
183.78 kN	18.087 kN	13.91 kN-m	1348 mm

**Compression and bending moment check:** Reading  $\chi_{LT}$ ,  $k_{yy}$  and  $k_{yz}$  from SAP2000 provides the values needed to calculate the combined axial and moment requirements (EC3: 6.61 and 6.62)



Table 3.16: Buckling factors for the combined axial and bending moment criterion

Section	$\chi_{LT}$	$k_{yy}$	$k_{yz}$	EC3: 6.61	EC3: 6.62
IPE 140	0.421	0.54	1.60	1.19	2.37
IPE 180	0.475	0.53	0.69	0.60	0.69

Table 3.17: Summary of capacity calculations

Section	IPE140	IPE180
Class	1	1
$\lambda$ check	Not ok	Ok
$M_{c,Rd}$	29.86 kN-m	56.25 kN-m
$M_{N,y,Rd}$	24.78 kN-m	56.25 kN-m
$M_{b,Rd}$	20.19 kN-m	46.87 kN-m
$V_{c,Rd}$	149.26 kN	219.68 kN
$N_{b,Rd}$	306.31 kN	554.18 kN
$M_{c,Rd} > M_{Ed}$	Ok	Ok
$M_{N,y,Rd} > M_{Ed}$	Ok	Ok
$M_{b,Rd} > M_{Ed}$	Ok	Ok
$V_{c,Rd} > V_{Ed}$	Ok	Ok
$N_{b,Rd} > N_{Ed}$	Ok	Ok
$6.61 \leq 1$	Not ok	Ok
$6.62 \leq 1$	Not ok	Ok
Suitable:	No	Yes

**Element 4B9** This beam element is fixed to beam 4BA and 4B8 and has a length of 2.7 meters. Effective length factor,  $k_e$ , is 0.5: effective length is 1.34 meters.

Table 3.18: Design load and critical length of element 4B9

$N_{Ed}$	$V_{Ed}$	$M_{Ed}$	$L_{cr}$
107.06 kN	18.087 kN	13.91 kN-m	1345 mm

**Compression and bending moment check:** Reading  $\chi_{LT}$ ,  $k_{yy}$  and  $k_{yz}$  from SAP2000 provides the values needed to calculate the combined axial and moment requirements (EC3: 6.61 and 6.62)

Table 3.19: Buckling factors for the combined axial and bending moment criterion

Section	$\chi_{LT}$	$k_{yy}$	$k_{yz}$	EC3: 6.61	EC3: 6.62
IPE 180	0.475	0.761	0.475	0.9589	0.6711

Table 3.20: Summary of capacity calculations

Section	IPE180
Class	1
$\lambda$ check	Not ok
$M_{c,Rd}$	56.25 <i>kN-m</i>
$M_{N,y,Rd}$	60.72 <i>kN-m</i>
$M_{b,Rd}$	46.87 <i>kN-m</i>
$V_{c,Rd}$	219.68 <i>kN</i>
$N_{b,Rd}$	554.29 <i>kN</i>
$M_{c,Rd} > M_{Ed}$	Ok
$M_{N,y,Rd} > M_{Ed}$	Ok
$M_{b,Rd} > M_{Ed}$	Ok
$V_{c,Rd} > V_{Ed}$	Ok
$N_{b,Rd} > N_{Ed}$	Ok
$6.61 \leq 1$	Ok
$6.62 \leq 1$	Ok
Suitable:	Yes

**Element 4BA** This beam element is fixed to beam 4BB and 4B9 and has a length of 3.0 meters. Effective length factor,  $k_e$ , is 0.5: effective length is 1.50 meters.

Table 3.21: Design load and critical length of element 4BA

$N_{Ed}$	$V_{Ed}$	$M_{Ed}$	$L_{cr}$
125.77 <i>kN</i>	110.69 <i>kN</i>	247.62 <i>kN-m</i>	1507 <i>mm</i>

**Compression and bending moment check:** Reading  $\chi_{LT}$ ,  $k_{yy}$  and  $k_{yz}$  from SAP2000 provides the values needed to calculate the combined axial and moment requirements (EC3: 6.61 and 6.62).

Table 3.22: Buckling factors for the combined axial and bending moment criterion

Section	$\chi_{LT}$	$k_{yy}$	$k_{yz}$	EC3: 6.61	EC3: 6.62
IPE 450	0.649	0.553	0.312	0.40	0.24
IPE 330	0.581	0.543	0.356	0.88	0.58
IPE 300	0.615	0.537	0.364	1.10	0.77

Table 3.23: Summary of capacity calculations

Section	IPE450	IPE330	IPE300
Class	1	1	
$\lambda$ check	Ok	Not ok	Not ok
$M_{c,Rd}$	575.43 kN-m	271.93 kN-m	212.45 kN-m
$M_{N,y,Rd}$	575.43 kN-m	271.93 kN-m	212.45 kN-m
$M_{b,Rd}$	588.71 kN-m	270.51 kN-m	208.73 kN-m
$V_{c,Rd}$	992.76 kN	601.46 kN	501.27 kN
$N_{b,Rd}$	2982 kN	1815 kN	1530 kN
$M_{c,Rd} > M_{Ed}$	Ok	Ok	Not ok
$M_{N,y,Rd} > M_{Ed}$	Ok	Ok	Not ok
$M_{b,Rd} > M_{Ed}$	Ok	Ok	Not ok
$V_{c,Rd} > V_{Ed}$	Ok	Ok	Ok
$N_{b,Rd} > N_{Ed}$	Ok	Ok	Ok
$6.61 \leq 1$	Ok	Ok	Ok
$6.62 \leq 1$	Ok	Ok	Not ok
Suitable:	Yes	Yes	No

**Element 4BB** This beam element is a critical member. It has a length of 5.1 meters, the longest of all the beams, and it is subjected to the highest loading: the accumulated snow loading. Because of this two lateral restraints are placed, one at mid-span and one at the end of the beam. These lateral restraints connect the '4BB' beams thus reducing the critical length for the buckling design. The points where the lateral restraints are connected act as pin supports with regard to the effective length factor. The start of the beam - that is connected to beam '4BA' - is seen as fixed, with two-pin supports: one in the middle and one at the end. The most conservative effective length factor is between the lateral restraints:  $k_e = 1.0$ . The effective length for buckling is therefore 2.549 meters.

The member is also the only one in tension instead of compression, which will effectively increase the buckling resistance.

Table 3.24: Design load and critical length of element 4BA

$N_{Ed}$	$V_{Ed}$	$M_{Ed}$	$L_{cr}$
30.78 kN (T)	222.08 kN	247.62 kN-m	2549 mm

**Compression and bending moment check:** Reading  $\chi_{LT}$ ,  $k_{yy}$  and  $k_{yz}$  from SAP2000 provides the values needed to calculate the combined axial and moment requirements (EC3: 6.61 and 6.62)

Table 3.25: Buckling factors for the combined axial and bending moment criterion

Section	$\chi_{LT}$	$k_{yy}$	$k_{yz}$	EC3: 6.61	EC3: 6.62
IPE 450	0.727	0.416	0.589	0.247	0.349
IPE 360	0.691	0.416	0.462	0.433	0.481
IPE 330	0.663	0.416	0.429	0.572	0.590

Table 3.26: Summary of capacity calculations

Section	IPE450	IPE360	IPE330
Class	1	1	1
$\lambda$ check	Ok	Ok	Ok
$M_{c,Rd}$	575.43 kN-m	344.51 kN-m	271.9 kN-m
$M_{N,y,Rd}$	575.43 kN-m	344.51 kN-m	271.9 kN-m
$M_{b,Rd}$	498.67 kN-m	281.98 kN-m	210.64 kN-m
$V_{c,Rd}$	992.76 kN	685.89 kN	601.46 kN
$N_{b,Rd}$	2392 kN	1650 kN	1339 kN
$M_{c,Rd} > M_{Ed}$	Ok	Ok	Ok
$M_{N,y,Rd} > M_{Ed}$	Ok	Ok	Ok
$M_{b,Rd} > M_{Ed}$	Ok	Ok	Not ok
$V_{c,Rd} > V_{Ed}$	Ok	Ok	Ok
$N_{b,Rd} > N_{Ed}$	Ok	Ok	Ok
$6.61 \leq 1$	Ok	Ok	Ok
$6.62 \leq 1$	Ok	Ok	Ok
Suitable:	Yes	Yes	No

### Continuous beam or changing sections

The original vision for beam elements 4B7 to 4BB was a single curved beam with a constant cross-section, but here a different section has been for every beam element.

There is a choice to be made here, between a single curved beam, which would be over-dimensioned for some parts, and suitable for some parts, and a curved composite beam with different cross-sections welded or bolted together. The advantage of a single section is that the analysis forward would be simpler as there is only one section to account for; there would be no need to look at how the different sections would be connected, and the construction process would presumably be simpler as well. The advantage of a curved beam composed of different sections would be potentially a lighter and cheaper structure, but they would have to be manually connected.

The decision to use a curved beam with constant cross-sections is made. The section for this member is IPE 360, as this capacity is needed for the 4BB part of the curved beam.

### 3.2.4 Design of ring elements

The ring is constructed by four different element types: the top beam, a compression member; the bottom beam, a tension member; columns connect the top beams to the bottom beams and lastly stiffeners connect the top of a column to the bottom of the adjacent column, making an 'X' between the columns.

The ring is subjected to very high loading, as all the trusses around are resting on the ring and it is the job of the ring to transfer the load of one truss to the truss on the opposite side.

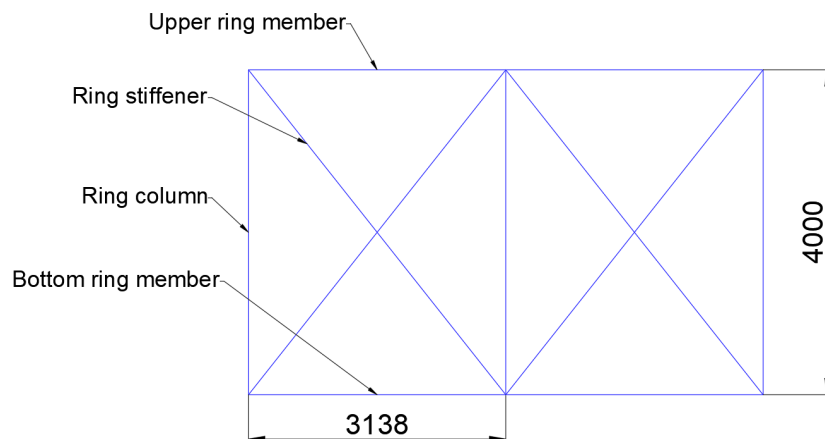


Figure 3.3: Ring element

#### Upper ring

Although this is a beam, subjected to both bending moment and shear forces, the compression force overshadows both.

Table 3.27: Design load and critical length of upper ring beam

$N_{Ed}$	$V_{Ed}$	$M_{Ed}$	$L_{cr}$
1140.55 kN (C)	3.37 kN	2.37 kN-m	3138 mm

Using the same formulas for finding trial sections for compression members a minimum cross-sectional area can be found:  $A_{min} = 3372 \text{ mm}^2$ , a HEA section would be most suitable and HEA-160 as an trial section.

Table 3.28: Summary of capacity calculations, upper ring

Section	A	$i_{min}$	$\alpha$	$N_{b,Rd}$
HEA160	3877 mm <sup>2</sup>	39.8 mm	0.34	1148 kN
HEA180	4525 mm <sup>2</sup>	45.2 mm	0.34	1381 kN

Section	$N_{Ed}$	$N_{pl,Rd}$	$N_{pl,Rd} > N_{Ed}$	$N_{b,Rd} > N_{Ed}$
HEA160	1140.55 kN	1310.84 kN	OK	Not oK
HEA180	1140.55 kN	1529.93 kN	OK	Ok

### Bottom ring

Subjected to almost the same load as the top ring, except in tension rather than compression, the minimum cross-sectional area is:  $A_{min} = 3444 \text{ mm}^2$ , a HEA section would be most suitable, with HEA-160 as a trial section.

Table 3.29: Design load and critical length of bottom ring beam

$N_{Ed}$	$V_{Ed}$	$M_{Ed}$	$L_{cr}$
1164.48 kN (T)	2.27 kN	15.974 kN-m	1569 mm

Table 3.30: Summary of capacity calculations, bottom ring

Section	A	$N_{Ed}$	$N_{pl,Rd}$	$N_{pl,Rd} > N_{Ed}$
HEA160	3877 mm <sup>2</sup>	1164.48 kN	1310 kN	Ok

### Ring column

The columns connecting the rings are subjected to a rather low loading and are in compression. A minimum area of  $A_{min} = 49.8 \text{ mm}^2$  is required, which is not a lot. Here a HEA or CHS would both be suitable. CHS 21.3 / 2.3 is chosen as a trial section.

Table 3.31: Design load and critical length of bottom ring beam

$N_{Ed}$	$V_{Ed}$	$M_{Ed}$	$L_{cr}$
16.837 kN (C)	0 kN	1.66 kN-m	2000 mm

Table 3.32: Summary of capacity calculations, upper ring

Section	A	$i_{min}$	$\alpha$	$N_{b,Rd}$
CHS 23.3 / 2.3	137 mm <sup>2</sup>	8.7 mm	0.21	1.22 kN
CHS 48.3 / 5	680 mm <sup>2</sup>	15.4 mm	0.21	18.54 kN
Section	$N_{Ed}$	$N_{pl,Rd}$	$N_{pl,Rd} > N_{Ed}$	$N_{b,Rd} > N_{Ed}$
CHS 23.3 / 2.3	16.837 kN	60.10 kN	Ok	Not ok
CHS 48.3 / 5	16.837 kN	229.96 kN	Ok	Ok

### 3.2.5 Steel design in SAP2000

SAP2000 has a steel design function that checks every member of the structure against the EC3 criteria. The software calculates all the required values and compares capacity with design load. It is very useful, as one can test different sections for an element without doing lengthy calculations. When comparing the manual calculations done here with the values from SAP2000, they are quite similar. One exception is that different geometry sometimes may be used, as buckling capacity in some cases differs.

Figure 3.5a and 3.5b show the result of the SAP2000 steel check, with the assigned sections and capacity ratio shown on the members. The chosen cross sections show capacity ratios mostly well under 1 with some close to 1. If a cross-section has a ratio over 1, it would need to be replaced with a cross-section with more capacity.

Two members are shown in red, and instead of a capacity ratio SAP2000 displaced "N/C". SAP2000 suggests that this section is too slender (admittedly the CHS 26.9 / 2.6 section is quite slender) and no capacity ratio is given. Both members are close to zero force members, so the loading is not the cause, the section is just too slender for SAP2000. The section is to be switched to a sturdier CHS 33.7/4.

Now some changes will be implemented to the model: the beam members (4BB - 4B7) are to be changed so that all the members are IPE 360 and the two previous discussed truss members changed to CHS 33.7/4. The steel check is then run again, and the capacity ratios are inspected. The new members have a higher self-weight which results in a slightly higher dead-load through the structure, which might overload other members.

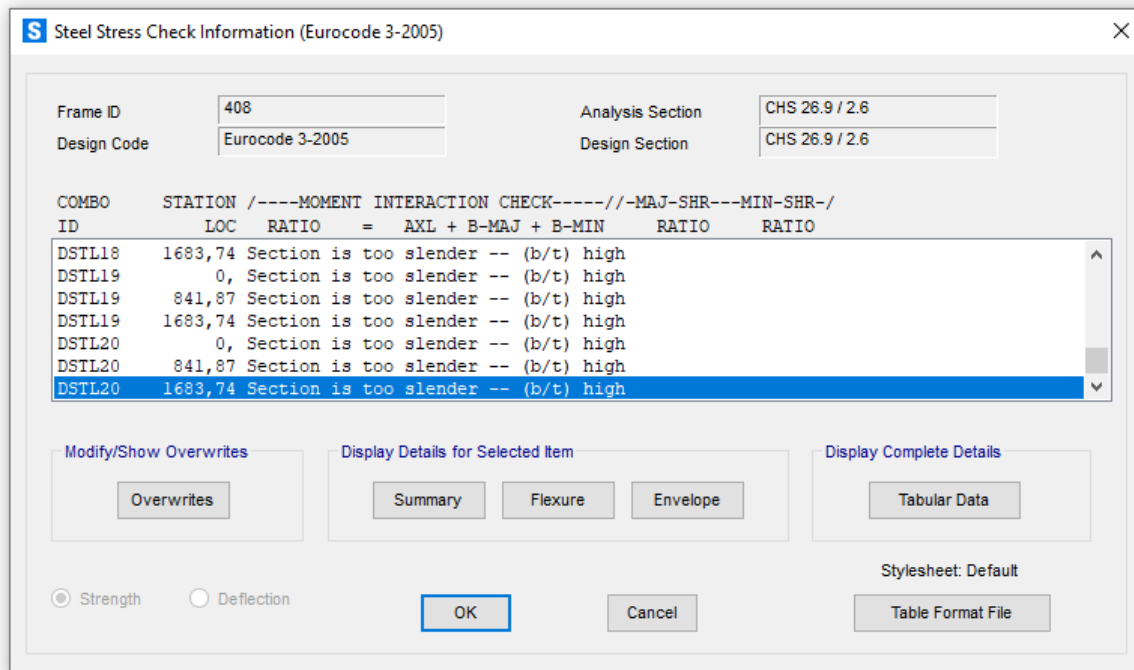
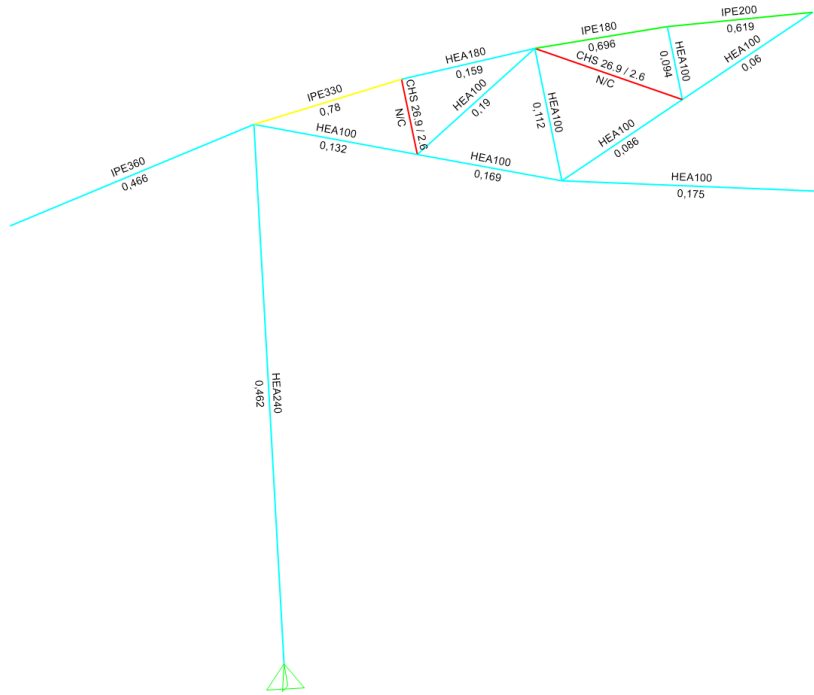


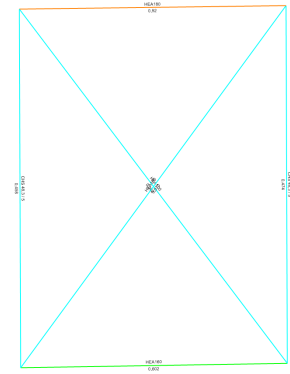
Figure 3.4: Steel stress check information for element 37B, before changes

Figure 3.5c and 3.5d show the result from running the steel check again with the changes to the cross-sections. The capacity ratio of all the members is under 1. The upper ring beam is close to failure with a capacity ratio of 0.984, but as long as it is under 1 it is okay, manual calculations confirm that capacity is not exceeded:  $N_{ed} = 859.77 \text{ kN} < N_{brd} = 998.88 \text{ kN}$ .

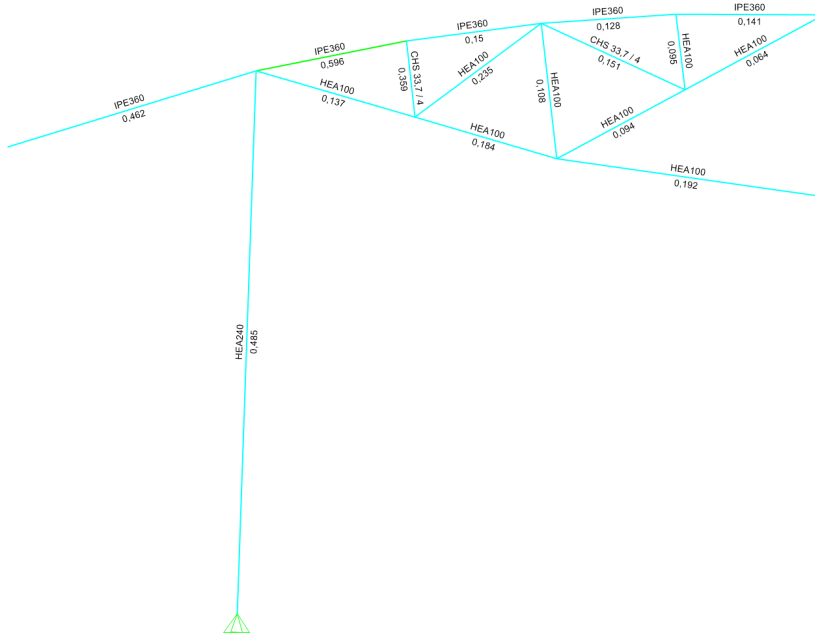




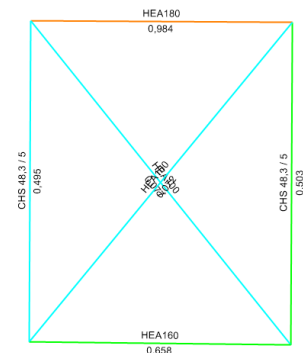
(a) Truss, before changes



(b) Ring, before changes



(c) Truss, after changes



(d) Ring, after changes

Figure 3.5: SAP2000 steel check for the structure in the finished position

### 3.2.6 Summary of design for final position

Now every element has been assigned a suitable section so that the structure can withstand the assigned dead-, live- and snow-load, in the final position. The sections are listed in table 3.33. These sections are the sections that will be used forwards in the analysis, where they may be changed if further analysis demands a higher capacity.

Table 3.33: Summation of the steel design for the structure in the final stage, with changes

Element	Section
Tension bars:	
37B	CHS 26.9/2.6 $\Rightarrow$ CHS 33.7/4
37E	CHS 26.9/2.6 $\Rightarrow$ CHS 33.7/4
385	HEA100
4D0	HEA100
4D1	HEA100
Compression bars:	
378	HEA100
37D	HEA100
37C	HEA100
48D	HEA240
4D2	HEA100
4D3	HEA100
Beams:	
4B7	IPE200 $\Rightarrow$ IPE360
4B8	IPE180 $\Rightarrow$ IPE360
4B9	IPE180 $\Rightarrow$ IPE360
4BA	IPE330 $\Rightarrow$ IPE360
4BB	IPE360
Ring elements:	
Upper ring	HEA180
Lower ring	HEA160
Ring column	CHS 48.3 / 5

## 3.3 Structure in starting position

In the previous chapter, a cross-section for all elements was assigned. These sections can now be used in a model for the lifting structure, which is geometrically different. The

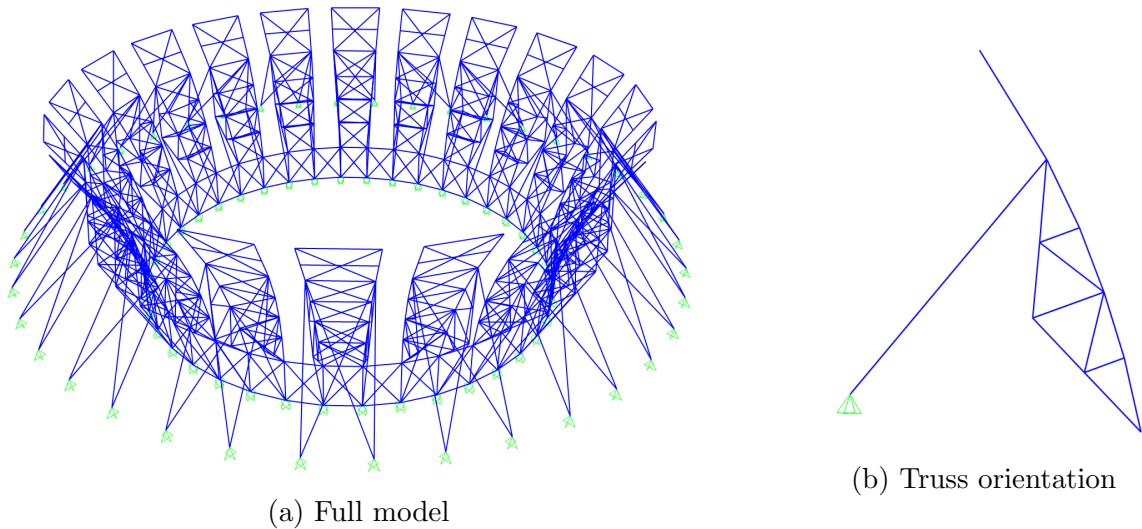


Figure 3.6: Model of the structure in the bottom position, in SAP2000

lifting models do not have the same number of bracings, and most importantly all the trusses are tilted forwards with the ring lowered, almost to the ground. The structure in this position is not subjected to any snow- or live-load, there is also no dead-load from the roof sheets, as the roof sheets are not present yet. The only load at this stage is the self-weight from the members themselves. The structure in the starting position should be able to stand on its own as the structure is prepared to be lifted.

The structure will start in the bottom position, then a force will be applied to lift the structure upwards. The design of the structure should be suitable and stable in the starting position and then also be suitable to withstand the applied jacking force. The ring of this structure is supported in the vertical direction by concrete blocks, these supports are added in SAP2000 as vertical restraints which restrict translation 3 (z-direction). Element 385 is not present on this model, as it is the jacking cable, not meant to absorb compression force. A safety factor of 1.35 is used for the dead load.

As shown in figure 3.6b the orientation of the truss is angled, compared to the final position, where member 48D is completely straight. Figure 3.7a shows the axial force in the truss, which for almost all members is a compression force, compared with the axial load for the truss in the final position where half were tension members.

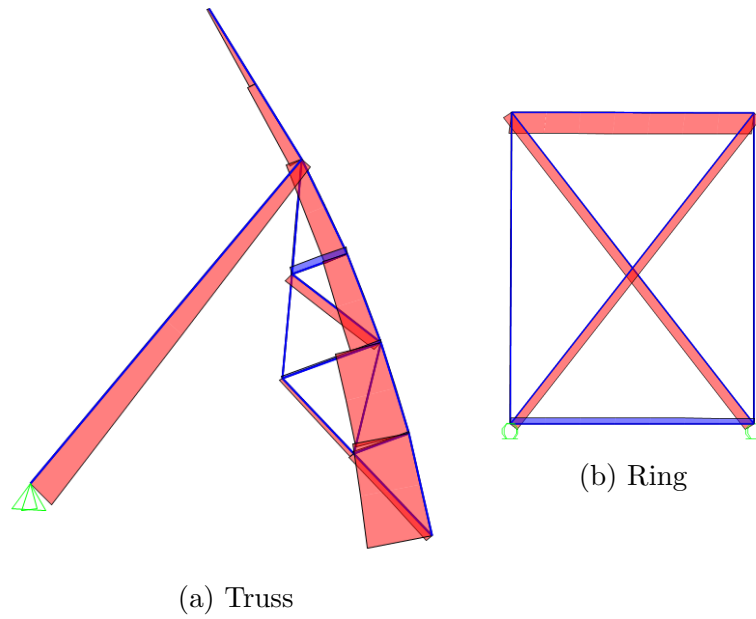


Figure 3.7: Axial force when the structure is in the bottom position, note the supports at the bottom of the ring in (b)

The element forces in this position is much lower for the final structure, because of the lack of external loading. Axial forces are significant lower, with moment and shear so low that they are negligible.

Table 3.34: Forces in the starting position

Element	Axial(P)	Shear(V2)	Moment(M3)
Tension bars:			
37B	2.697 <i>kN</i>	0 <i>kN</i>	0 <i>kN</i>
37E	0.124 <i>kN</i>	0 <i>kN</i>	0 <i>kN</i>
378	0.947 <i>kN</i>	0.3 <i>kN</i>	0.2 <i>kN</i>
Compression bars:			
4D0	2.12 <i>kN</i>	0 <i>kN</i>	0 <i>kN</i>
4D1	0.4 <i>kN</i>	0 <i>kN</i>	0 <i>kN</i>
37C	3.28 <i>kN</i>	0.2 <i>kN</i>	0.2 <i>kN</i>
48D	11.78 <i>kN</i>	2.9 <i>kN</i>	8.7 <i>kN</i>
4D2	1.46 <i>kN</i>	0.22 <i>kN</i>	0.16 <i>kN</i>
4D3	2.33 <i>kN</i>	0.24 <i>kN</i>	0.20 <i>kN</i>
Beams:			
4B7	17.77 <i>kN</i> (C)	0.43 <i>kN</i>	0.34 <i>kN-m</i>
4B8	15.56 <i>kN</i> (C)	0.36 <i>kN</i>	0.42 <i>kN-m</i>
4B9	9.526 <i>kN</i> (C)	0.699 <i>kN</i>	0.95 <i>kN-m</i>
4BA	7.27 <i>kN</i> (C)	3.53 <i>kN</i>	8.21 <i>kN-m</i>
4BB	4.4 <i>kN</i> (T)	2.83 <i>kN</i>	8.315 <i>kN-m</i>
Ring elements:			
Upper ring	27.11 <i>kN</i> (C)	0.73 <i>kN</i>	0.43 <i>kN-m</i>
Lower ring	7.138 <i>kN</i> (T)	0.63 <i>kN</i>	0.25 <i>kN-m</i>
Ring column	5.11 <i>kN</i> (C)	0 <i>kN</i>	0 <i>kN-m</i>
C = compression, T = tension			

The element forces can be read in table 3.34. There are no forces that demand any attention - all are below the element forces in the final structure. Running the SAP2000 steel check to confirm that the section are okay shows no red section (fig 3.8).



Table 3.35: Axial forces in the lifting position, 1.0 and 2.5 safety factor on dead load

Element	Axial(P) X 1.0	Axial(P) X 2.5
Tension bars:		
37B	6 <i>kN</i>	15 <i>kN</i>
37E	1.28 <i>kN</i>	3.2 <i>kN</i>
378	1.313 <i>kN</i>	3.28 <i>kN</i>
37D	0.387 <i>kN</i>	0.96 <i>kN</i>
385	137.61 <i>kN</i>	344.02 <i>kN</i>
4D0	44.41 <i>kN</i>	111.02 <i>kN</i>
4D1	49.628 <i>kN</i>	124.07 <i>kN</i>
Compression bars:		
37C	6.783 <i>kN</i>	16.95 <i>kN</i>
48D	33.787 <i>kN</i>	84.46 <i>kN</i>
4D2	101.775 <i>kN</i>	254.43 <i>kN</i>
4D3	101.512 <i>kN</i>	253.78 <i>kN</i>
Beams:		
4B7	35.3 <i>kN</i> (C)	88.25 <i>kN</i>
4B8	43.7 <i>kN</i> (C)	109.29 <i>kN</i>
4B9	34.18 <i>kN</i> (C)	85.45 <i>kN</i>
4BA	32.95 <i>kN</i> (C)	82.38 <i>kN</i>
4BB	3.2 <i>kN</i> (C)	8.12 <i>kN</i>
Ring elements:		
Upper ring	493.99 <i>kN</i> (C)	1234.97 <i>kN</i>
Lower ring	433.95 <i>kN</i> (T)	1084.89 <i>kN</i>
Ring column	29.374 <i>kN</i> (C)	73.43 <i>kN</i>
C = compression, T = tension		

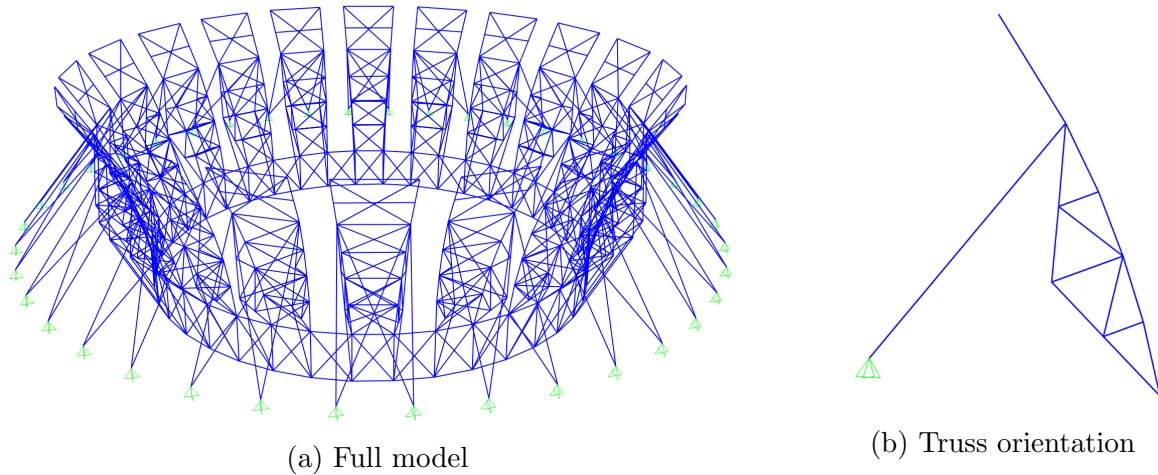


Figure 3.9: Model of the structure in the lifting position, in SAP2000

### 3.4.1 New members

The members that exceeded a capacity ratio of 1.0 need a more suitable cross-section to pass SAP2000's steel checks with a safety factor of 2.5. Some members experience a lot higher load in this analysis than in the previous analysis.

#### Element 4D2

This element is subjected to a relatively low load in the two first analyses,  $30.626\text{ kN}$  and  $1.46\text{ kN}$ . With a safety factor of 2.5, the axial load is  $254.43\text{ kN}$ . A minimum cross-sectional area is therefore:  $A_{min} = 2389\text{ mm}^2$ , with HEA120 being the closest in cross-sectional area. This cross-section has a buckling resistance,  $N_{brd}$ , of  $371.67\text{ kN}$  and is suitable.

#### Element 4D3

This element is similar to element 4D2, in both maximum loading and element length so a HEA120 section is also suitable here.

#### Upper ring element

With a safety factor of 2.5, this is loaded slightly higher than in the complete structure analysis, with an axial load of  $1234.975\text{ kN}$ . This load requires a minimum area of  $A_{min} = 3652.7\text{ mm}^2$ , which is less than the HEA180 provides, but this section does not provide enough buckling resistance. A HEA200 provides a buckling resistance of  $1286.1\text{ kN}$  for this element which is suitable.



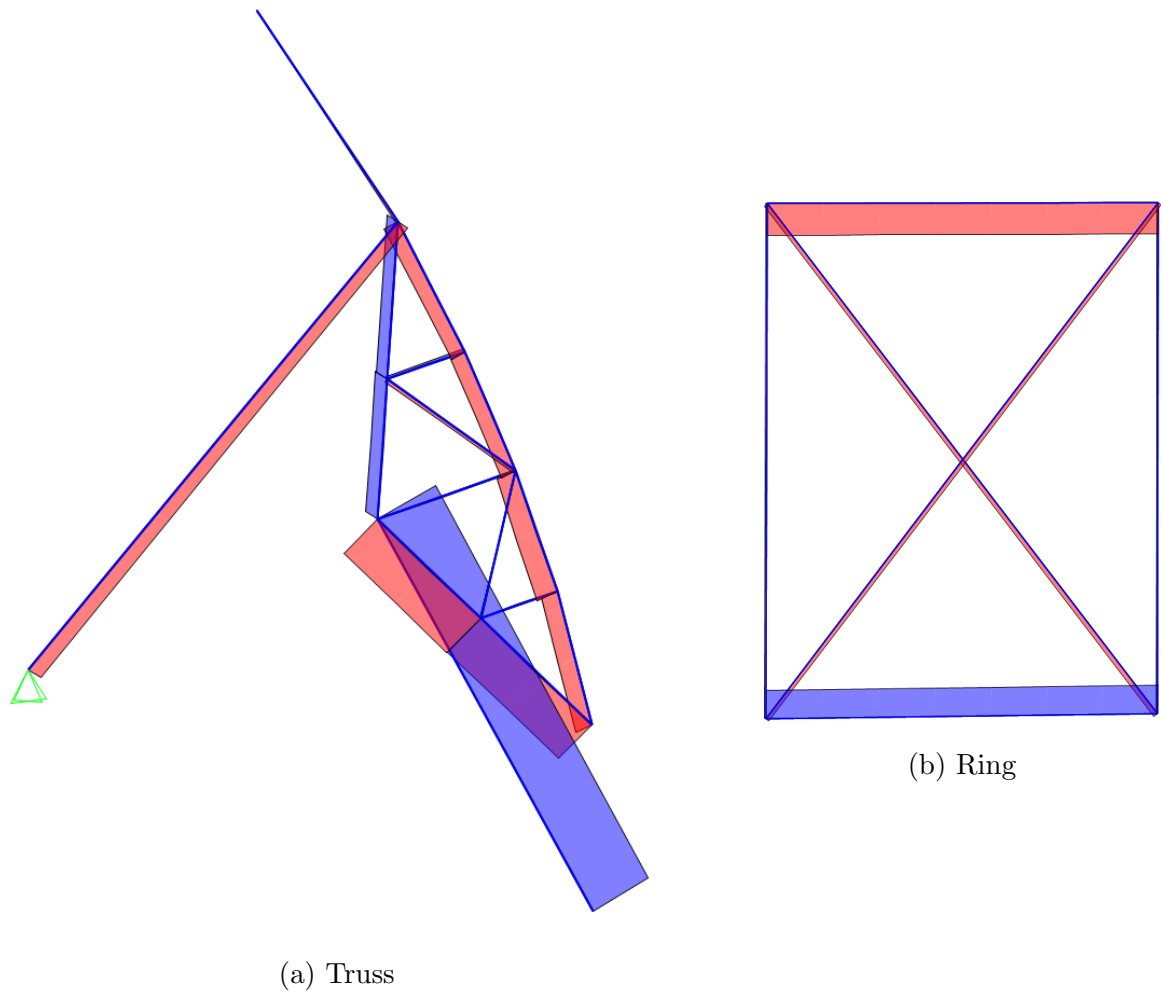
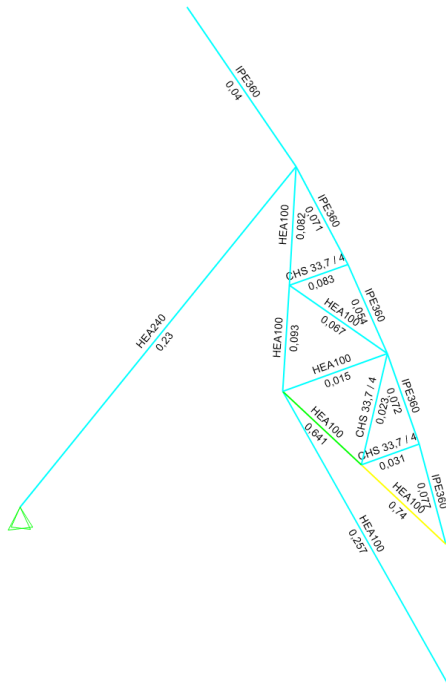
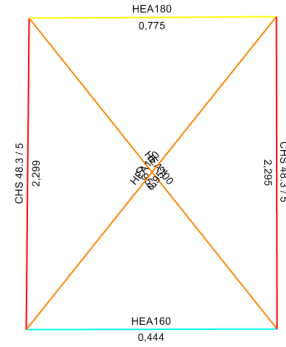


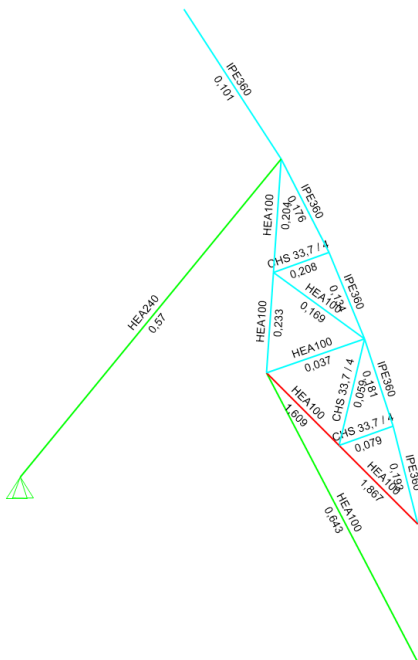
Figure 3.10: Axial load (tension blue, compression red), lifting structure, for both analysis (same shape)



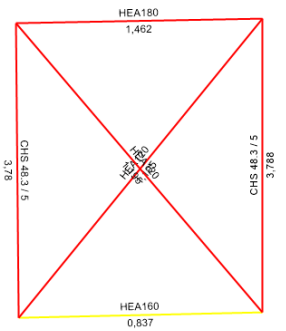
(a) Truss, safety factor 1.0



(b) Ring, safety factor 1.0



(c) Truss, safety factor 2.5



(d) Ring, safety factor 2.5

Figure 3.11: SAP2000 steel design / check for structure, lifting structure

### Ring column

The element is subjected axial load of  $73.43\text{ kN}$ , up from an axial load of  $16.837\text{ kN}$ , which is a sizable increase. A new minimum area of  $A_{min} = 217.43\text{ mm}^2$  is required, which is far below the currently provided area of the CHS 48.3/5 section:  $A = 680\text{ mm}^2$ , but this section only provides a buckling resistance,  $N_{brd}$ , of  $18.546\text{ kN}$ . The section CHS 101.6/8 provides a buckling resistance of  $221.731\text{ kN}$ , and thus suitable.

Finding a cross-section for this member was not an easy task. Around 10 different sections which promised to be suitable were tried, but they all displayed a capacity ratio over 1.0 in SAP2000. The section had to be increased to a section with almost five times the original cross-sectional area to display a capacity ratio under 1.0. It is therefore believed that this member and to some degree the entire ring is in an extremely unfavourable position. What end up happening was that when trying larger sections these sections would, because of the increased self-weight, increase the design axial load in the ring column and therefore make the section not suitable. There could have been a situation where no physical possible section would be suitable, because of the geometry, self-weight and safety factors. It is important to mention that a cross-section made of S355 steel was tried, this member might have been a candidate for high-strength steel material, as the self weigh is the same (same section of S355 and S450 weight the same per meter, density  $\rho \approx 7850\text{ kg/m}^3$  [18] for both), but capacity is higher.

### Ring stiffeners

These members was assigned the standard HEA100 section that was assigned to all the bracing/stiffeners, which was suitable until now. Changing the cross-section to a HEA120 is enough to satisfy the SAP2000 steel check.

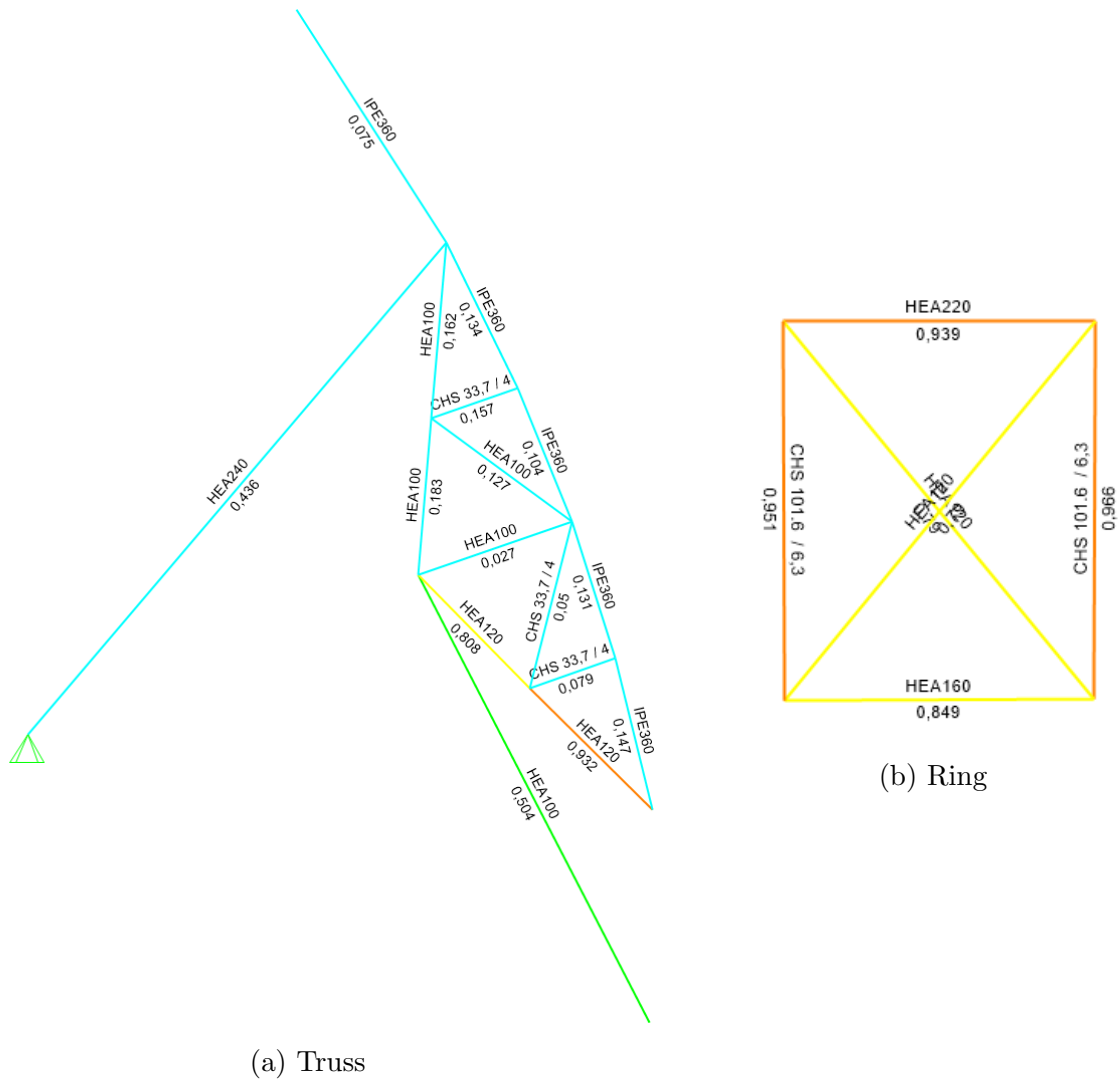


Figure 3.12: SAP2000 steel design / check for structure, lifting structure, new members (all pass)

### 3.4.2 Temperature loading - equation to post-tension

Using the equations from chapter 6, an appropriate temperature loading that emulate the jacking/post-tension can be found. An fictive material and cross section is made in SAP2000, with an temperature coefficient of 0.0001.

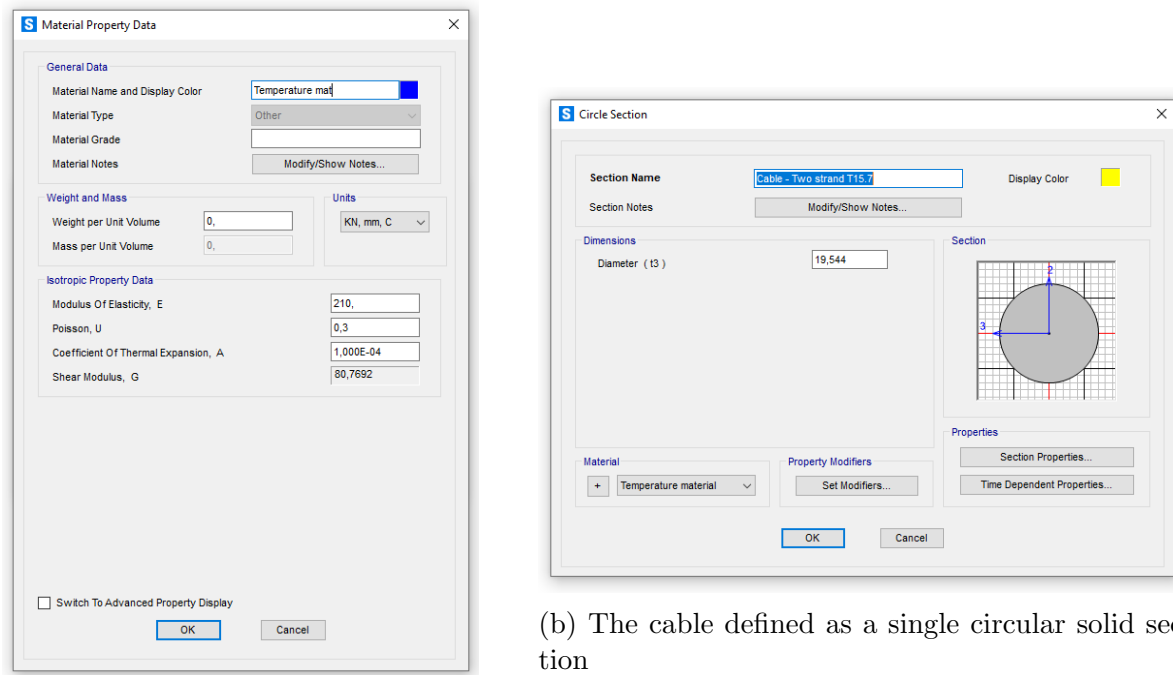


Figure 3.13: SAP2000 temperature material and cable

Using this new cross section, material and the tension force in element 385 from the analysis with a safety factor of 1.0,  $125.924 \text{ kN}$ , the change in temperature can be calculated:

$$\Delta T = \frac{N}{A \cdot E \cdot \alpha} = \frac{-125.924 \text{ kN}}{300 \text{ mm}^2 \cdot 210 \text{ kN/mm}^2 \cdot 0.0001} = -19.98^\circ \text{C} \quad (3.1)$$

This temperature is then added as a frame temperature loading to element 385. With only the dead-load on the structure, the ring is displaced  $210.78 \text{ mm}$  downwards. The goal was that this temperature loading would negate the displacement caused by the self-weight of the structure, such that the displacement would be zero. This was not the case as the ring had a downwards displacement of  $84.37 \text{ mm}$  with the calculated temperature, so the displacement was reduced, but not negated.

The next step then was to obtain zero vertical displacement (U3) of the ring. The calculated temperature reduced the displacement a bit, but not enough, a larger temperature load was needed. Once zero vertical displacement was obtained a marginal increase in the temperature loading could be applied to get the jacking force needed to move the structure upwards.

Table 3.36: Temperature loading, and the associating axial force and displacement

$\Delta T$	N ( $\Delta T$ + Dead)	U3 ( $\Delta T$ + Dead)
0°C	125.92 <i>kN</i>	-210.78 <i>mm</i>
-19.98°C	127.54 <i>kN</i>	-84.37 <i>mm</i>
-30°C	128.34 <i>kN</i>	-20.97 <i>mm</i>
-33°C	128.59 <i>kN</i>	-1.99 <i>mm</i>
-33.31°C	128.65 <i>kN</i>	-0.035 <i>mm</i>
-34.893°C	128.743 <i>kN</i>	9.98 <i>mm</i>

Interpolation the values approximates a temperature load that produces a near zero displacement, the accompanying force of 128.65 *kN*, if applied by the jacks will negate the displacement caused by the self weight. But this was not the goal. The goal is to lift the structure upwards. To reach this goal a temperature load of a larger magnitude is required. To start the lifting a displacement of 10 *mm* upwards should suffice. Again approximating a temperature, this time to obtain a 10 *mm* displacement. A temperature load of -34.893°C will produce this displacement, with 128.743 *kN* as the accommodation tension force. This is the force that the jacks will produce to start the lifting.

The formula for estimation temperature load, found by interpolation the results in table 3.36. Where  $y$  is the temperature and  $x$  is the displacement of the ring:

$$y = -0.1583x - 33.31 \quad (3.2)$$

As the ring and structure is moving upwards, the load needed from the jacks to continue the lifting is reducing, because more of the weight of the structure is transferred to the supports - the angle of element 48D is reduced as the structure is lifted.

To obtain the final jacking load, the model for the completed structure is used, without the bracing between the truss pairs and other members that are not in the lifting model. Applying only the dead load, with an safety factor of 1.0, displays a value of 34.969 *kN* in element 385. This is force that the jacks need to provide to lift the structure the last step. So there is an decrease jacking force required to continue the lifting. If the jacking force is reducing linear or non-linear is not clear from these analysis, more models at different stages in the lifting would be required to obtain this information. Looking at the figure 12 in the Xàtiva detailing paper [8] shows that the jacking force drops rapidly in the first half of the lifting and in the second half also reducing but less. This might be the case for this thesis structure as well, but it is not know. But it is highly likely that the highest jacking force is at the start of the lifting, which means that this is the most critical situation that the structure will experience.

### 3.4.3 Jacking system

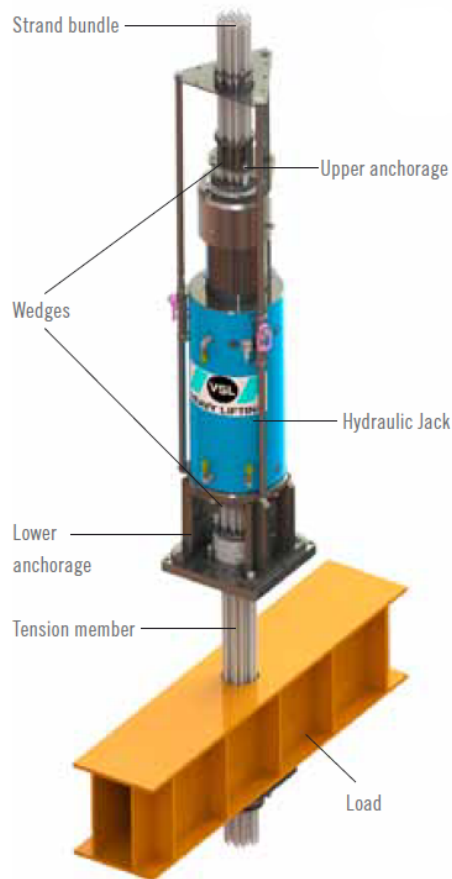
After the ring and the truss have been constructed, a cable is installed in place for element 385. These cables will be individually jacked by a jack mounted to each truss.

The jack is to be installed at the bottom of element 385, where the cable meets the ring. From the temperature loading test, it was found that the jacking force at the start is  $128.743\text{ kN}$  so the cable should be able to withstand this load, but the cable should also be able to meet the requirement from the 2.5 safety factor analysis: a tension force of  $344.02\text{ kN}$ . The cable chosen is a Y 1860 S7 15.7 cable [19], often used to prestress concrete. The cable has the following data:

- Diameter ( $mm$ ) = 15.7
- Tensile strength ( $MPa$ ) = 1860
- Cross sectional area ( $mm^2$ ) = 150
- Mass per meter ( $g/m$ ) = 1172
- Characteristic value of maximum force ( $kN - min$ ) = 279
- Maximum value of maximum force ( $kN$ ) = 321
- Characteristic value of 0.1% ( $kN - min$ ) = 246
- Modulus of elasticity ( $kN/mm^2$ ) = 195
- Minimum total elongation (%) = 3.5

With an characteristic value of maximum force of  $279\text{ kN}$ , at least one of these cables are required, to exceed the tension force from the 2.5 safety factor analysis.

The jack chosen is a VSL Strand lifting unit [20]. With a required lifting tension force of  $128.743\text{ kN}$ , type SLU-40 is suitable, with a jacking capacity of  $416\text{ kN}$ . This type has a capacity of four strands, so additional strands can be added for a higher safety margin. The jack weighs 280 kg, which is  $280/9.81 = 28.5\text{ N}$ , which is fairly light and a marginal increase in self-weight to the structure. This weight will not be added to any model.



(a) The VSL strand jacking system [20]



(b) Jack mounted at the bottom of the ring, Xàtiva bullring [1]

Figure 3.14: VSL Jack

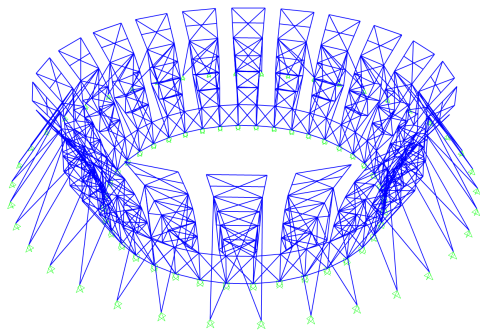
### 3.4.4 Animation of the lifting

Applying temperature loading with a higher magnitude will displace the structure higher and can show what the lifting process will look like. Figure 3.15 shows the displacement with the temperature from table 3.37, respectively. The displacement for 100% is not shown, because strange deformation happens with such a high-temperature loading, as can be seen, start happening at figure 3.15e, figure 3.15f is, therefore, the model for the complete structure.

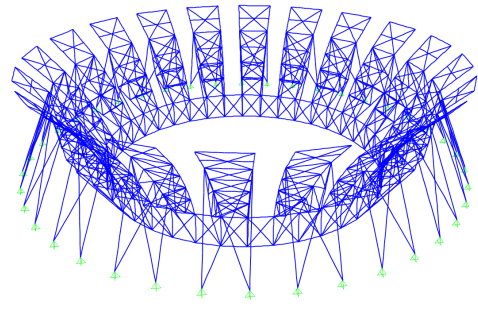


Table 3.37: The temperature load needed to displace the structure

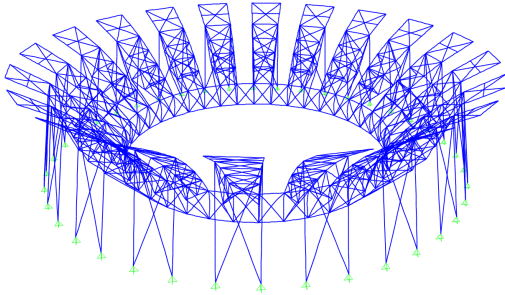
% of distance	$\Delta T$	U3 ( $\Delta T$ + Dead)
0	-33.31°C	-0.035 mm
20	-499.58°C	2949.98 mm
40	-965.85°C	5900.00 mm
60	-1432.13°C	8850.08 mm
80	-1898.40°C	11800.10 mm
100	-2364.68°C	14750 mm



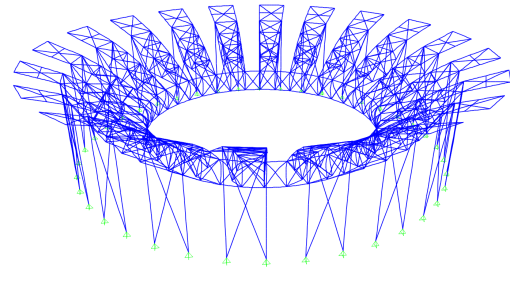
(a) Starting position



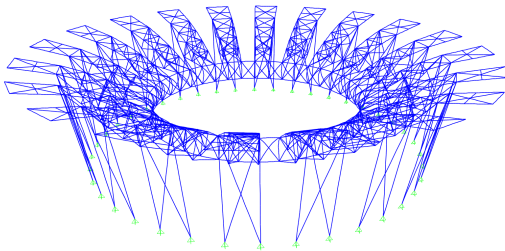
(b) 20% traveled



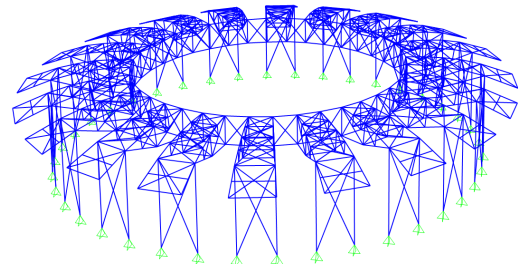
(c) 40% traveled



(d) 60% traveled



(e) 80% traveled



(f) 100% traveled

Figure 3.15: Structure in different position in the lifting process

### 3.4.5 Summary

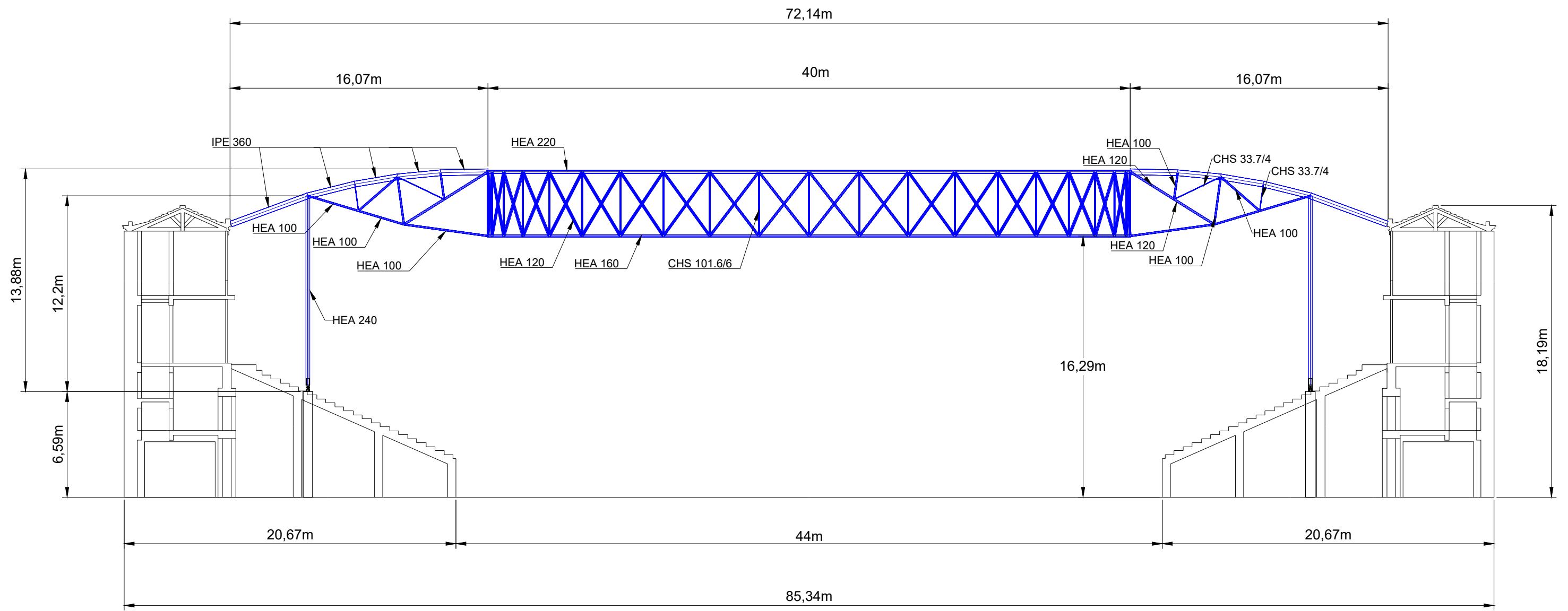
Now the structure has been checked in the position right after the lifting has started, with an high safety factor. Some members needed to be redesigned to accommodate this phase, those changes can be seen in Table 3.38.

Then the required jacking force to start and end the lifting was discovered, at the start:  $128.743\text{ kN}$  and at the end:  $34.969\text{ kN}$ .

On the next page there is an section drawing of the structure in the finished position, with the chosen steel design. More detailed drawing can be found in Appendix A.

Table 3.38: Changes to accommodate the lifting phase

Element	Section
Compression bars:	
4D2	HEA100 $\Rightarrow$ HEA120
4D3	HEA100 $\Rightarrow$ HEA120
Ring elements:	
Upper ring	HEA180 $\Rightarrow$ HEA220
Ring column	CHS 60.3/5 $\Rightarrow$ CHS 101.6/6.3



Sindre Jakobsen - Master thesis Alicante bullring roof		Fag	Format
		RIB	A3
Steel drawing Section A-A (two trusses)		Dato	06.06.2022
		Format/Målestokk:	1:250
University of Stavanger	Status	Konstr./Tegnet	Kontrollert
		Tegningsnr.	Godkjent
		3	

## 3.5 Design of connections

Now the structure has been subjected to three different scenarios and suitable cross sections which fit all scenarios have been assigned. Now there are two parts left of the steel design: the design of connections and adding additional capacity to members. The last part means adding a flange in the middle of a section to avoid buckling or LTB, or it could be to add bracing along the web (transverse stiffeners) to account for transverse forces and to avoid web buckling/bearing failure of the web. It is outside the scope to design these stiffeners, but the design of some critical connections will be attempted.

For the connection design, the most unfavourable scenarios are to be chosen, out of the three scenarios presented. The connections are crucial as they connect the members and transfer the load throughout the structure. Some of the connections will require rotation and some will not. Bolts, welds and pins will be used for the different connections. The literature used is the 1993-1-8 Eurocode [21], which describes the design of joints. Not every connection will be designed, instead, the critical joints will be looked at: joint 1, joint 5, joint 7 and joint 11.

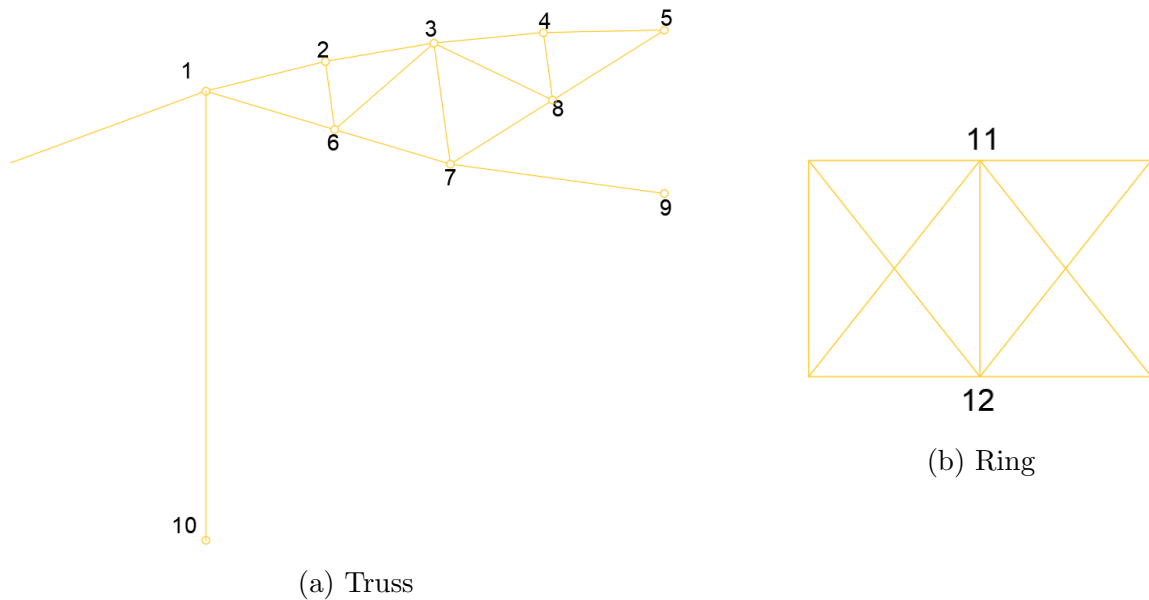


Figure 3.16: Assigned joint numbers

### 3.5.1 Joint 5

This joint is the connection between the ring and the curved beam (4B7 - 4BB), there is also a bar (4D3) connected to the beam 4B7 near this point. Both of the connections at this point are plate-pin connections. The beam will be connected by a pin, with welded plates connection the pin to the members. There will be two plates welded to the ring member and one plate welded to the beam (4B7). The plates welded to the ring member will require only half the thickness of the plate welded to the beam member.

Table 3.39: Forces in the members at joint 5, from the different phases

Joint 5	Axial	Shear	Moment
Finished			
4B7	144.42 kN (C)	20.06 kN	0 kN-m
4D3	2.51 kN (C)	0.26 kN	0.00 kN-m
Bottom			
4B7	17.77 kN (C)	0.436 kN	0.34 kN-m
4D3	2.338 kN (C)	0.25 kN	0.00 kN-m
Lifting			
4B7	70.043 kN (C)	2.686 kN	2.317 kN-m
4D3	193.63 kN (C)	0.407 kN	0.00 kN-m

The critical loading for this joint is shown in table 3.39.

As seen both the members are compression members, with some shear force in the beam(4B7). The connection between the ring and the beam will have to endure both the axial force from the beam and the bar. The scenario that cause the highest combined axial force is the lifting scenario, with an combined force of:  $70.043 \text{ kN} + 193.63 \text{ kN} = 263.674 \text{ kN}$ . There are three critical values when calculation the size of these plates:  $a$ ,  $c$  and the thickness,  $t$ . The thickness is chosen as  $12 \text{ mm}$ , the two other values can then be calculated by table 3.9 in EN 1993-1-8:

$$a \geq \frac{F_{Sd} \gamma_{M0}}{2t f_y} + \frac{2d_0}{3} \quad (3.3)$$

$$c \geq \frac{F_{Sd} \gamma_{M0}}{2t f_y} + \frac{d_0}{3} \quad (3.4)$$

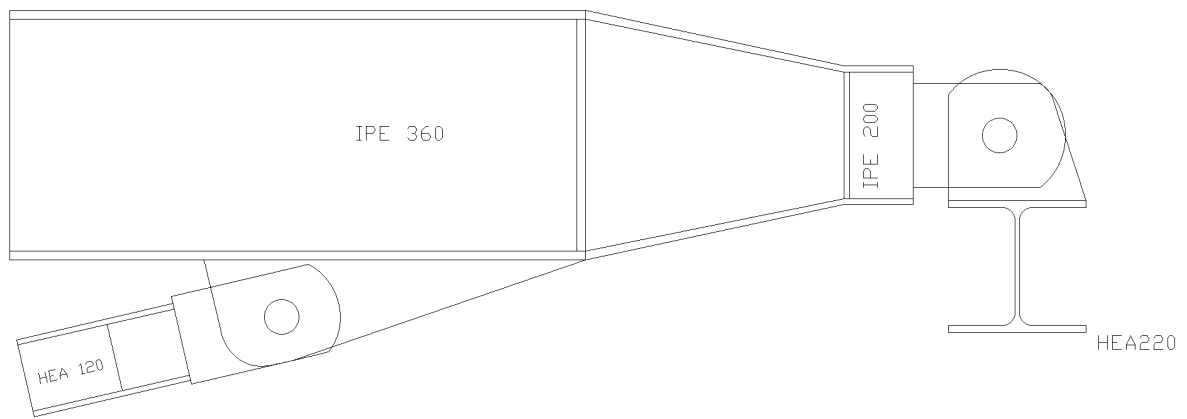
where:

- $F_{Sd}$  = the axial force in the member
- $d_0$  = the diameter of the pin hole

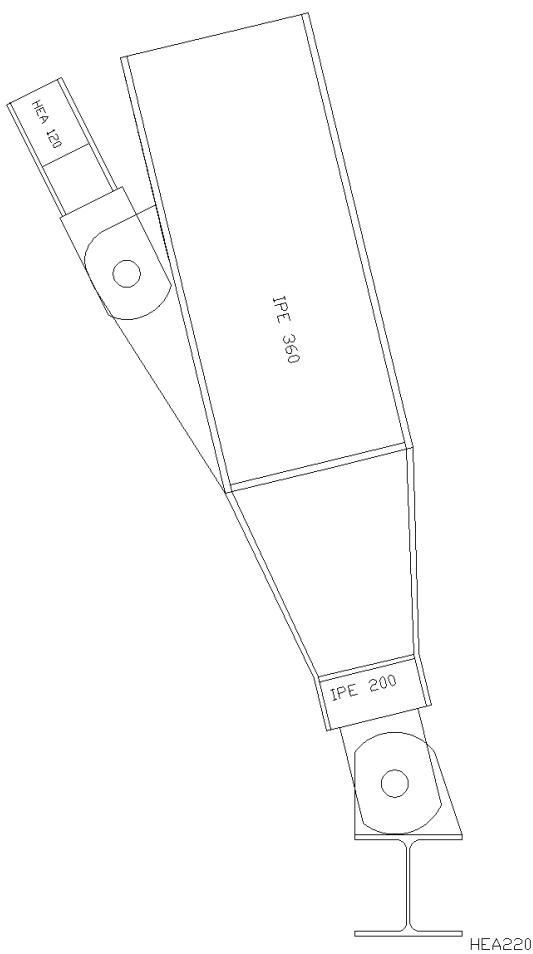
The plates need to welded to the members, weld capacity is given by the following formula [22]:

$$\sqrt{\sigma_{\perp}^2 + 3(\tau_{\perp}^2 + \tau_{\parallel}^2)} \leq \frac{f_u}{\gamma_{M2} \beta_w} \quad (3.5)$$

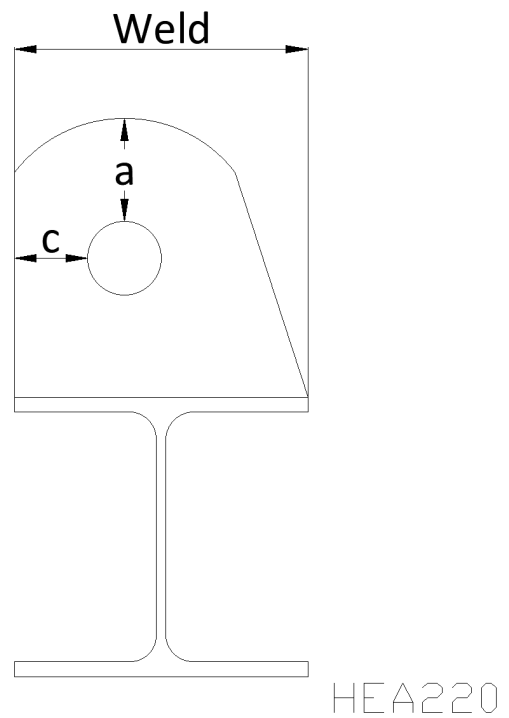
where  $\sigma$  and  $\tau$  is the stresses in the weld, depending on the load direction on the weld. In the bottom position the weld between the ring and the beam is in pure compression, but in the finished position this weld is in primarily shear with some compression force. The



(a) Finished position of members



(b) Members before lifting



(c) Plate on ring flange

Figure 3.17: Drawings of proposed connection design between 4B7, 4D3 and top ring

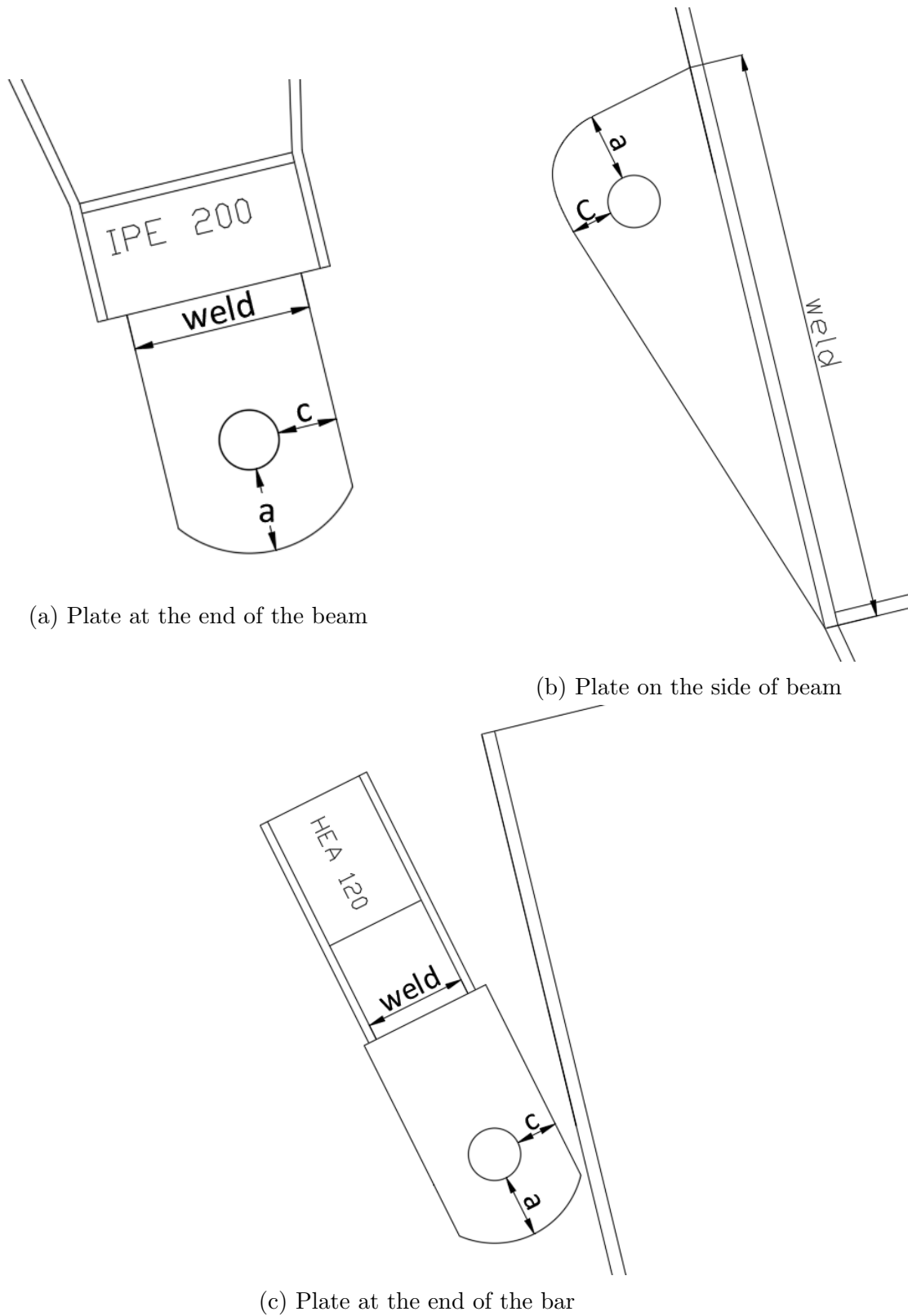


Figure 3.18: Drawings of proposed connection design between 4B7, 4D3 and top ring

weld connecting the plate to the bar is always in compression, and the weld connecting the plate to the beam flange is only subjected to shear force. Shear stress in a fillet weld is given by [22]:

$$\tau_{\parallel} = \frac{F_n}{L \cdot a} \quad (3.6)$$

and stress from an normal force is given by:

$$\sigma_{\perp} = \tau_{\perp} = \frac{F_s}{\sqrt{2} \cdot L \cdot a} \quad (3.7)$$

where:

- $F_n$  = half the axial force
- $F_s$  = half the shear force
- $L$  = weld length
- $a$  = effective throat size
- $\beta_w$  = correlation factor
- $f_u$  = breaking strength of the steel
- $\gamma_{M2}$  = safety factor

With an trial throat size of 8 mm the weld length can be calculated. The dimensions a, c (for the plates) and weld length is given in Table 3.40.

Table 3.40: Minimum dimensions, for joint 5

Joint 5	a	c	weld length, L
4D3 - 4B7	41.66 mm	25.00 mm	26.69 mm
4B7 - upper ring			
- lifting phase	64.28 mm	47.61 mm	62.80 mm
- final phase	50.587 mm	33.92 mm	34.79 mm

The values in Table 3.40 are the minimum length for respective dimensions. The highest lengths from the table, between the lifting phase and final phase are chosen. All the calculated values are within the dimension of the connection member so there is no need to extend the connections to accommodate a large weld length.

The pin can also be subjected to failure. Shear resistance, bearing resistance and moment resistance have to be checked. These values are given by Table 3.10 in EN 1993-1-8 [21]:

$$F_{v,Rd} = 0.6 A d f_{up} / \gamma_{M2} \geq F_{v,Ed} \quad (3.8)$$



$$F_{b,Rd} = 1.5 t d f_y / \gamma_{M0} \geq F_{b,Ed} \quad (3.9)$$

$$M_{Rd} = 1.5 W_{el} f_{up} / \gamma_{M0} \geq M_{Ed} \quad (3.10)$$

where:

- $d$  = diameter of the pin
- $f_y$  = lower of the design strengths of the pin and the connected part
- $f_{up}$  = ultimate tensile strength of the pin
- $f_{yp}$  = the yield strength of the pin
- $t$  = thickness of the connected part
- $A$  = cross-sectional area of a pin

A trial diameter of 50 mm was chosen for the pin. The steel is S355 with an ultimate tensile strength of 470 MPa to 630 MPa [23], where  $f_{up}$  is chosen to be 470 MPa. The capacity provided is then:

$$F_{v,Rd} = 0.6 A d f_{up} / \gamma_{M2} = 442.95 \text{ kN} \quad (3.11)$$

$$F_{b,Rd} = 1.5 t d f_y / \gamma_{M0} = 319.5 \text{ kN} \quad (3.12)$$

The elastic section modulus for a circular solid section, like this pin, is given by [22]:

$$W_{el} = \frac{I}{y} = \frac{\pi d^3}{32} = 12271.84 \text{ mm}^3 \quad (3.13)$$

Moment capacity is then:

$$M_{Rd} = 1.5 W_{el} f_{up} / \gamma_{M0} = 8651.62 \text{ kN-mm} \quad (3.14)$$

The design bearing force on the pin is simply the axial force, and the shear force is half the axial force. The design moment in the pin is given by:

$$M_{Ed} = \frac{F_{Ed}}{8} (b + 4c + 2a) = 1452 \text{ kN-mm} \quad (3.15)$$

$a$  is the thickness, 6 mm, of the two plates connected to member 4B7.  $b$  is the thickness of the single plate connected to the ring member, 12 mm.  $c$  is the distance between opposite plates. There is no need for a distance between these plates, but a little distance is realistic, 5 mm should suffice (more conservative).

$$F_{v,Rd} = 442.95 \text{ kN} \geq F_{v,Ed} = 263.67 \text{ kN} \rightarrow \text{OK} \quad (3.16)$$

$$F_{b,Rd} = 319.5 \text{ kN} \geq F_{b,Ed} = 131.83 \text{ kN} \rightarrow \text{OK} \quad (3.17)$$

$$M_{Rd} = 8651.62 \text{ kN-mm} \geq M_{Ed} = 1452 \text{ kN-mm} \rightarrow \text{OK} \quad (3.18)$$

### 3.5.2 Joint 11/12

Joint 11 and 12 are similar joints, with the same forces - since the three members connecting the the two joints are all bar members. The members that connect at this joint is the ring column, that connects the upper and lower ring, and the stiffeners, that connect the corners of the ring structure.

A plate will be welded to the bottom of the upper ring member, this plate is connected to another plate with bolts, the second plate is welded to circular ring column, extending down the member as far as the weld need to be.

Table 3.41: Forces in the members at joint 11/12, from the different phases

Joint 5	Axial	Shear	Moment
Finished			
Ring column	76.477 kN (C)	0.00 kN	0.00 kN-m
Ring stiffeners	41.557 kN (T)	0.11 kN	0.8 kN-m
Bottom			
Ring column	4.843 kN (C)	0.00 kN	0 kN-m
Ring stiffeners	11.83 kN (C)	0.352 kN	0.3 kN-m
Lifting			
Ring column	79.523 kN (C)	0.1 kN	0.37 kN-m
Ring stiffeners	92.412 kN (C)	0.345 kN	0.409 kN-m

As the table shows these are both axial force dominated members. The ring stiffeners changes between being in tension and compression, where the compression load is the most critical. The ring column is always in compression with the lifting phase providing the critical load.  $F_{Ed}$  for the column is then 79.523 kN and 92.412 kN for the ring stiffeners

The bolts is in the design category A: Bearing type. The bolts used is of class 8.8 and will be solely subjected to shear. The amount of bolts required is the determining factor for the size of the plate. The shear capacity through the threaded part of an 8.8 bolt is given by the formula [22] :

$$F_{d,v}^* = \frac{0.6 f_{u,b} A_s}{1.25} \quad (3.19)$$

A single bolt of size M16 has a shear capacity of 60.3 kN [22], so two bolts of this size is enough for both the members. Regardless of the unused capacity a minimum of four bolts is used. This bolt will require the following spacing [21]:

- End distance  $e_1 = 1.2 d_0 = 1.2 \cdot 16 = 19.2 \text{ mm}$
- Edge distance  $e_2 = 1.2 d_0 = 1.2 \cdot 16 = 19.2 \text{ mm}$

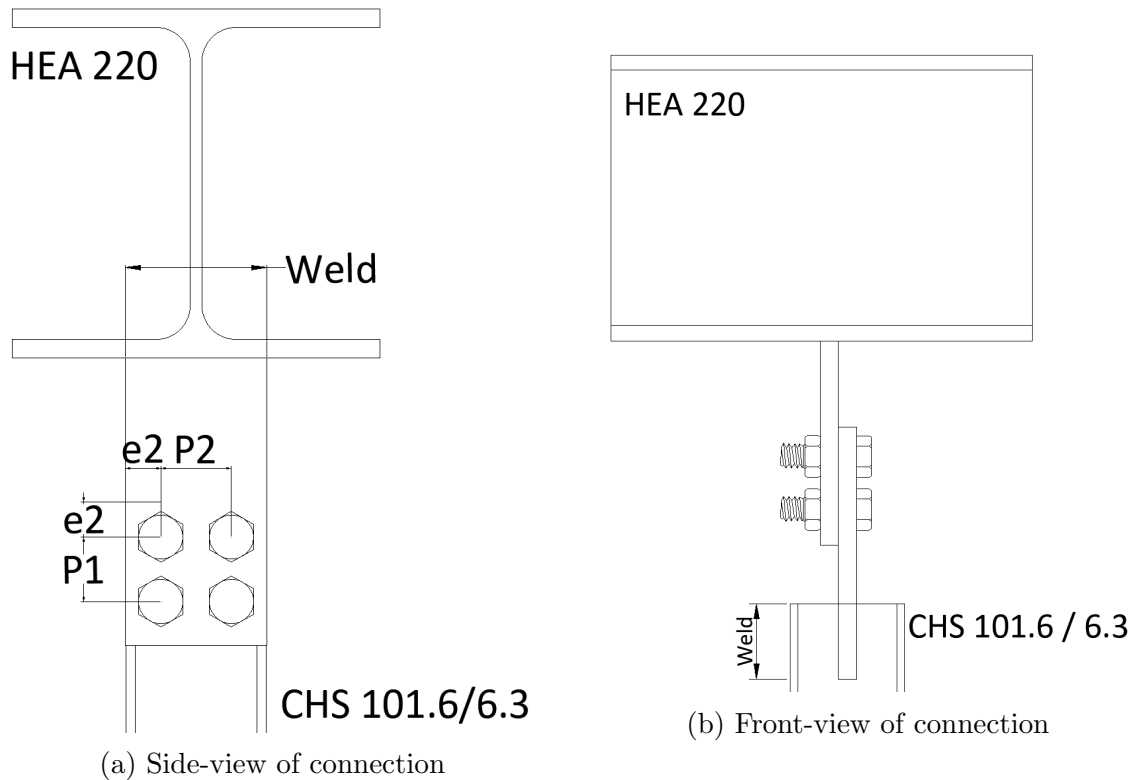


Figure 3.19: Drawings of proposed connection design between top ring member and ring column

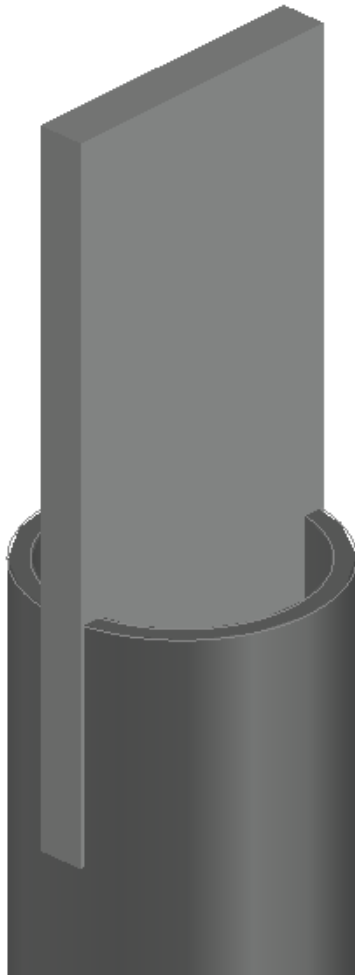
- Spacing  $p_1 = 2.2 d_0 = 2.2 \cdot 16 = 35.2 \text{ mm}$
- Spacing  $p_2 = 2.4 d_0 = 2.4 \cdot 16 = 38.4 \text{ mm}$

With this spacing the plate will have a minimum width of  $76.8 \text{ mm}$ . Choosing a thickness of  $12 \text{ mm}$  gives the plate an axial load capacity of  $76.8 \text{ mm} \cdot 12 \text{ mm} \cdot 355 \text{ N/mm} = 327.2 \text{ kN}$ , which is enough for both connections. Removing the area that the bolt hole occupies, since there is a tension load, provides a axial load capacity of  $190.84 \text{ kN}$ , which is still enough for both connections.

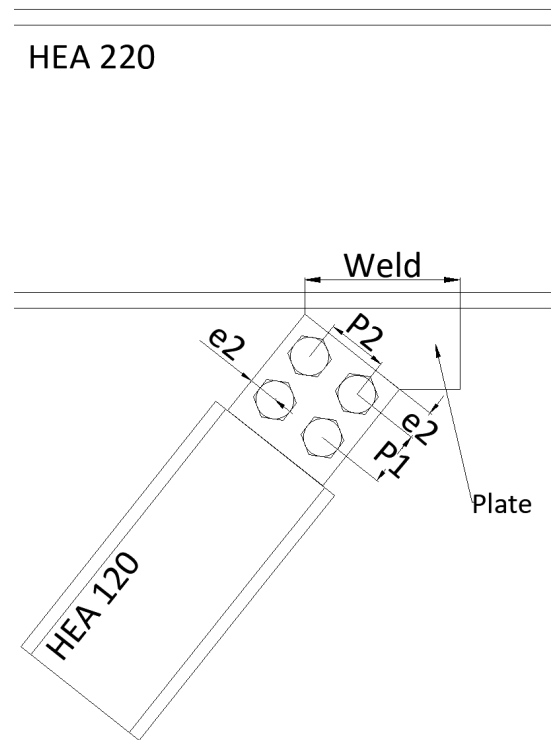
Using the highest axial load from table, the weld length is calculated to be  $22.06 \text{ mm}$ , which is less than the recommended weld length for load carrying weld. The effective length should not be less than  $30 \text{ mm}$  or six times the throat thickness [21]. With an throat thickness of  $8 \text{ mm}$ , the minimum length is  $48 \text{ mm}$ . This length will be the minimum for the welds in the two connections.

The plate that connects the bolts to the ring column extends down into a cut in the circular section, as far as the weld length need to be. Since the plate will be able to be welded on two sides the weld length can be reduced, but since the calculated weld length is under the minimum, the weld still needs to be above the minimum. An extension of  $50 \text{ mm}$  will suffice.

The stiffeners are connected to the ring with similar plates and bolts as the column.



(a) Extension of plate in ring circular section, column



(b) Connection between ring stiffener and top ring member

The plate is rotated to the same orientation as the member, and the plate is extended such that there is a part that is parallel to the top ring member, and can be welded here. The joint is mirrored for the stiffener in the opposite direction.

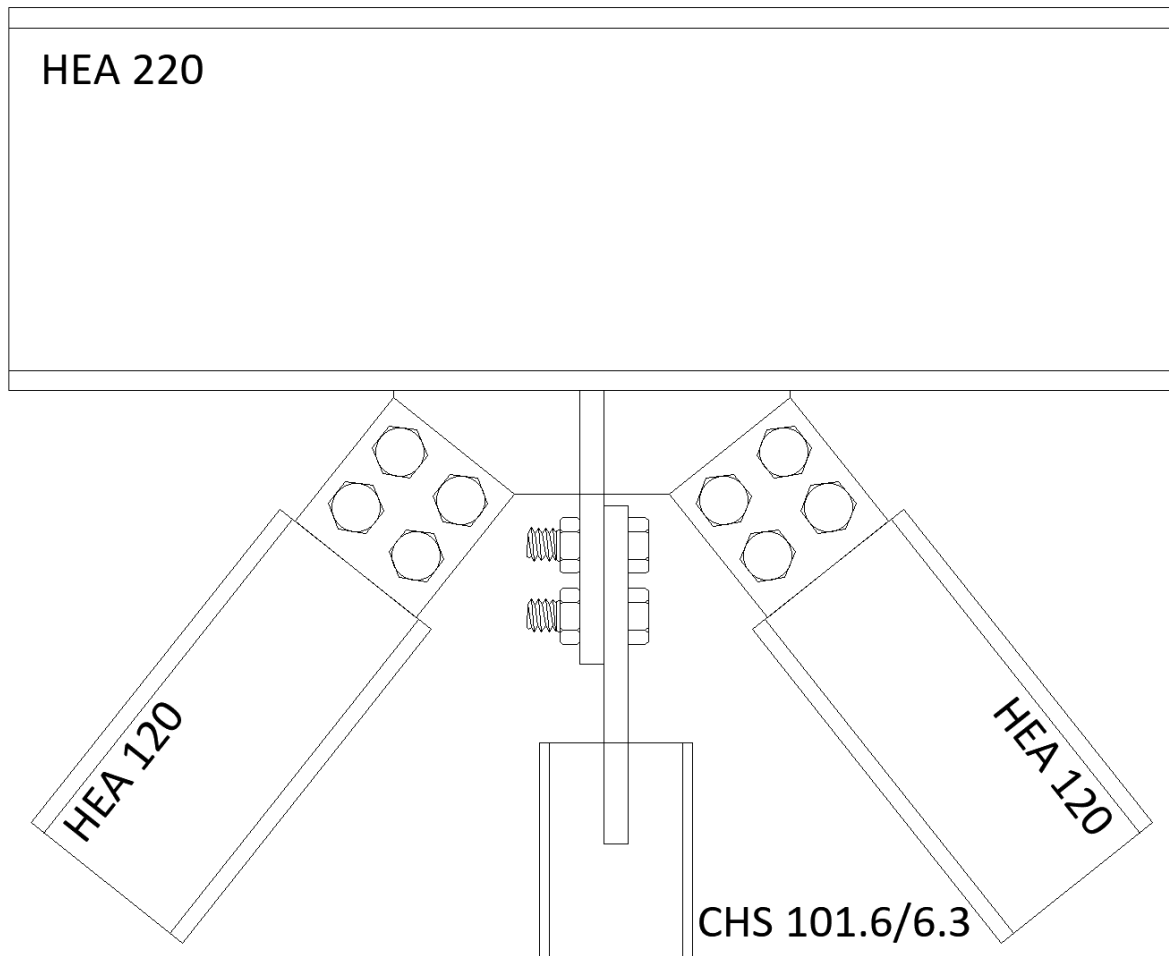


Figure 3.21: Illustration of entire joint 11

### 3.5.3 Joint 7

Joint 7 is an pin-plate connection such as joint 5. The joint connects four members: 4D1, 378, 4D2 and 385/cable with a single pin. This is the joint that the jacks will pull/rotate to lift the structure, so this is be a critical joint.

Table 3.42: Forces in the members at joint 7, from the different phases

Joint 7	Axial		Axial	
Finished			Bottom	
4D1	139.295 <i>kN</i> (T)		4D1	0.4 <i>kN</i> (C)
378	7.98 <i>kN</i> (C)		378	0.947 <i>kN</i> (C)
4D2	18.47 <i>kN</i> (C)		4D2	1.46 <i>kN</i> (C)
385/Cable	149.68 <i>kN</i> (T)		385/Cable	N/A
Lifting				
4D1	128.12 <i>kN</i> (T)			
378	3.12 <i>kN</i> (C)			
4D2	261.98 <i>kN</i> (C)			
385/Cable	354.47 <i>kN</i> (T)			

As shown in table 3.42, most of the critical forces occur in the lifting phase except for the tension in member 4D1, which is highest when the structure is in the finished state. The weld length, and the plate dimensions:  $a$  and  $c$ , is calculated using the same approach as in joint 5. A thickness of 10 *mm* is used for the plate accompanying member 385, with a thickness of 8 *mm* for the rest. Weld throat thickness is 0.75 times the thickness of the plate. The pin is 118 *mm* long and has a diameter of 50 *mm*. A 5 *mm* spacing between the plates on the pin is used.

Table 3.43: Minimum dimensions for joint 7

Joint 7	$a$	$c$	weld length, L
4D1	45.59 <i>mm</i>	28.92 <i>mm</i>	22.17 <i>mm</i>
378	34.03 <i>mm</i>	17.36 <i>mm</i>	1.27 <i>mm</i>
4D2	56.39 <i>mm</i>	39.72 <i>mm</i>	41.7 <i>mm</i>
385/Cable	58.29 <i>mm</i>	41.62 <i>mm</i>	45.14 <i>mm</i>

Using 60 *mm* for both  $a$  and  $c$  produces a circular plate with an rectangular part that attaches to the section, which is used for all the members in this connection. The plate extends 60 *mm* into the section and is welded with welds parallel to the direction of the section. The plate that connects to member 378 to the pin are a single plate of double the thickness of the other plates, 16 *mm*, and is positioned in the middle. Member 378/cable need to first be able to connect the cables to the joint, and then switch to the steel section. Figure 3.23 shows a plate with three holes where the cables can be connected. When the ring/truss is in the final position, the cables can be removed and the steel member (HEA100) can be installed.

Using the max axial force to check the pin for shear, which is the force in member 378

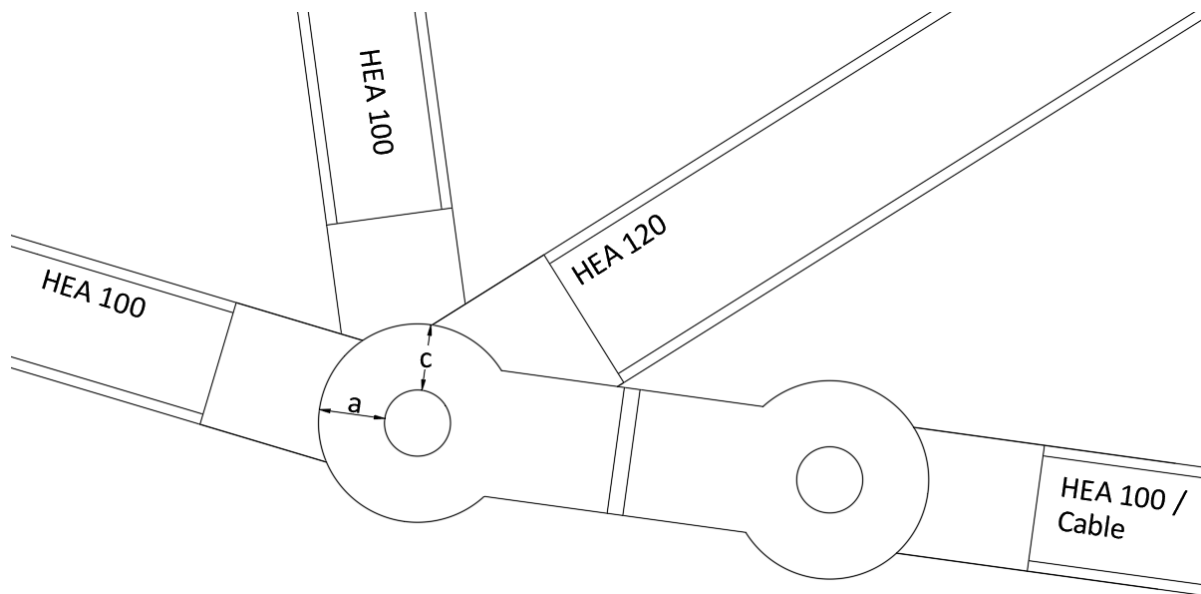


Figure 3.22: Illustration of the entire joint, with  $a$  and  $c$  dimensions

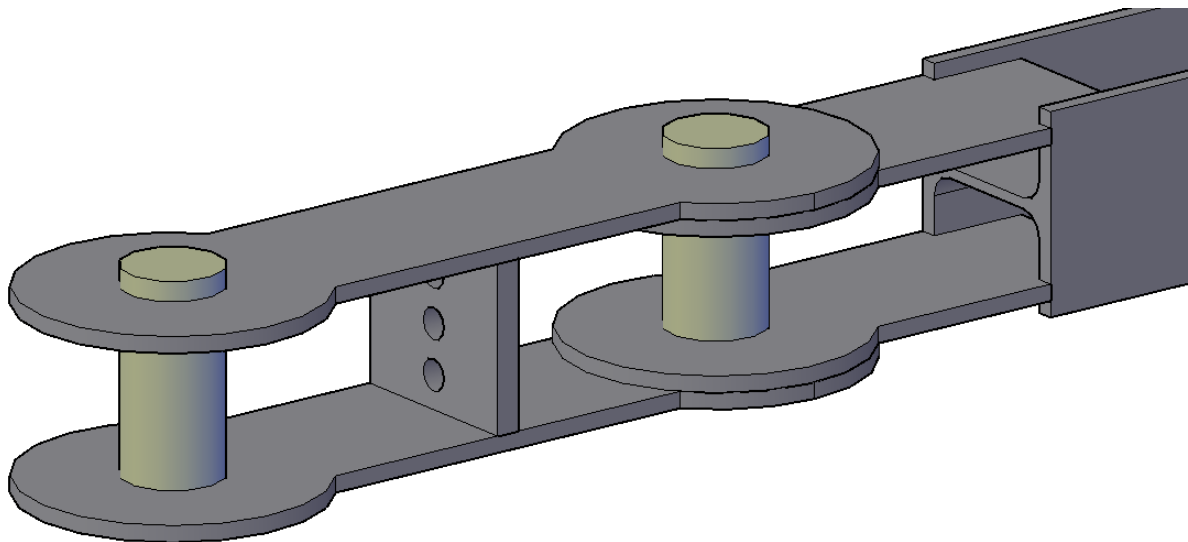


Figure 3.23: Member 385 with connection for the cables

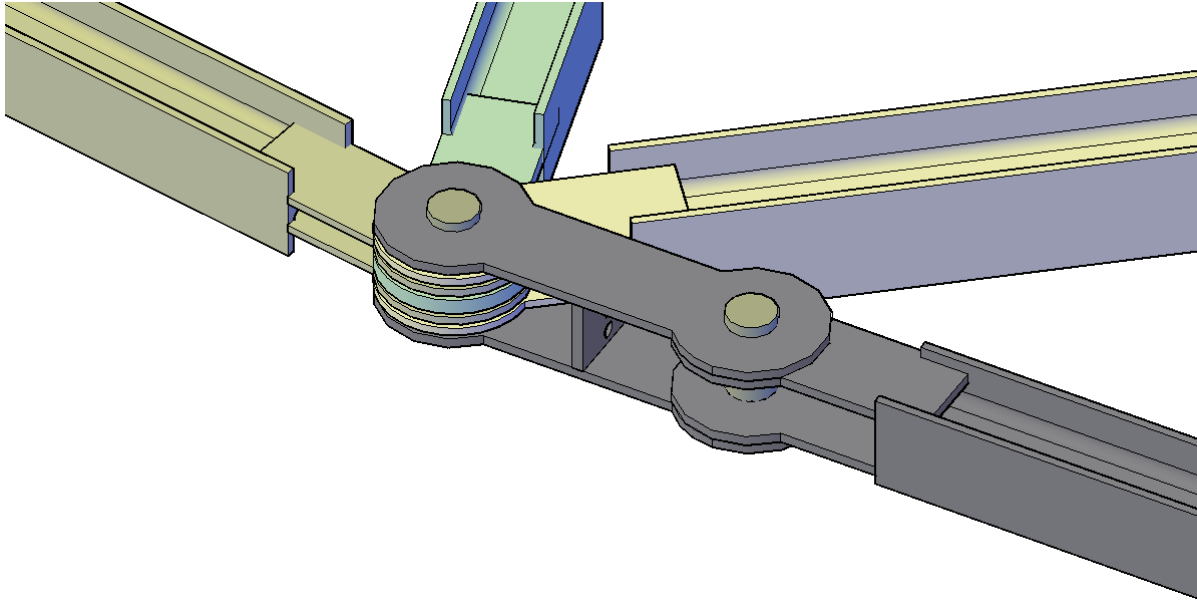


Figure 3.24: Illustration of the entire joint 7

and checking member 378 and 385 for bearing failure (since the plate thickness differ from the two).

$$F_{v,Rd} = 0.6 A d f_{up} / \gamma_{M2} = 442.95 \text{ kN} \quad (3.20)$$

$$F_{b,Rd,4D2} = 1.5 t d f_y / \gamma_{M0} = 426 \text{ kN} \quad (3.21)$$

$$F_{b,Rd,385} = 1.5 t d f_y / \gamma_{M0} = 532.5 \text{ kN} \quad (3.22)$$

$$M_{Rd} = 1.5 W_{el} f_{up} / \gamma_{M0} = 8.65 \text{ kN-m} \quad (3.23)$$

The design bearing force on the pin is simply the axial force, and the shear force is half the axial force. The most critical moment is obtained by only taking member 378 and member 385 into account.  $a$  is then  $10 \text{ mm}$ ,  $b$  is  $16 \text{ mm}$  and  $c$  is  $31 \text{ mm}$ . The design bending moment in the pin is then:

$$M_{Ed} = \frac{F_{Ed}}{8} (b + 4c + 2a) = 7089.4 \text{ kN-mm} \quad (3.24)$$

Comparing the design force with the design capacity:

$$F_{v,Rd} = 442.95 \text{ kN} \geq F_{v,Ed} = 177.23 \text{ kN} \rightarrow \text{OK} \quad (3.25)$$

$$F_{b,Rd,4D2} = 426 \text{ kN} \geq F_{b,Ed} = 261.98 \text{ kN} \rightarrow \text{OK} \quad (3.26)$$

$$F_{b,Rd,385} = 532.5 \text{ kN} \geq F_{b,Ed} = 354.47 \text{ kN} \rightarrow \text{OK} \quad (3.27)$$

$$M_{Rd} = 8.65 \text{ kN-m} \geq M_{Ed} = 7.08 \text{ kN-m} \rightarrow \text{OK} \quad (3.28)$$

All the trial dimensions are okay!



Table 3.44: Forces in the members at joint 1, from the different phases

Joint 7	Axial		Axial	
Finished			Bottom	
48B	214.94 kN (C)	48B	11.78 kN (C)	
Lifting				
48B	86.59 kN (C)			

Table 3.45: Minimum dimensions for joint 1

Joint 1	<i>a</i>	<i>c</i>	weld length(shear)	weld length (axial)
4D8	52.25 mm	35.58 mm	34.21 mm	27.93 mm

### 3.5.4 Joint 1

Joint 1 is also an pin-plate joint, like joint 5 and 7. This joint connects the primary column - member 4D8 - to the beam members 4BA/4BB. A single plate will be connected to the column, and two plates connected to the underside of the beam. The single plate will have a thickness of 16 mm and the two plates will have a thickness of 8 mm. Using 0.75 times the thickness of the plate as weld throat thickness.

The pin has a diameter of 50 mm and has the same capacity as the pin in the previous joint:

$$F_{v,Rd} = 0.6 A d f_{up} / \gamma_{M2} = 442.95 \text{ kN} \quad (3.29)$$

$$F_{b,Rd} = 1.5 t d f_y / \gamma_{M0} = 426 \text{ kN} \quad (3.30)$$

$$M_{Rd} = 1.5 W_{el} f_{up} / \gamma_{M0} = 8.65 \text{ kN-m} \quad (3.31)$$

The design bearing force on the pin is simply the axial force, and the shear force is half the axial force. The values for calculating the moment in the pin: *a* is 8 mm, *b* is 16 mm and *c* is 5 mm,

$$M_{Ed} = \frac{F_{Ed}}{8} (b + 4c + 2a) = 1.39 \text{ kN-m} \quad (3.32)$$

Comparing the design force with the design capacity:

$$F_{v,Rd} = 442.95 \text{ kN} \geq F_{v,Ed} = 177.23 \text{ kN} \rightarrow \text{OK} \quad (3.33)$$

$$F_{b,Rd,AD2} = 426 \text{ kN} \geq F_{b,Ed} = 261.98 \text{ kN} \rightarrow \text{OK} \quad (3.34)$$

$$F_{b,Rd,385} = 532.5 \text{ kN} \geq F_{b,Ed} = 354.47 \text{ kN} \rightarrow \text{OK} \quad (3.35)$$

$$M_{Rd} = 8.65 \text{ kN-m} \geq M_{Ed} = 1.39 \text{ kN-m} \rightarrow \text{OK} \quad (3.36)$$

All the trial dimensions are okay!

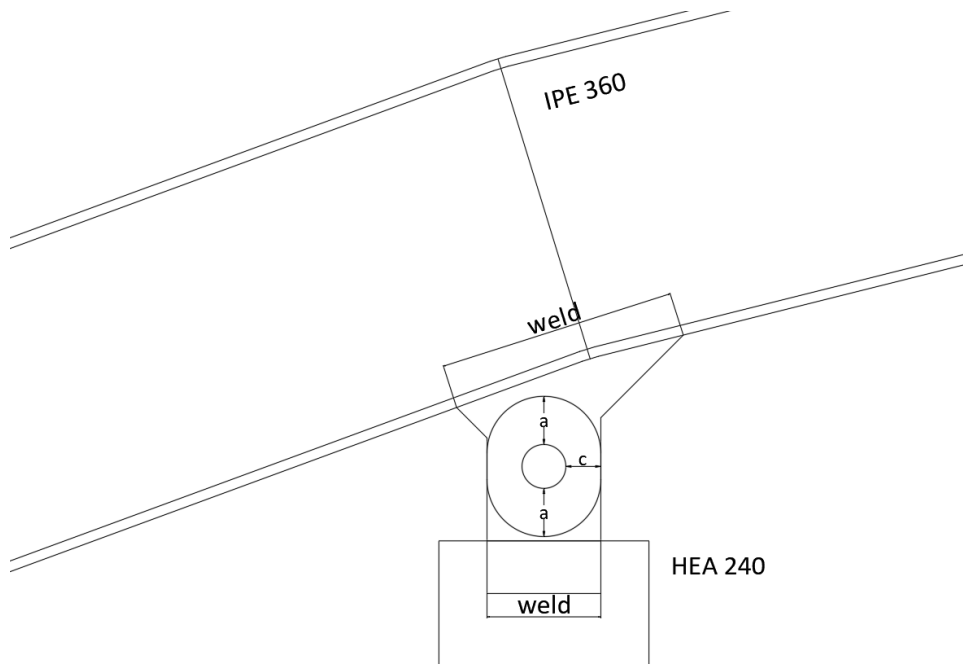
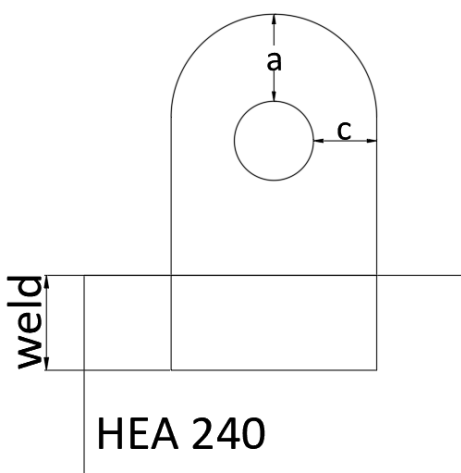
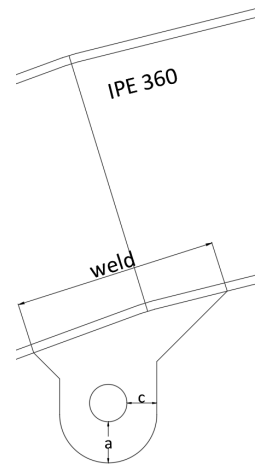


Figure 3.25: Illustration of the entire joint 1



(a) Plate welded to column



(b) Plate on the underside of beam

Figure 3.26: Drawings of proposed connection design between 4B7, 4D3 and top ring

# Chapter 4

## Discussion

### 4.1 Geometry

Three structural analysis has been conducted and suitable steel sections that suit all the phase have been chosen. Some details on the structure have been designed and calculated. The plausibility of the structure and the construction has been challenged and solutions have been presented.

Working with such an old structure provided some challenges, as the drawings were old and without accurate dimensions. The key dimensions of the old structure were measured, and different roof solutions were sketched. Decisions about the size and shape of the roof had to be made early so that the thesis could progress forwards, that is why some dimensions were arbitrarily chosen. That is the nature of every project I presume, not everything can be scientific, and decisions may be made on experience alone.

Some of the dimensions and orientations could have been different, and it might have been beneficial to compare e.g. different truss shapes, the curvature of the roof or the number of trusses around the ring, but what was thought to be the best decision was always chosen. If this was a real project more research could be made to find a comparable or better shape of the truss/roof.

Drawing and modelling in Autocad were great, as the drawing tools are numerous and helpful. One could easily make changes to a model and producing the three models was trouble-free, in contrast to the drawing tools in analysis software which often are time-consuming and tedious to use. Being able to effortlessly export the Autocad models to SAP2000 was a solace.

### 4.2 Analysis

The analysis was the most time-consuming part of the thesis. The models had to go through multiple iterations before the current designs were reached. The analysis models could then produce the desired result: element forces. Using these forces a suitable steel design was reached and using the forces near the joints, some connections could be

designed. Had the scope permitted it all the connections would have had a design proposed, but some key connections were nevertheless designed.

The design proposed in this thesis is done to the best ability with the resources available, but if this was to be built, a deeper analysis would be recommended. Parts that would have to be examined close would be all connections, bracing/stiffeners, ground conditions, support foundation, accidental situations/loading from the accidental situation and a more thorough environmental loading analysis. More models could be made at different stages of the lifting i.e with an interval of 20% and five models or with a smaller interval and more models, to get a deeper understanding of the lifting process.

The jacks also don't pull with a constant force throughout the lifting, instead, it pulls in strokes of 160 *mm* to 550 *mm* [20]. The cable in this thesis starts with a length of 9.4 meters and is reduced to a length of 5.2 meters with a shortening of 4.2 meters, it would therefore require a minimum of 8 strokes to a maximum of 27 strokes, depending on the stroke length used. As the lifting should be as smooth as possible operation, using a short stroke length and more strokes is preferable. In the Detailing and Constructions of Xàtiva [8] they used 39 strokes and a measured cable shortening of 5.374 meters, with an average shortening of 0.137 meters per stroke. More information should (ideally provided by the producers of the jacks) be gathered about jacks and their limitations. A rough plan of how many strokes and the shortening of the cable at the strokes should be made.

The jacking force was also measured in Xàtiva [1]: starting at 262.5 *kN* and ending with 136.60 *kN*, at no point increasing: always decreasing between strokes. The force is not decreasing linearly, but rather more rapidly at the start and slower at the end of the lifting; a formula (equation 4.1) that tries to predict the jacking force is made, which correlates quite well.

$$T = \frac{2bd}{h(c \sin\beta - b \cos\beta)} ((W_n + W_m) \cdot \sin\alpha \tan\beta + W_m \cos\beta) \quad (4.1)$$

This information is crucial when planning what jacking force to use. There are two ways this information could have been found for the structure in this thesis: more models at the different stages of the lifting (time-consuming) or constructing a similar formula to predict the jacking force. A function of the tension force in the cable with regards to the angle of a member or the position of a joint could have been made. The Xàtiva detailing paper uses a method of virtual work to derive this function, where the weight of the structure was applied at two hinges (the equivalent of this thesis hinge 2 and 3). The method of joints could also be used, but since the self-weight of all the members has to be accounted for the expression would be quite lengthy. This was ultimately outside of the scope of the thesis.

### 4.3 Xàtiva roof

A comparison of the roof structure in this thesis and the roof in Xàtiva can not easily be made, as only general dimensions are given about the Xàtiva roof, but some can be

made. Comparing the inner ring: Xàtiva roof has a diameter of 42 meters, while the thesis roof has a ring diameter of 44 meters, so a little larger span. The other ring of the Xàtiva roof is 102 meters, but the thesis roof is only 72 meters. The Xàtiva roof is larger and covers a larger seating area, as appose to the thesis roof which can't span longer because of the old roof at the outer edge of the Alicante structure. The difference in outer diameter is probably why the Xàtiva structure is heavier with a weight of  $4200\text{ kN}$  ( $428280.72\text{ kg}$ ), as appose to the weight of the structure in this thesis which is  $1409\text{ kN}$ . Although the Xàtiva roof is most likely not designed to carry a high snow load, a heavier design was chosen. HEB600 members are used for the ring in Xàtiva, here HEA220 are used. The curved beam is in Xàtiva a 500 mm deep double T curved beam, whereas in this thesis a curved IPE 360 is used. The difference in sections chosen is again probably from the increased capacity required for a longer span.

The truss has the same shape because the effort required to test the suitability of different truss shapes, that is suitable for the self-raising process, was not justified. There was a possibility that a design that when analysed would fail but changing the cross-sections of members would increase the self-weight and again make the same member (or other members) fail, resulting in a vicious cycle of increasing capacity but also increasing the load. This almost happen to the ring column, but a suitable member was found. When using high safety factors and lengthy spans there is a possibility of this happening.

## 4.4 Conclusion

The thesis aimed to explore the Pantadome system and the possibility of the modified Pantadome system used in Xàtiva to be used in a location in Norway. Now the roof was designed for a structure in Alicante because that structure was similar to the structure in Xàtiva and also had drawings available, but the roof system and design can be changed to suit the building in Norway. The important part is the knowledge gained about the self-raising system and procedure.

The theory behind the self-raising system is quite brilliant and so was the idea of using post-tension jacks to facilitate the lifting. Reading the paper from Mukogawa Women's University [9], provided great insight into the mechanics of the different versions of the system and the models shown in the paper were intriguing. These papers were the main motivation behind starting this research.

A suitable geometry, design of steel elements and design of connections was found, though a deeper analysis could be done. When starting the thesis the challenges that awaited were not clear, so it was difficult to allocate time and resources, but the results produced are satisfactory. It has been shown that a design for the use of the self-lifting system can be found using digital analysis tools and that equating a post-tension force with a temperate loading to find the jacking force, can be of value.

This paper intends to expand the knowledge about the self-raising lifting system and motivate further research. This thesis can be used as a starting point for more specified research regarding a structure like this.

### 4.4.1 Forward research

Additional research on the Pantadome system could continue in multiple directions. Not many papers were found when researching the system, so there are ample research directions one could pursue.

The system could be tried theoretically on existing structures, built with more traditional methods, to see if the structure could be built using the pantadome system. Doing this can map out what types of structure fits the system and what does not. Now the system has been used on structures that are circular or oval shaped (or closely similar to these shapes), maybe the system can be suitable for other shapes: a square or a half-circle, with some modifications.

Another direction for research is comparing the Pantadome system and traditional construction methods with regards to construction time and cost, on simple structure which can be a theoretical structure or real. Looking at differences in time and cost could provide information about the commercial use of the pantadome system. The system might only have a use for extreme structure (where cost and time are not the main limitations), or it might have a more wide-spread commercial use.

Research could be done on the system it self, the system did not use jacks in the first iteration: the system was changed to the self-raising system with jacks. Maybe the the jacks could be replaced with something else, there might be a more elegant self-raising method to be discovered. The paper from Mukogawa Women's University [9] explains some different versions of the system, one with an electric motor and a spool winding in a wire, maybe this could be designed on a larger scale.

# Bibliography

- [1] C. Lázaro, A. Domingo, M. Kawaguchi, A. Candenás, and F. Palacios, *Renovation of the bullring arena of Xàtiva (Spain)*. Mar. 2015.
- [2] K. Mamoru, “Application of Pantadome system to long-span roof structures,” en, 1994. DOI: 10.5169/SEALS-54125. [Online]. Available: <https://www.e-periodica.ch/digbib/view?pid=bse-re-003:1994:71::112> (visited on 05/30/2022).
- [3] *Plaza de toros de Alicante*, en, Jan. 2022. [Online]. Available: [https://es.wikipedia.org/w/index.php?title=Plaza\\_de\\_toros\\_de\\_Alicante&oldid=140741065](https://es.wikipedia.org/w/index.php?title=Plaza_de_toros_de_Alicante&oldid=140741065) (visited on 05/19/2022).
- [4] *Google Maps*, en-NO. [Online]. Available: <https://www.google.com/maps/@38.3525915,-0.4844371,110m/data=!3m1!1e3> (visited on 06/11/2022).
- [5] *Plaza de Toros y Museo Taurino de Alicante*. [Online]. Available: [https://lh3.googleusercontent.com/p/AF1QipNmA9btjqjUGs11M7Rg0\\_n0zZfilQyE\\_A9GMoSQ=s1600-w1600](https://lh3.googleusercontent.com/p/AF1QipNmA9btjqjUGs11M7Rg0_n0zZfilQyE_A9GMoSQ=s1600-w1600) (visited on 06/11/2022).
- [6] *La Audiencia Provincial confirma la absolución del arquitecto de Xàtiva en el caso de la plaza de toros*, es, Section: ribera-costera, Feb. 2020. [Online]. Available: <https://www.lasprovincias.es/ribera-costera/audiencia-provincial-confirma-20200214233017-ntvo.html> (visited on 06/11/2022).
- [7] *Båndtekkning*, nb-NO, Figur kuppelhallen. [Online]. Available: <https://lieblikk.no/tak/bandtekkning/> (visited on 05/20/2022).
- [8] C. Lázaro and A. Domingo, “Detailing and Construction of the *Pantadome* Roof Structure for a Bullring in Xàtiva (Spain),” en, *International Journal of Space Structures*, vol. 25, no. 4, pp. 229–241, Dec. 2010, ISSN: 0956-0599, 2059-8033. DOI: 10.1260/0266-3511.25.4.229. [Online]. Available: <http://journals.sagepub.com/doi/10.1260/0266-3511.25.4.229> (visited on 05/30/2022).
- [9] H. Tagawa, Y. Tazaki, K. Yanagisawa, S. Okazaki, and M. Kawaguchi, *Design and Fabrication of Modern Ger utilizing Pantadome Systems in Architectural Design Class*. Sep. 2016. [Online]. Available: [https://www.researchgate.net/publication/330442280\\_Design\\_and\\_Fabrication\\_of\\_Modern\\_Ger\\_utilizing\\_Pantadome\\_Systems\\_in\\_Architectural\\_Design\\_Class](https://www.researchgate.net/publication/330442280_Design_and_Fabrication_of_Modern_Ger_utilizing_Pantadome_Systems_in_Architectural_Design_Class) (visited on 06/13/2022).

- [10] *Waddell "A" Truss Bridge*, en, Page Version ID: 1064577605, Jan. 2022. [Online]. Available: [https://en.wikipedia.org/w/index.php?title=Waddell\\_%22A%22\\_Truss\\_Bridge&oldid=1064577605](https://en.wikipedia.org/w/index.php?title=Waddell_%22A%22_Truss_Bridge&oldid=1064577605) (visited on 05/21/2022).
- [11] "Eurocode 1: Actions on structures - Part 1-3: General actions - Snow loads," European Committee for Standardization (CEN), Tech. Rep. NS-EN 1991-1-3: 2003 + A1: 2015 + NA: 2018. [Online]. Available: <https://www.standard.no/no/Nettbutikk/produktkatalogen/Produktpresentasjon/?ProductID=1004200> (visited on 06/11/2022).
- [12] "Eurocode 1: Actions on structures - Part 1-4: General actions - Wind actions," European Committee for Standardization (CEN), Tech. Rep. NS-EN 1991-1-4: 2005/NA: 2009. [Online]. Available: <https://www.standard.no/no/Nettbutikk/produktkatalogen/Produktpresentasjon/?ProductID=392208> (visited on 06/11/2022).
- [13] "Eurocode 1: Actions on structures - Part-1-1: General actions - Densities, self-weight, imposed loads for building," European Committee for Standardization (CEN), Tech. Rep. NS-EN 1991-1-1: 2002 + NA: 2019. [Online]. Available: <https://www.standard.no/no/Nettbutikk/produktkatalogen/Produktpresentasjon/?ProductID=1015211> (visited on 06/11/2022).
- [14] *T70 - Bærende takprofil — Plannja*, no. [Online]. Available: <https://www.plannja.no/proffkunder/husfabrikker/produkter/ovrige-profiler/ovrige-profiler-produkter/t70> (visited on 06/11/2022).
- [15] "Eurocode: Basis of structural design," European Committee for Standardization (CEN), Tech. Rep. NS-EN 1990:2002+A1:2005+NA:2016. [Online]. Available: <https://www.standard.no/no/Nettbutikk/produktkatalogen/Produktpresentasjon/?ProductID=814830> (visited on 06/11/2022).
- [16] A. P. Boresi and R. J. Schmidt, *Advanced mechanics of materials*, 6th ed. New York: John Wiley & Sons, 2003, ISBN: 978-0-471-43881-6.
- [17] "Eurocode 3: Design of steel structures - Part 1-1: General rules and rules for buildings," European Committee for Standardization (CEN), Tech. Rep. NS-EN 1993-1-1: 2005 + A1: 2014 + NA: 2015. [Online]. Available: <https://www.standard.no/no/Nettbutikk/produktkatalogen/Produktpresentasjon/?ProductID=755701> (visited on 06/11/2022).
- [18] *Table of material properties for structural steel S235, S275, S355, S420*, en. [Online]. Available: <https://eurocodeapplied.com/design/en1993/steel-design-properties> (visited on 06/12/2022).
- [19] *Data sheet Strand T15.7*, Feb. 2015. [Online]. Available: [https://barsandrods.arcelormittal.com/repository2/fanny/Strand\\_7\\_15.7\\_EN.pdf](https://barsandrods.arcelormittal.com/repository2/fanny/Strand_7_15.7_EN.pdf) (visited on 06/11/2022).
- [20] *Heavy lifting company — VSL*, en-US. [Online]. Available: <https://vsl.com/home/technologies/heavy-lifting/> (visited on 06/12/2022).



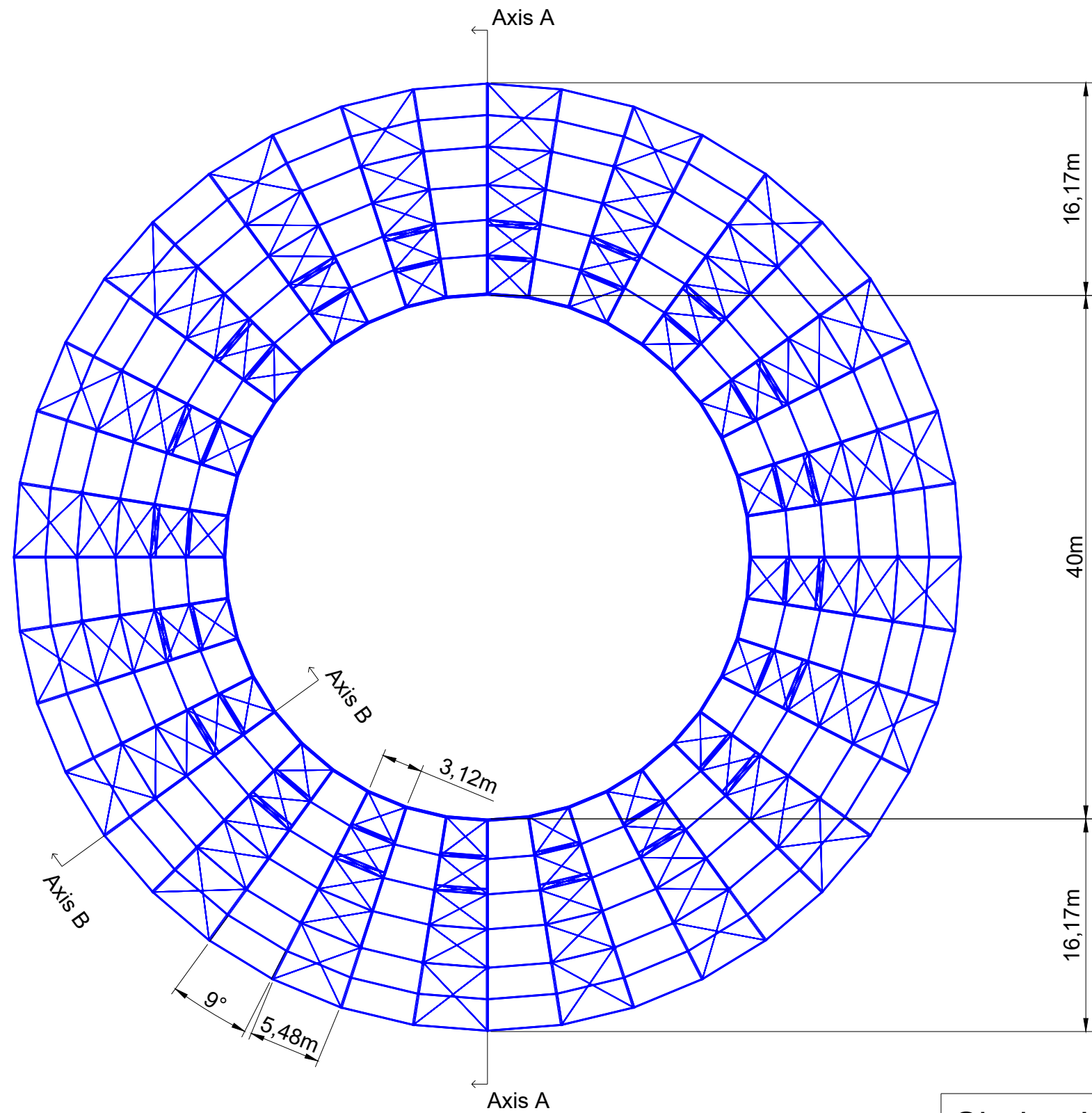
- [21] “Eurocode 3: Design of steel structures - Part 1-8: Design of joints,” European Committee for Standardization (CEN), Tech. Rep. NS-EN 1993-1-8: 2005 + NA: 2009. [Online]. Available: <https://www.standard.no/no/Nettbutikk/produktkatalogen/Produktpresentasjon/?ProductID=396860> (visited on 06/11/2022).
- [22] Norges tekniske høgskole and Institutt for konstruksjonsteknikk, *Stålkonstruksjoner profiler og formler*, Norwegian, 3. utgave. Trondheim: Tapir, 1993, OCLC: 1028253971, ISBN: 978-82-519-1151-1.
- [23] E. team, *Table of properties for steel tubes / circular hollow sections CHS*, en. [Online]. Available: <https://eurocodeapplied.com/design/en1993/chs-design-properties> (visited on 05/03/2022).
- [24] “Eurocode 3: Design of steel structures - Part 1-5: Plated structural elements,” European Committee for Standardization (CEN), Tech. Rep. NS-EN 1993-1-5: 2006 + AC + A1: 2017 + A2: 2019 + NA:2019. [Online]. Available: <https://www.standard.no/no/Nettbutikk/produktkatalogen/Produktpresentasjon/?ProductID=1094401> (visited on 06/14/2022).
- [25] *Visit Plaza de Toros y Museo Taurino de Alicante on your trip to Alicante*, en. [Online]. Available: <https://www.inspirock.com/spain/alicante/plaza-de-toros-y-museo-taurino-de-alicante-a4271635059> (visited on 06/11/2022).

# Appendix A

## Drawings

Here are more detailed drawing of the building, in the finished position and in the starting position. List of drawings:

1. Plan view finished position, new roof, wire-frame
2. Plan view finished position, new roof and Alicante bullring, conceptual
3. Section A-A view finished position, new roof, wire-frame
4. Section B-B view finished position, new roof truss, wire-frame
5. Plan view truss pair, new roof, conceptual
6. Single ring section, new roof, conceptual
7. Plan view starting position, new roof, wire-frame
8. Plan view starting position, new roof and Alicante bullring, conceptual
9. Section view starting position, new roof, wire-frame
10. 3D view finished position, new roof, Alicante bullring, and roof sheets, conceptual
11. 3D view finished position, new roof and Alicante bullring, conceptual
12. 3D view starting position, new roof and Alicante bullring, conceptual
13. 3D view section finished position, new roof and Alicante bullring, conceptual
14. 3D view section starting position, new roof and Alicante bullring, conceptual
15. 3D view section finished position, new roof, Alicante bullring and roof sheets, conceptual



Sindre Jakobsen - Master thesis  
Alicante bullring roof

Fag  
RIB

Format  
A3

Dato  
06.06.2022

Steel drawing  
Plan, new roof only

Format/Målestokk:  
1:400

University of  
Stavanger

Status

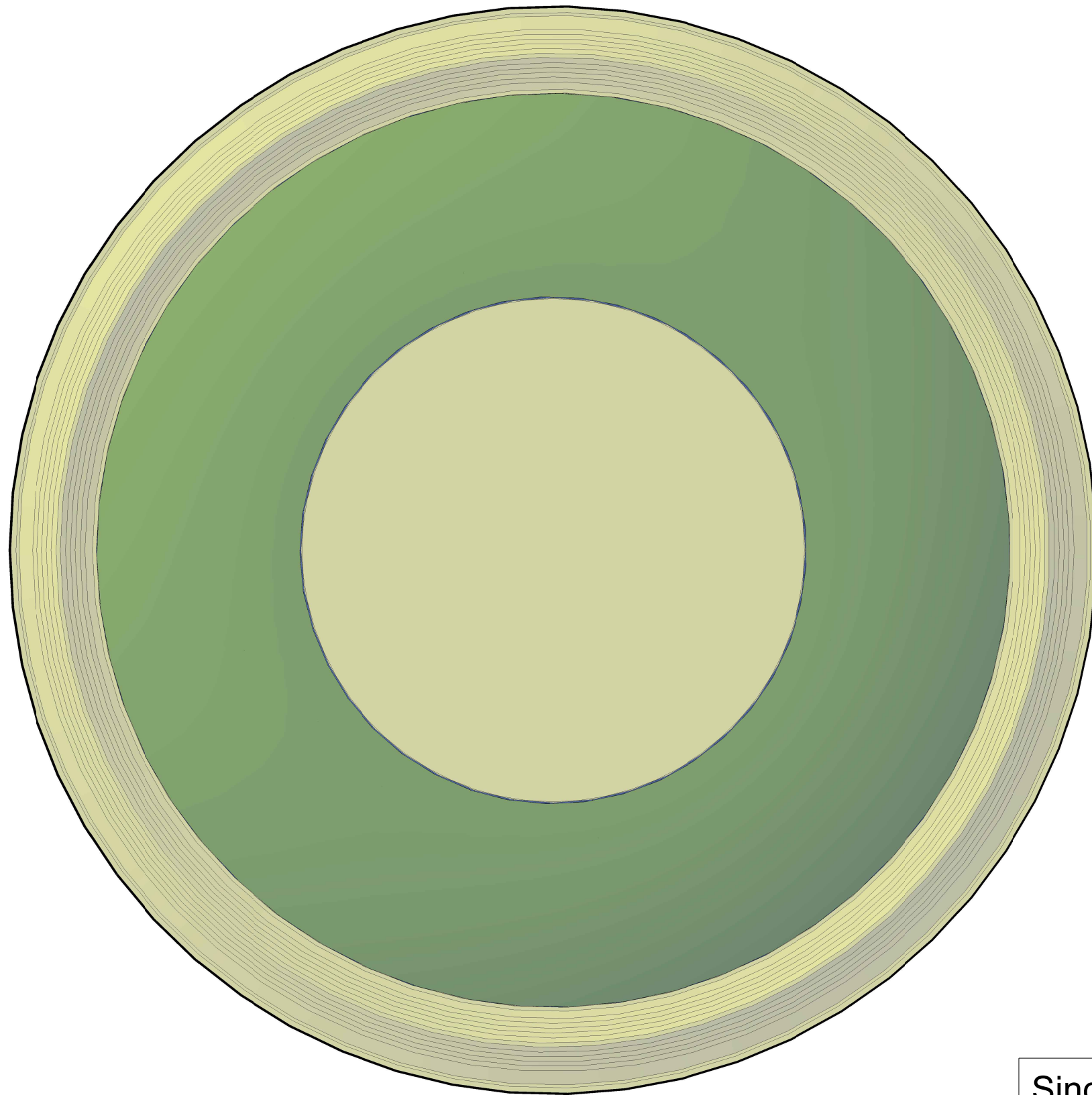
Konstr./Tegnet

Kontrollert

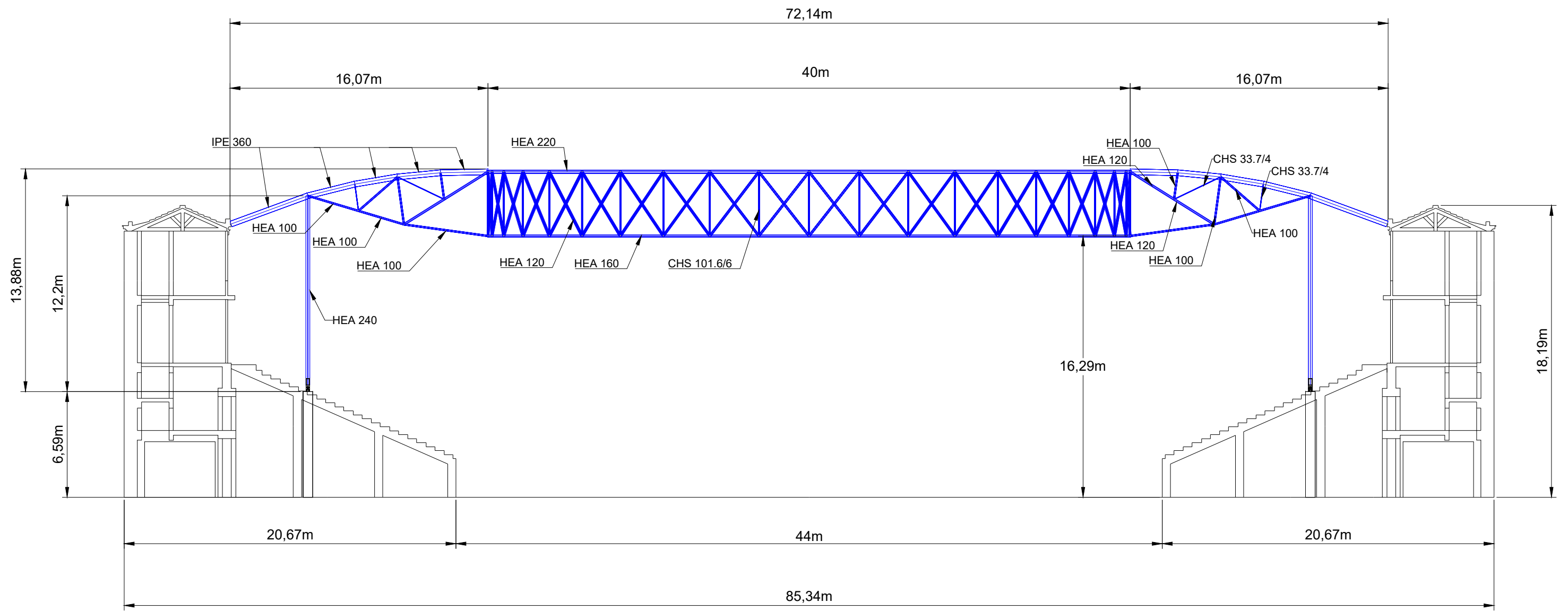
Godkjent

Tegningsnr.

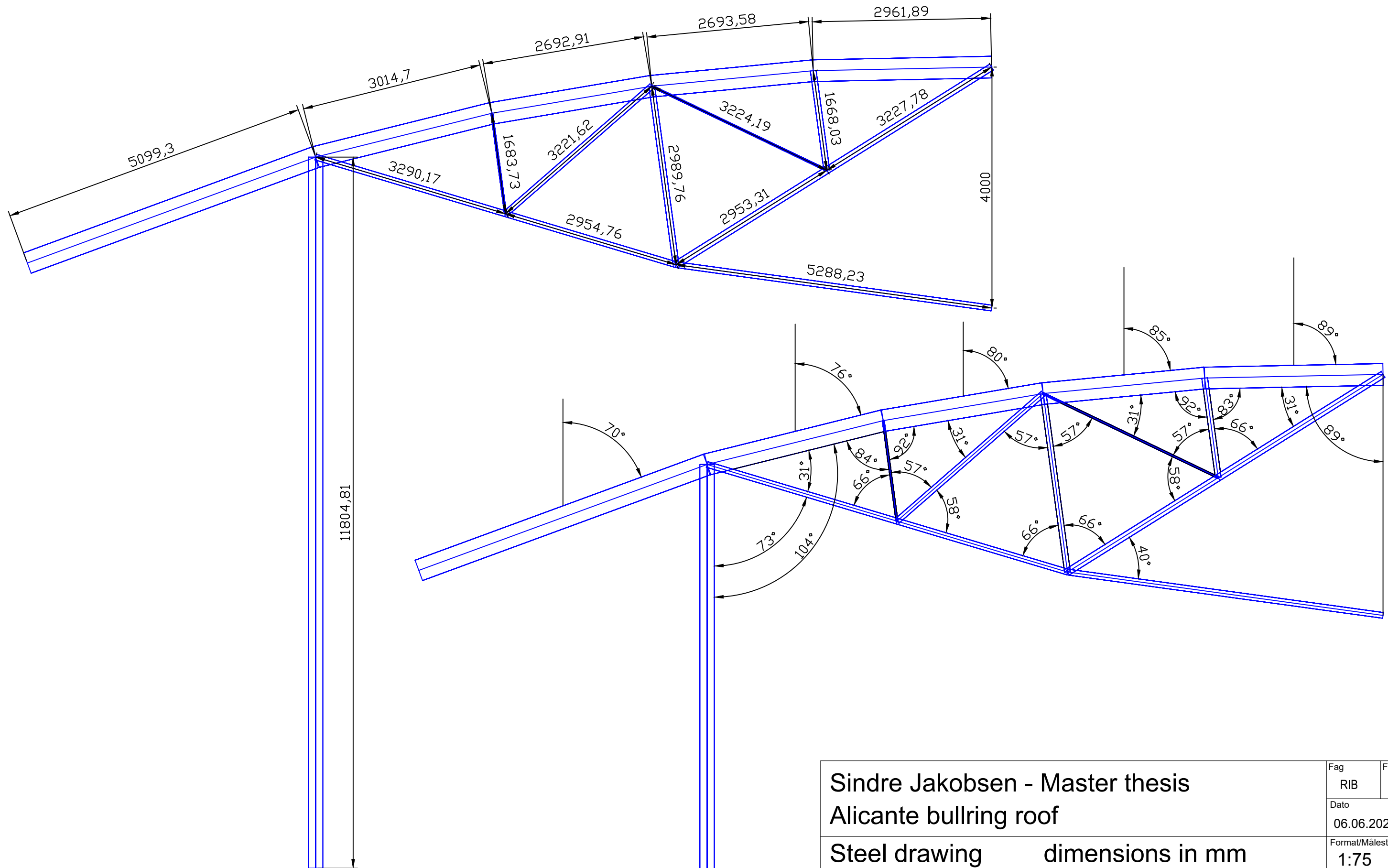
1



Sindre Jakobsen - Master thesis Alicante bullring roof		Fag	Format
		RIB	A3
Steel drawing Plan, new roof and old structure		Dato	
		06.06.2022	
University of Stavanger		Format/Målestokk:	
		1:400	
Status	Konstr./Tegnet	Kontrollert	Godkjent
	Tegningsnr.		
	2		



Sindre Jakobsen - Master thesis Alicante bullring roof		Fag	Format
		RIB	A3
Steel drawing Section A-A (two trusses)		Dato	Format/Målestokk:
		06.06.2022	1:250
University of Stavanger	Status	Konstr./Tegnet	Kontrollert
		Tegningsnr.	Godkjent
		3	



Sindre Jakobsen - Master thesis  
Alicante bullring roof

Steel drawing      dimensions in mm  
Truss section B-B

Fag  
RIB      Format  
A3

Dato  
06.06.2022

Format/Målestokk:  
1:75

University of  
Stavanger

Status

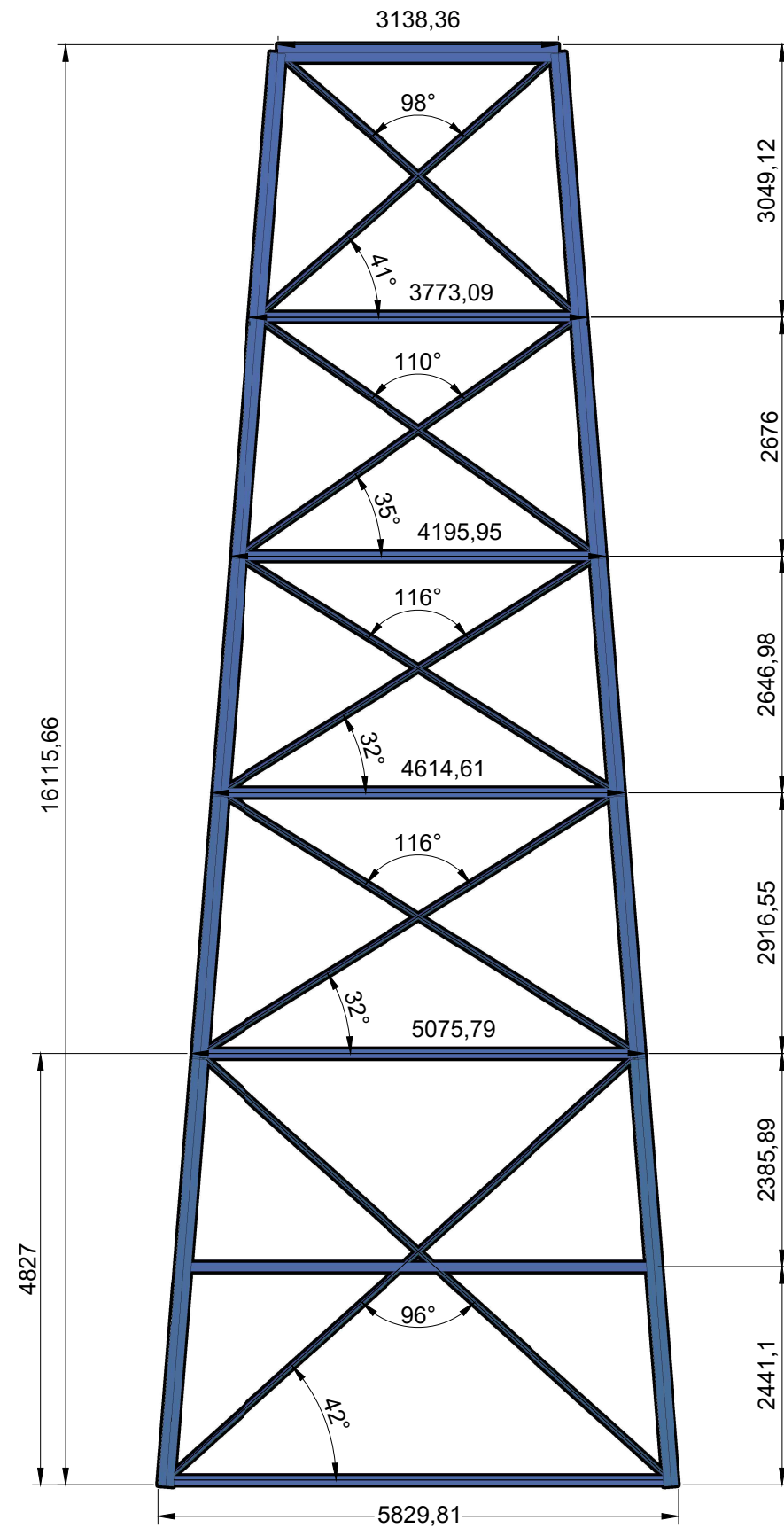
Konstr./Tegnet

Kontrollert

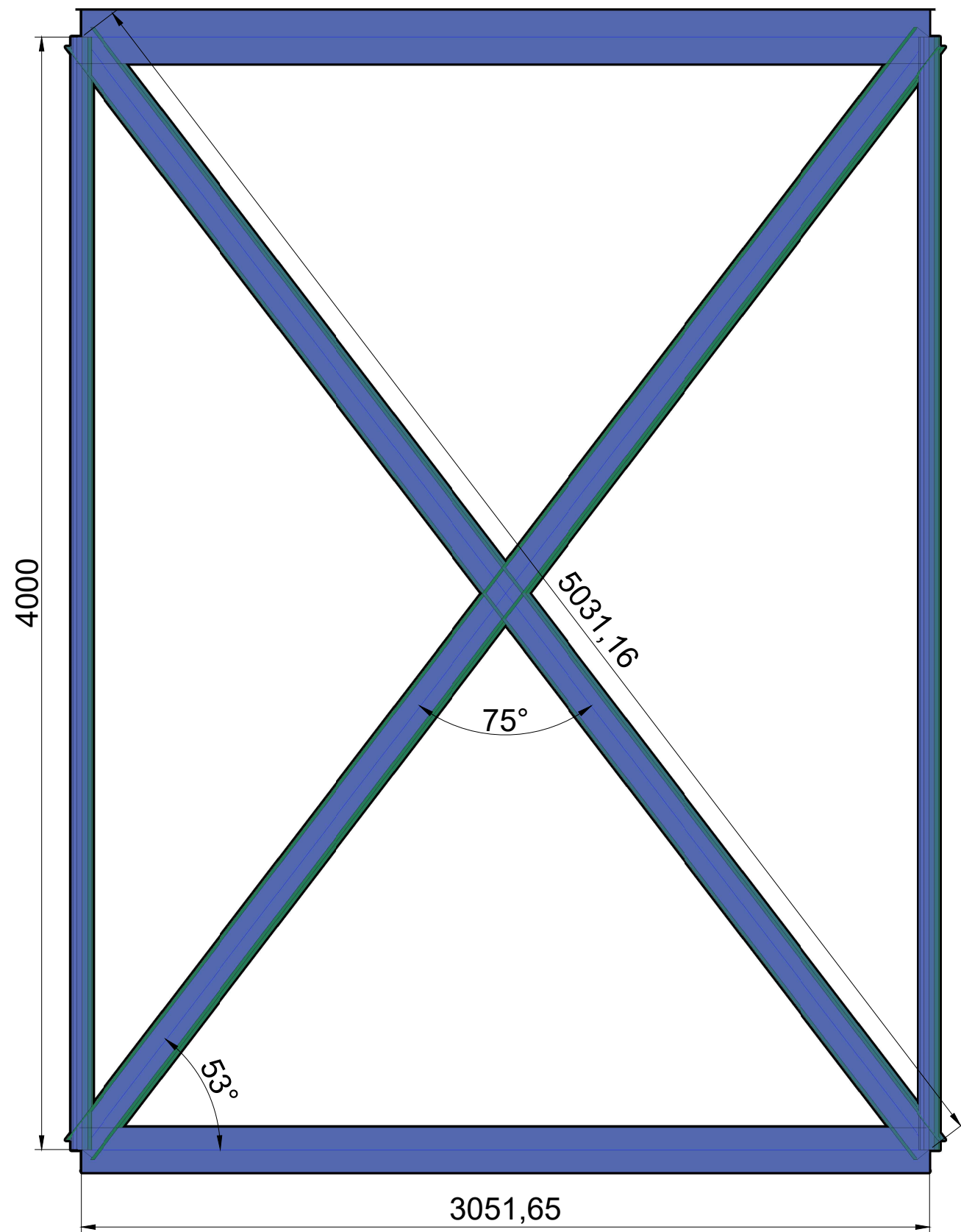
Godkjent

Tegningsnr.

4



Sindre Jakobsen - Master thesis Alicante bullring roof		Fag	Format
		RIB	A3
Steel drawing      dimensions in mm Truss pair, plan view		Dato	
		06.06.2022	
University of Stavanger		Format/Målestokk:	
		1:75	
Status	Konstr./Tegnet	Kontrollert	Godkjent
	Tegningsnr.		
	5		



Sindre Jakobsen - Master thesis  
Alicante bullring roof

Steel drawing  
Single ring section

Dimensions in mm

Fag	Format
RIB	A3

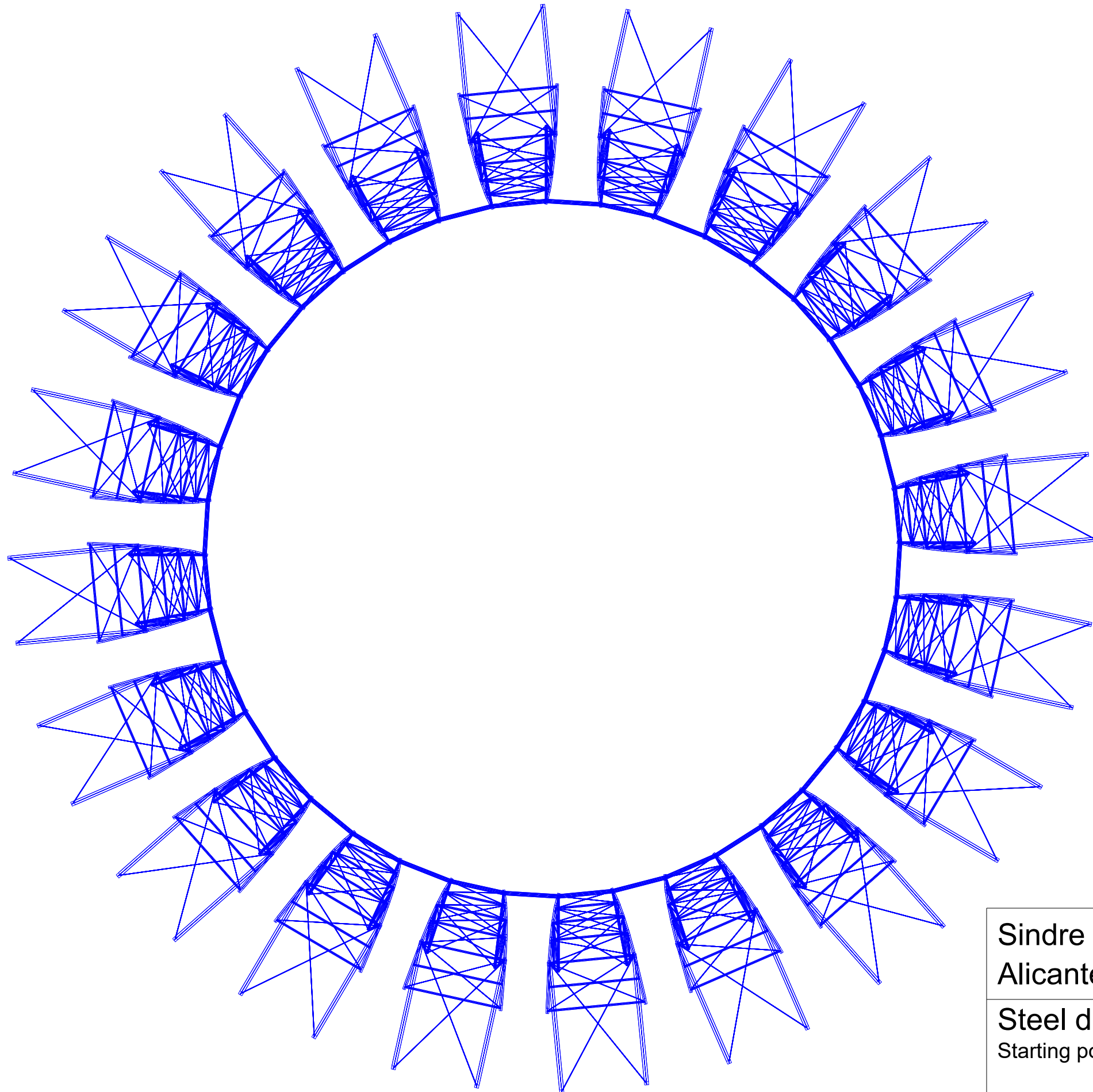
Dato
11.06.2022

Format/Målestokk:
1:20

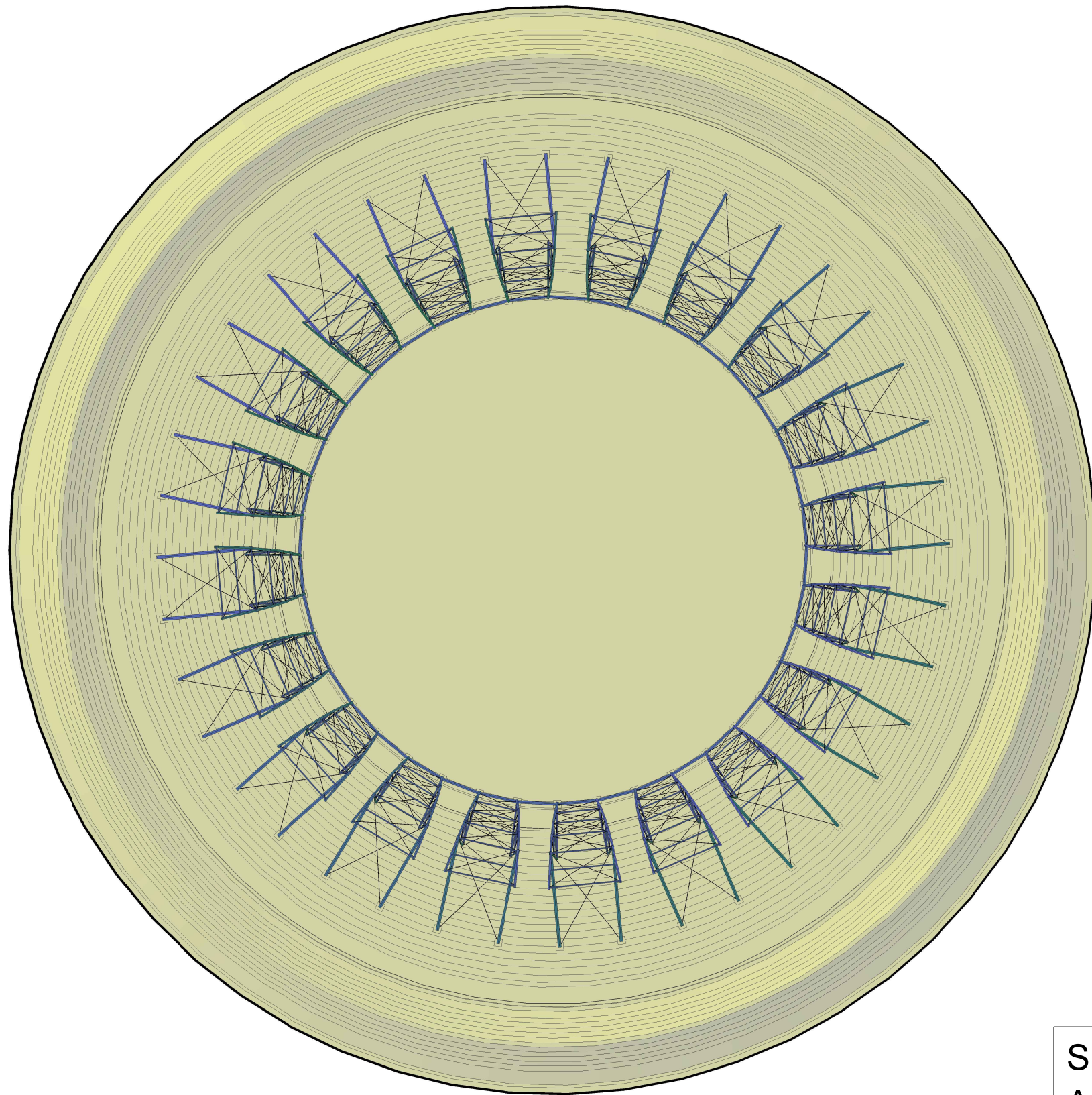
University of  
Stavanger

Status	Konstr./Tegnet	Kontrollert	Godkjent
	Tegningsnr. <b>6</b>		

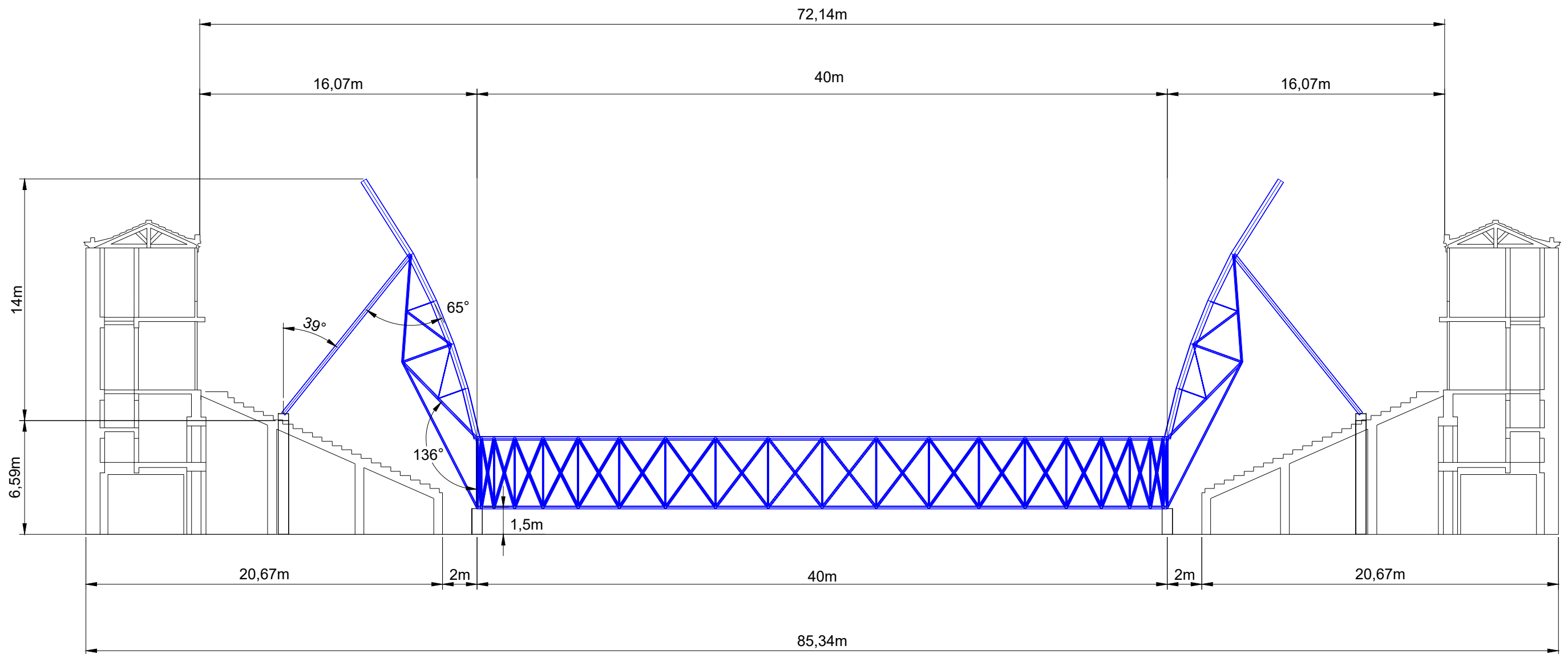




<b>Sindre Jakobsen - Master thesis</b> <b>Alicante bullring roof</b>		Fag	Format	
		RIB	A3	
<b>Steel drawing</b> Starting position plan view, new roof only		Dato	11.06.2022	
		Format/Målestokk:	1:250	
<b>University of Stavanger</b>	Status	Konstr./Tegnet	Kontrollert	Godkjent
		Tegningsnr. <b>7</b>		



Sindre Jakobsen - Master thesis Alicante bullring roof		Fag	Format	
		RIB	A3	
Steel drawing Starting position plan view, new roof and old structure		Dato	Format/Målestokk:	
		06.06.2022	1:400	
University of Stavanger	Status	Konstr./Tegnet	Kontrollert	Godkjent
		Tegningsnr. 8		



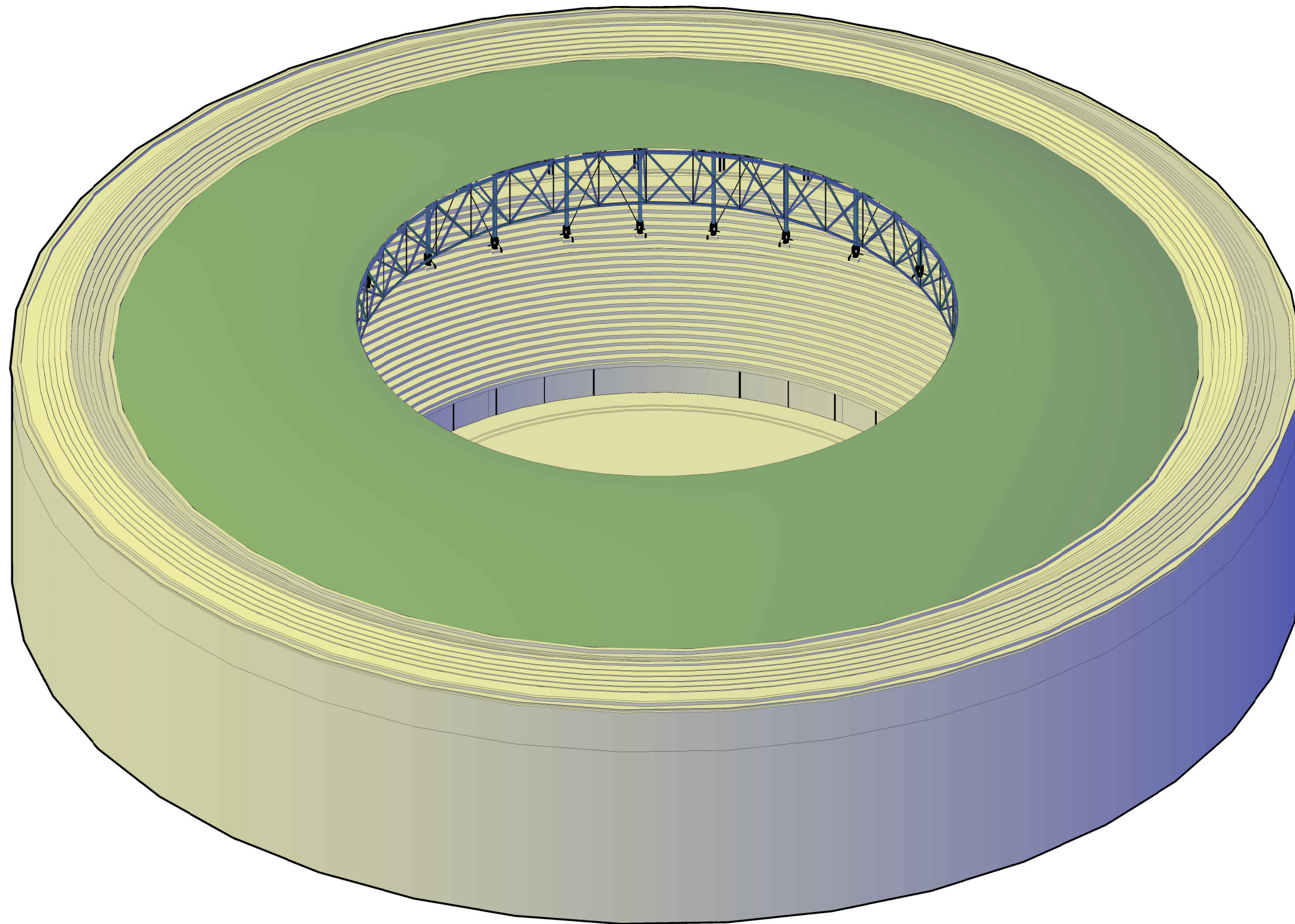
Sindre Jakobsen - Master thesis  
Alicante bullring roof

Steel drawing  
Section A-A (two trusses)  
Starting position

University of  
Stavanger

Fag	Format		
RIB	A3		
Dato			
11.06.2022			
Format/Målestokk:			
1:250			
Status	Konstr./Tegnet	Kontrollert	Godkjent
Tegningsnr.			
9			





Sindre Jakobsen - Master thesis  
 Alicante bullring roof

Steel drawing  
 3D, new roof and old structure and roof sheets

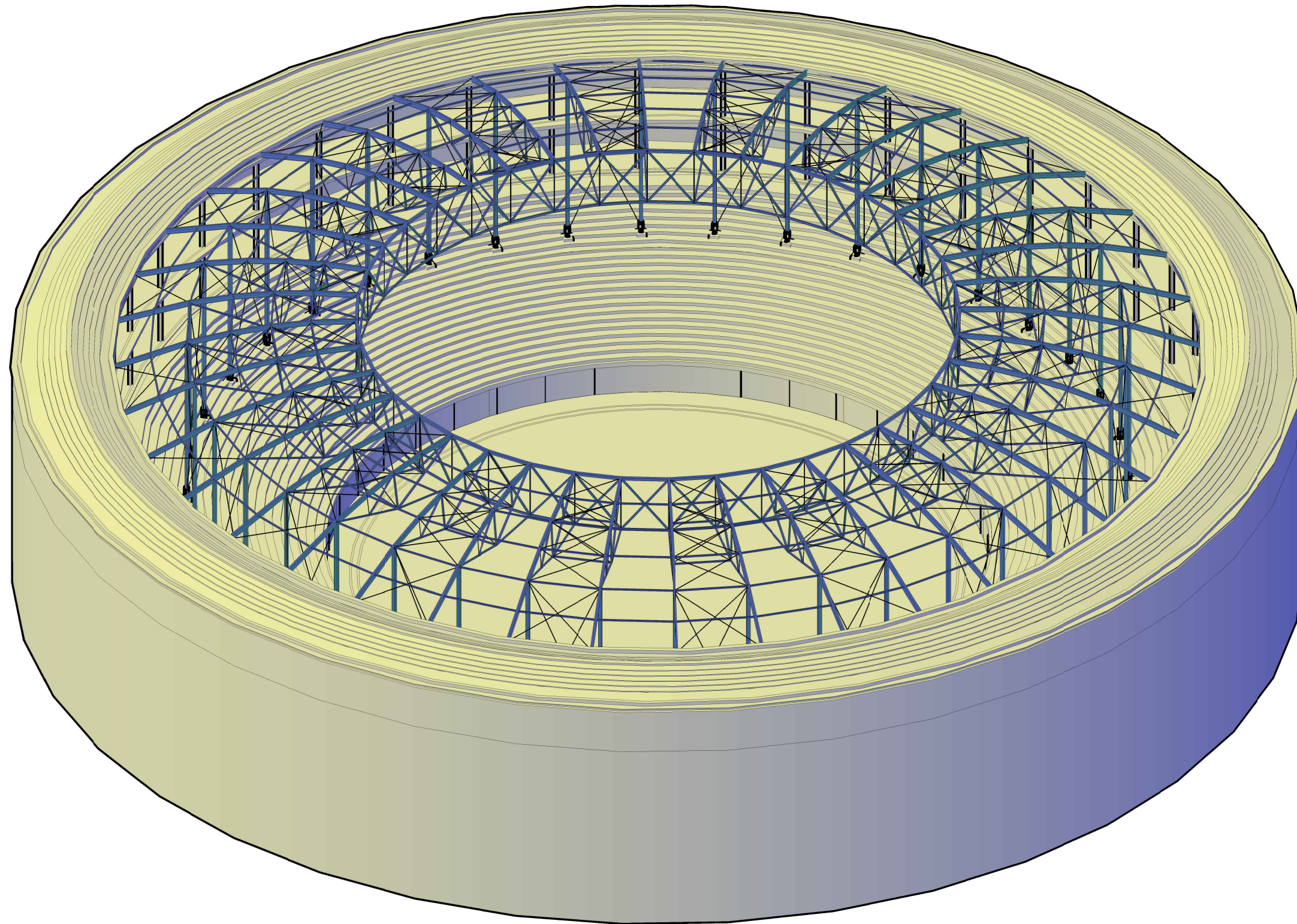
Fag	Format
RIB	A3
Dato	
06.06.2022	

Format/Målestokk:
1:300

University of  
 Stavanger

Status	Konstr./Tegnet	Kontrollert	Godkjent
Tegningsnr.			
10			





Sindre Jakobsen - Master thesis  
 Alicante bullring roof

Steel drawing  
 3D, new roof and old structure

Fag	Format
RIB	A3

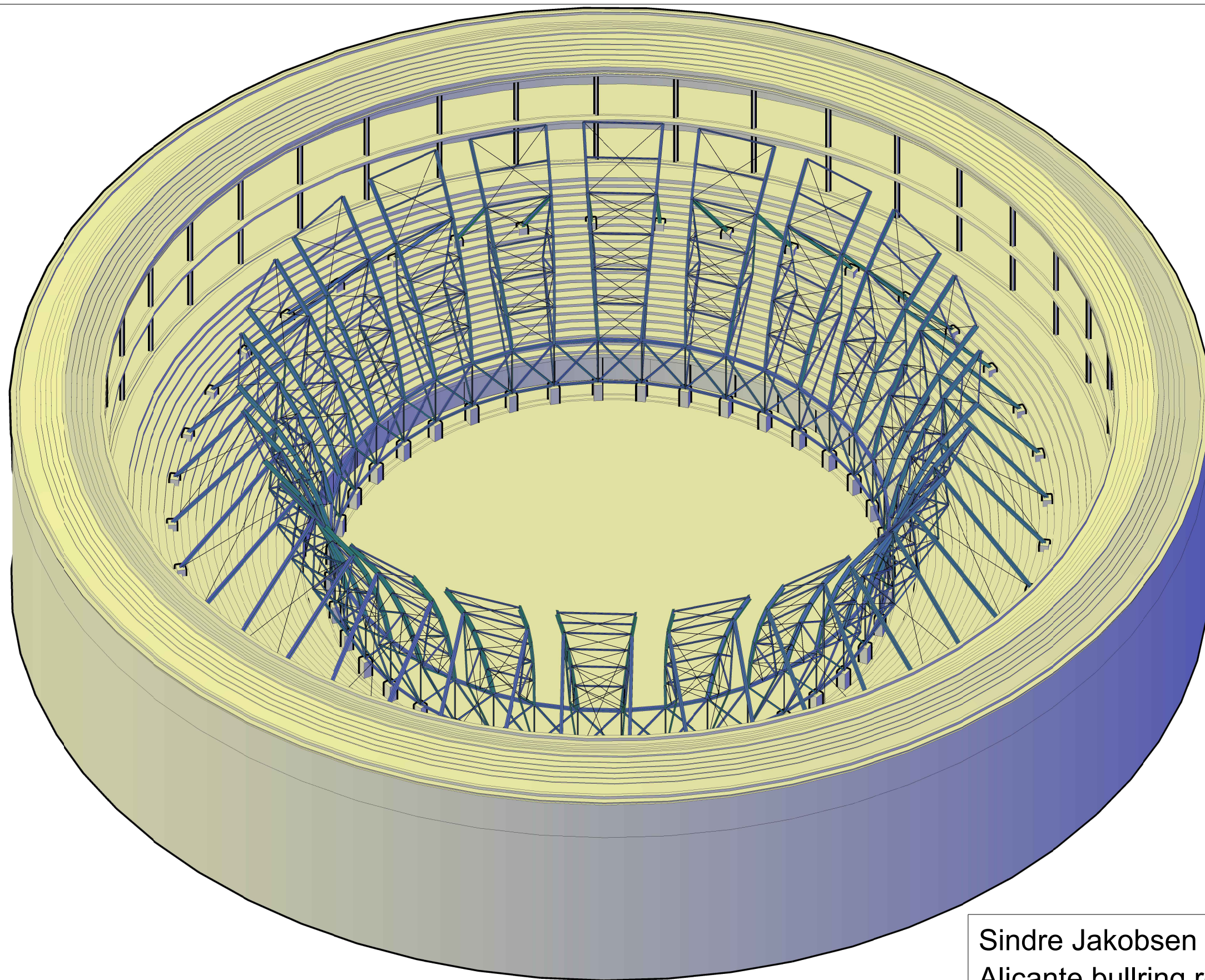
Dato
06.06.2022

Format/Målestokk:
1:300

University of  
 Stavanger

Status	Konstr./Tegnet	Kontrollert	Godkjent
	Tegningsnr. <b>11</b>		





Sindre Jakobsen - Master thesis  
 Alicante bullring roof

Steel drawing  
 Starting position 3D view, new roof and old structure

University of  
 Stavanger

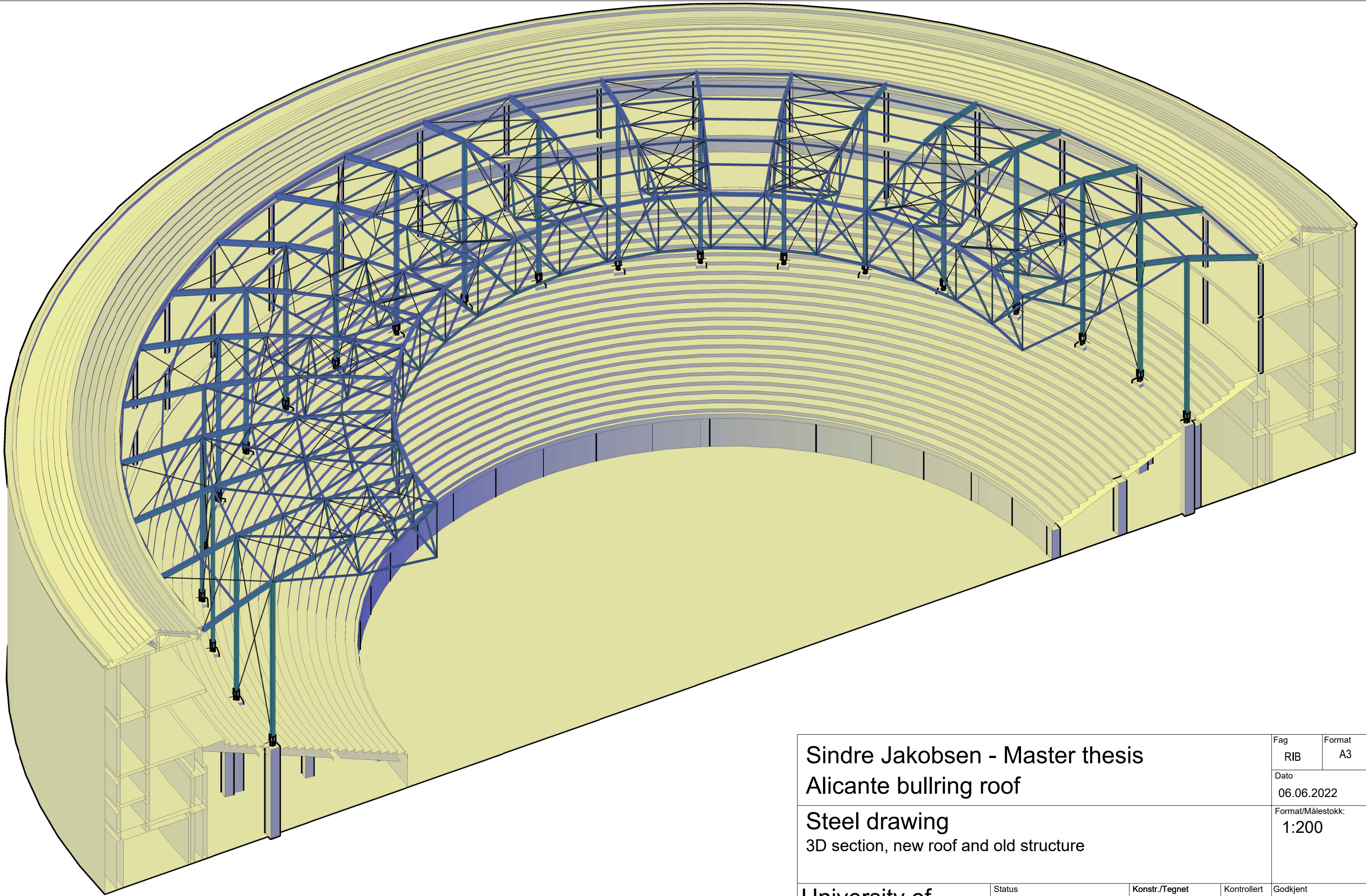
Fag	Format
RIB	A3

Dato
06.06.2022

Format/Målestokk:
1:300

Status	Konstr./Tegnet	Kontrollert	Godkjent
	Tegningsnr.		
	12		





Sindre Jakobsen - Master thesis  
 Alicante bullring roof

Steel drawing  
 3D section, new roof and old structure

Fag	Format
RIB	A3

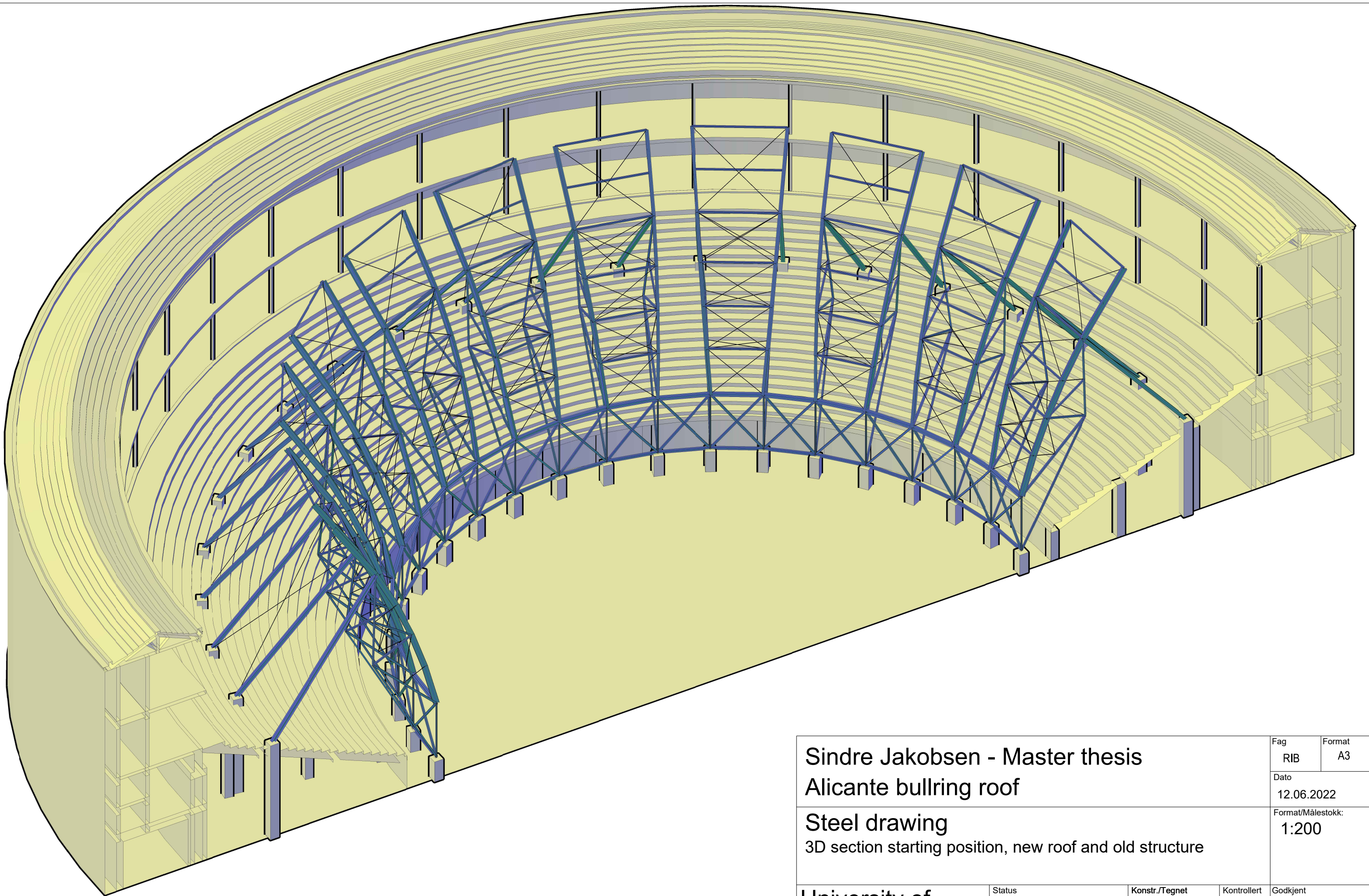
Dato
06.06.2022

Format/Målestokk:
1:200

University of  
 Stavanger

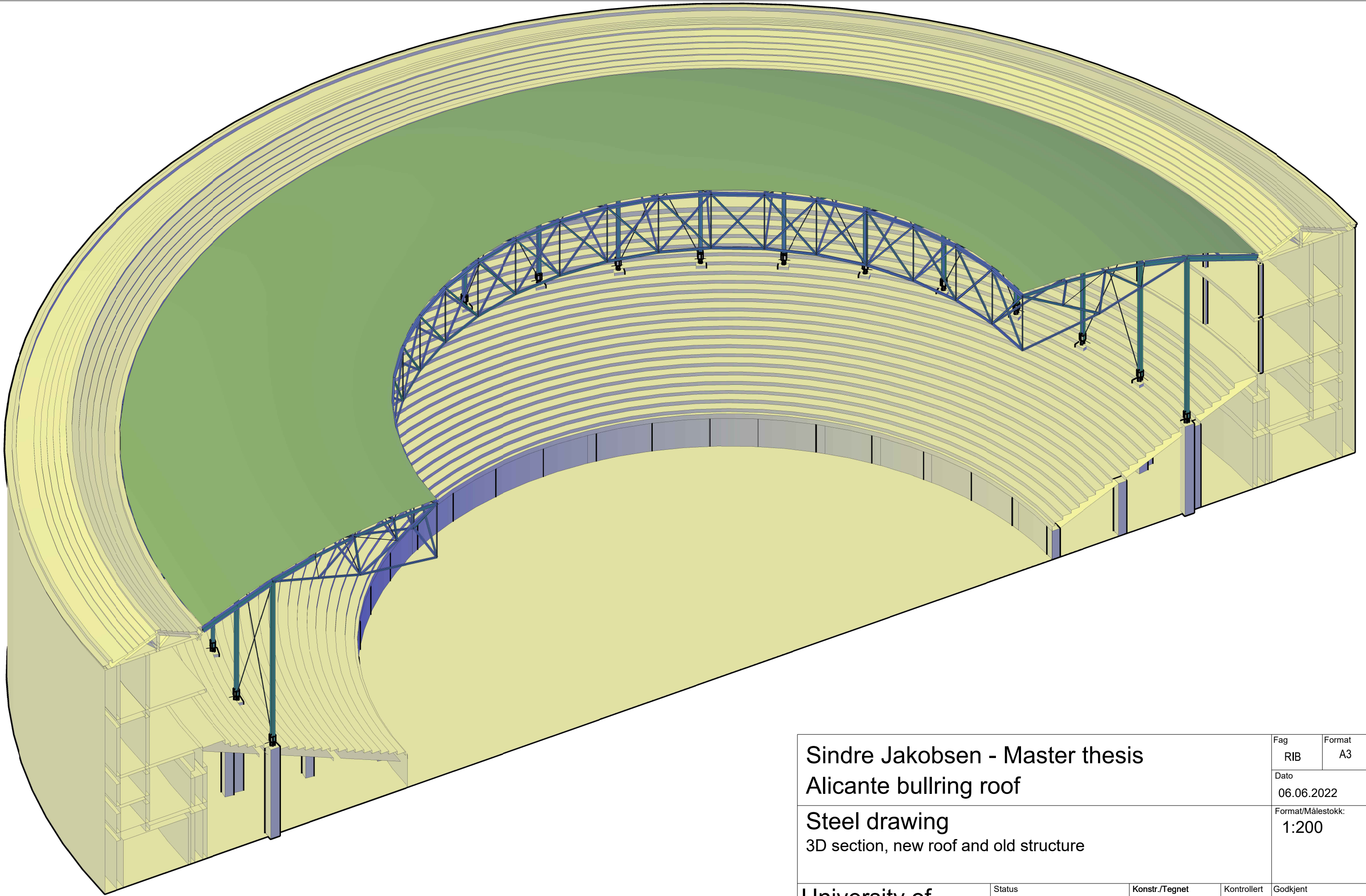
Status	Konstr./Tegnet	Kontrollert	Godkjent
	Tegningsnr. 13		





Sindre Jakobsen - Master thesis Alicante bullring roof	Fag	Format		
	RIB	A3		
Steel drawing 3D section starting position, new roof and old structure	Dato			
	12.06.2022			
	Format/Målestokk:			
	1:200			
University of Stavanger	Status	Konstr./Tegnet	Kontrollert	Godkjent
		Tegningsnr.		
		14		





Sindre Jakobsen - Master thesis  
 Alicante bullring roof

Steel drawing  
 3D section, new roof and old structure

Fag	Format
RIB	A3

Dato
06.06.2022

Format/Målestokk:
1:200

University of  
 Stavanger

Status	Konstr./Tegnet	Kontrollert	Godkjent
	Tegningsnr. 15		

# Appendix B

## Design of steel members

The design of steel members follows Eurocode 3: EN1993: Design of Steel Structures. Most of the formulas needed for the design are given by NS-EN 1993-1-1:2005 + A1:2014 + NA:2015 [17], which were used to design the steel section in this thesis. Here is a summary of the equations and checks used.

### B.1 Tension members

Tension members should pass this check:

$$\frac{N_{Ed}}{N_{t,Rd}} \leq 1 \quad (\text{EC3 eq:6.5})$$

where:

- $N_{Ed} = N_{t,Ed} =$  Axial load (P)
- $N_{t,Rd} =$  Tension capacity

We have that:

$$N_{t,Rd} = f_y \cdot A \quad (\text{B.1})$$

Minimum cross sectional area is then:

$$A_{min} \geq \frac{N_{t,Ed} \cdot \gamma_{M0}}{f_y} \quad (\text{B.2})$$

Capacity is given by:

$$N_{pl,Rd} = \frac{A f_y}{\gamma_{M0}} \quad (\text{EC3 eq: 6.6})$$

where:

- $f_y =$  yield strength of the steel used, here S355 steel is used for most of the members

- $A$  = Gross area of cross section
- $A_{min}$  = Minimum cross section area required
- $\gamma_{M0}$  = Partial safety factor (1.05)

## B.2 Compression members

The design of compression members is similar to tension members, but require that there is no buckling failure, to have a section to test for buckling a trial section has to be found first:

$$\text{Guess: } \chi_{trial} = 0.3 \quad (\text{B.3})$$

then

$$N_{b,Rd} = \frac{\chi A f_y}{\gamma_{M1}} \quad (\text{EC3 eq: 6.47})$$

solving for  $A$  and neglecting the partial safety factor:

$$A_{min} \geq \frac{N_{Ed}}{\chi f_y} \quad (\text{B.4})$$

Calculation the minimum area for the compression members and choosing a section with a larger area will provide the a trial section.

### B.2.1 Class classification

To estimate to what degree buckling can occur, the sections are classified. There are four classes, where class 1 is a thicker section that will not buckle, to class 4 which is a slender/thin-walled section that is especially prone to buckling.

The web and the flange are classified separately, where the highest class of the two is the class of the section. Table 5.2 in the EC3 is used, for the web:

$$\text{Class 1: } \frac{c_w}{t_w} \leq 33 \varepsilon \quad (\text{B.5})$$

$$\text{Class 2: } \frac{c_w}{t_w} \leq 38 \varepsilon \quad (\text{B.6})$$

$$\text{Class 3: } \frac{c_w}{t_w} \leq 42 \varepsilon \quad (\text{B.7})$$

$$\text{Class 4: } \frac{c_w}{t_w} > 42 \varepsilon \quad (\text{B.8})$$

where:

- $c_w$  = the length of the web minus the root radius on both sides

- $t_w$  = the thickness of the web

For the flange:

$$\text{Class 1: } \frac{c_f}{t_f} \leq 9 \varepsilon \quad (\text{B.9})$$

$$\text{Class 2: } \frac{c_f}{t_f} \leq 10 \varepsilon \quad (\text{B.10})$$

$$\text{Class 3: } \frac{c_f}{t_f} \leq 14 \varepsilon \quad (\text{B.11})$$

$$\text{Class 4: } \frac{c_f}{t_f} > 14 \varepsilon \quad (\text{B.12})$$

where:

- $c_f$  = outstanding flange length on one side
- $t_f$  = the thickness of the flange
- $\varepsilon = \sqrt{235/f_y}$ , for  $f_y = 355$ ,  $\varepsilon = 0.81$

### B.2.2 Buckling capacity

To following equation should be true to prevent buckling:

$$\frac{N_{Ed}}{N_{b,Rd}} \leq 1.0 \quad (\text{EC3 eq:6.46})$$

where  $N_{Ed}$  is the design load and  $N_{b,Rd}$  is the buckling resistance. For class 3,  $N_{b,Rd}$  is given by:

$$N_{b,Rd} = \frac{\chi A f_y}{\gamma_{M1}} \quad (\text{EC3 eq:6.47})$$

and for class 4:

$$N_{b,Rd} = \frac{\chi A_{\text{eff}} f_y}{\gamma_{M1}} \quad (\text{EC3 eq:6.48})$$

based on the trial sections the actual value for  $\chi$  can now be calculated:

$$\chi = \frac{1}{\Phi + \sqrt{\Phi^2 - \bar{\lambda}^2}}, \quad \chi \leq 1.0 \quad (\text{EC3 eq:6.49})$$

where

$$\Phi = 0.5 \left[ 1 + \alpha (\bar{\lambda} - 0.2) + \bar{\lambda}^2 \right]$$

$$\bar{\lambda} = \sqrt{\frac{A f_y}{N_{cr}}} = \frac{L_{cr}}{i} \frac{1}{\lambda_1} \quad \text{for class 1, 2 or 3} \quad (\text{EC3 eq:6.50})$$

$$\bar{\lambda} = \sqrt{\frac{A f_y}{N_{cr}}} = \frac{L_{cr}}{i} \frac{\sqrt{\frac{A_{\text{eff}}}{A}}}{\lambda_1} \quad \text{for class 4} \quad (\text{EC3 eq:6.51})$$

- $\alpha$  = imperfection factor for the respective buckling curve
- $N_{cr}$  = ideal force for the respective buckling curve based on the gross sectional area
- $L_{cr}$  = buckling length in the considered buckling plane
- $i$  = radius of gyration

The members can buckle in their local y-axis or z-axis, the final buckling resistance will therefore be the lowest resistance of the two. Using the lowest  $i$  and the respectful  $\alpha$  value to that axis, when calculation will accomplice this.

## B.3 Beam members

The beam members 4B7, 4B8, 4B9, 4BA and 4BB is in reality a single curved beam and must therefor have the same cross-section, but the parts of the curved beam will be designed individual and a single section will be chosen that is suitable for all the parts.

### B.3.1 Trial design

First a trail section has to be chosen for the members, the section will then be tested against the checks in the EC3, which for beams are numerous.

$$\text{Guess: } \chi_{Lt,trial} = 0.5 \quad (\text{B.13})$$

$$W_{pl,min} = \frac{\gamma_{M0} M_{y,Ed}}{\chi_{Lt,trial} f_y} \quad (\text{B.14})$$

### B.3.2 Class classification

Similar to compression bars, beam has to be classified to estimate to what degree buckling can occur. The class calculation for the flange is the same, but the web is different, as only the part of the web in compression can buckle. To find this area the plastic neutral axis has to be located. Where the plastic neutral axis is on the section depends on the axial load, so the axis will be different for the different elements.

If there were no axial loading on the beams the following equation could be used:

$$\sum F_x = 0 \Rightarrow C_w - T_w = 0 \quad (\text{B.15})$$

when there is an axial load:

$$\sum F_x = 0 \Rightarrow C_w - T_w = N_{Ed} \quad (\text{B.16})$$

where:

- $C_w$  = the area of the web in compression times the yield strength of the material
- $T_w$  = the area of the web in tension times the yield strength of the material

When there is no axial load, the C and T value will be equal, but as the axial load rises, a larger area of the section will be in compression.

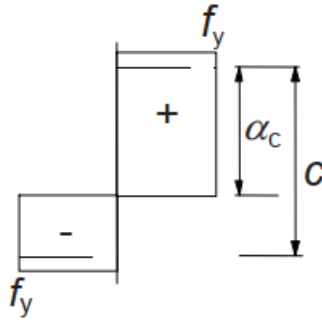


Figure B.1: Figure from table 5.2 in EC3 [17]

Expanding the equation:

$$\alpha_c \cdot t_w \cdot f_y - (C - \alpha_c) \cdot t_w \cdot f_y = N_{Ed} \quad (\text{B.17})$$

$$\alpha_c = C \cdot \alpha \quad (\text{B.18})$$

Rearranging for  $\alpha$ :

$$\alpha = \left[ \frac{N_{Ed}}{f_y t_w C} + 1 \right] \cdot \frac{1}{2} \quad (\text{B.19})$$

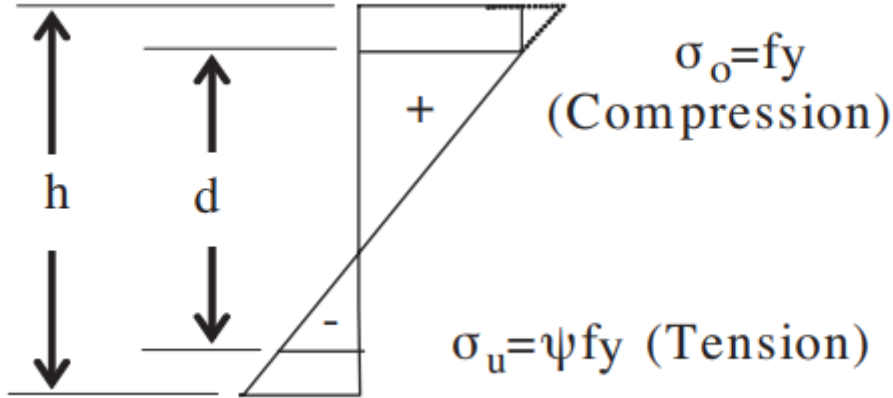


Figure B.2: PSI notation, Design of Steel Structures to Eurocode, page 409 [17]

The equations for the class of the web depends on the value of  $\alpha$ :

$$\begin{aligned}
 \text{Class 1:} \quad & \text{for } \alpha > 0.5 : \frac{c_w}{t_w} \leq \frac{396\varepsilon}{13\alpha - 1} \\
 & \text{for } \alpha \leq 0.5 : \frac{c_w}{t_w} \leq \frac{36\varepsilon}{\alpha} \\
 \text{Class 2:} \quad & \text{for } \alpha > 0.5 : \frac{c_w}{t_w} \leq \frac{456\varepsilon}{13\alpha - 1} \\
 & \text{for } \alpha \leq 0.5 : \frac{c_w}{t_w} \leq \frac{41.5\varepsilon}{\alpha} \\
 \text{Class 3:} \quad & \text{for } \psi > -1 : \frac{c_w}{t_w} \leq \frac{42\varepsilon}{0.67 + 0.33\psi} \\
 & \text{for } \psi \leq -1 : \frac{c_w}{t_w} \leq 62\varepsilon(1 - \psi)\sqrt{-\psi} \\
 \text{Class 4:} \quad & \text{for } \psi > -1 : \frac{c_w}{t_w} > \frac{42\varepsilon}{0.67 + 0.33\psi} \\
 & \text{for } \psi \leq -1 : \frac{c_w}{t_w} > 62\varepsilon(1 - \psi)\sqrt{-\psi}
 \end{aligned}$$

The stress- or strain-ratio,  $\psi$ , is calculated by dividing the stress at the top of the web by the stress at the bottom of the web, when the top of the web has reached yield stress:

$$\sigma_o = \frac{N_{Ed}}{A} + \frac{M_{Ed}}{I_y} z = f_y \quad (\text{B.20})$$

$$\sigma_u = \frac{N_{Ed}}{A} - \frac{M_{Ed}}{I_y} z \quad (\text{B.21})$$

$$\psi = \frac{\sigma_o}{\sigma_u} \quad (\text{B.22})$$

The classification of the flange is the same as for compression bars:

$$\begin{aligned} \text{Class 1: } & \frac{c_f}{t_f} \leq 9 \varepsilon \\ \text{Class 2: } & \frac{c_f}{t_f} \leq 10 \varepsilon \\ \text{Class 3: } & \frac{c_f}{t_f} \leq 14 \varepsilon \\ \text{Class 4: } & \frac{c_f}{t_f} > 14 \varepsilon \end{aligned}$$

Table B.1: Class for beam sections

Element	Trial section	$N_{Ed}$	$\alpha$	$\psi$	Class
4B7	IPE140	158.20 kN (C)	0.922	-0.728	1
4B8	IPE140	183.78 kN (C)	0.99	-0.684	1
4B9	IPE180	107.06 kN (C)	0.69	-0.873	1
4BA	IPE450	125.77 kN (C)	0.549	-0.964	1
4BB	IPE450	30.785 kN (T)	0.487	-1.00	1

### B.3.3 Bending moment resistance - Yield capacity

For cross sections belonging to class 1 or 2:

$$M_{c,Rd} = M_{pl,Rd} = \frac{W_{pl,y} f_y}{\gamma_{M0}} \quad (\text{EC3: 6.13})$$

For cross sections belonging to class 3:

$$M_{c,Rd} = M_{el,Rd} = \frac{W_{el,min} f_y}{\gamma_{M0}} \quad (\text{EC3: 6.14})$$

For cross sections belonging to class 4:

$$M_{c,Rd} = M_{pl,Rd} = \frac{W_{eff,min} f_y}{\gamma_{M0}} \quad (\text{EC3: 6.15})$$

where:

- $W_{pl,y}$  = Plastic section modulus
- $W_{el,min}$  = minimum elastic section modulus
- $W_{eff,min}$  = Effective minimum section modulus



### B.3.4 Bending moment resistance - Local buckling of flange

If the flange is class 4 it is subjected to local buckling; the effective area of the flange is reduced.

None of the sections are class 4.

### B.3.5 Bending moment resistance - Lateral (flexural) torsional buckling of beam

The following criteria (referred to as the  $\lambda$  check) has to stand to confirm no lateral torsional buckling:

$$\bar{\lambda}_f = \frac{k_c L_c}{i_{f,z} \lambda_1} \leq \bar{\lambda}_{c0} \frac{M_{c,Rd}}{M_{y,Ed}} \quad (\text{EC3: 6.59})$$

where:

- $i_{f,z}$  = radius of gyration of the flange in compression plus 1/3 of the web in compression
- $\lambda_1 = 93.3 \varepsilon$
- $k_c$  = correction factor, table 6.6 EC3
- $L_c$  = length of member

If check is okay:

$$M_{b,Rd} = M_{c,Rd} \quad (\text{B.23})$$

If the EC3: 6.59 check fails, the member may be subjected to lateral torsional buckling and  $M_{b,Rd}$  has to be calculated.

$M_{b,Rd}$  - **Simplified method/conservative method:**

$$M_{b,Rd} = k_{fl} \chi M_{c,Rd} \quad (\text{EC3: 6.60})$$

- $k_{fl}$  = modification factor that account for that the method is safe, given by the national annex to be 1.10
- $\chi$  = the same factor that is used in the calculation of buckling capacity of column, can also be read from figure 6.4 EC3, curve C

### B.3.6 Reduced moment capacity due to axial load

For class 1 and 2 I- and H-sections the axial load can be neglected if these two criterias are met:

$$N_{Ed} \leq 0.25 N_{pl,Rd} \quad (\text{B.24})$$

and

$$N_{Ed} \leq \frac{0.5 h_w t_w f_y}{\gamma_{M0}} \quad (\text{B.25})$$

if one of the criteria is not met, the section has a reduced moment capacity that has to be calculated. The new moment capacity,  $M_{N,y,Rd}$ , is given by:

$$M_{N,y,Rd} = M_{pl,y,Rd} \frac{(1-n)}{(1-0.5a)} \quad \text{but} \quad M_{N,y,Rd} \leq M_{pl,y,Rd} \quad (\text{EC3: 6.36})$$

where:

$$n = \frac{N_{Ed}}{N_{pl,Rd}} \quad (\text{B.26})$$

$$a = \frac{(A - 2bt_f)}{A} \quad \text{but} \quad a \leq 0.5 \quad (\text{B.27})$$

The reduced bending moment resistance for class 3 and 4 are not shown, as these sections will try to be avoided.

### B.3.7 Members subjected to compression and bending moment

Members that is subjected to compression and bending moment should meet the following criterias:

$$\frac{N_{Ed}}{\chi_y N_{Rk}/\gamma_{m1}} + k_{yy} \frac{M_{y,Ed} + \Delta M_{y,Ed}}{\chi_{LT} M_{y,Rk}/\gamma_{m1}} + k_{yz} \frac{M_{z,Ed} + \Delta M_{z,Ed}}{M_{z,Rk}/\gamma_{m1}} \leq 1 \quad (\text{EC3: 6.61})$$

$$\frac{N_{Ed}}{\chi_z N_{Rk}/\gamma_{m1}} + k_{yz} \frac{M_{y,Ed} + \Delta M_{y,Ed}}{\chi_{LT} M_{y,Rk}/\gamma_{m1}} + k_{zz} \frac{M_{z,Ed} + \Delta M_{z,Ed}}{M_{z,Rk}/\gamma_{m1}} \leq 1 \quad (\text{EC3: 6.62})$$

None of the beam members are subjected to bi-axial bending moment; only bending about the primary axis. The last part of the equations can be neglected:

$$\frac{N_{Ed}}{\chi_y N_{Rk}/\gamma_{m1}} + k_{yy} \frac{M_{y,Ed} + \Delta M_{y,Ed}}{\chi_{LT} M_{y,Rk}/\gamma_{m1}} \leq 1 \quad (\text{B.28})$$

$$\frac{N_{Ed}}{\chi_z N_{Rk}/\gamma_{m1}} + k_{zy} \frac{M_{y,Ed} + \Delta M_{y,Ed}}{\chi_{LT} M_{y,Rk}/\gamma_{m1}} \leq 1 \quad (\text{B.29})$$

Some of these values are known from previous capacity calculations, and some are new:  $N_{Rk}$  and  $M_{y,Rk}$ , which is simply the respective axial/bending moment capacity without the safety factor  $\gamma_{M0}$ .  $\Delta M_{y,Ed}$  is the moment produced by a eccentricity,  $e_{Ny}$ , but is only applicable for class 4 sections. There is also  $\chi_{LT}$  which is quite lengthy to calculate, as  $M_{cr}$ : elastic critical moment, has to be calculated. Luckily SAP2000's steel design rapport can provide this value and the  $\chi_{LT}$  value.

### B.3.8 Shear resistance - Yielding of web

The design shear resistance,  $V_{c,Rd}$ , depends on the class of the section:

$$V_{c,Rd} = V_{pl,Rd} = \frac{A_v (f_y / \sqrt{3})}{\gamma_{M0}} \quad (\text{B.30})$$

where:

- $A_v$  = shear area

$$\frac{V_{Ed}}{V_{c,Rd}} \leq 1.1 \quad (\text{B.31})$$

### B.3.9 Shear resistance - Shear buckling

For thick webs eq B.31 check is enough, but if the web is slender, the shear buckling capacity has to be checked. This theory is from NS-EN 1993-1-5: Plated structural elements [24]. First is a check to determine if the section may be subjected to shear buckling:

$$\text{Unstiffened web: } \frac{h_w}{t} > \frac{72}{\eta} \varepsilon \quad (\text{B.32})$$

$$\text{Stiffened web: } \frac{h_w}{t} > \frac{31}{\eta} \varepsilon \sqrt{k_\tau} \quad (\text{B.33})$$

$\eta$  is a factor dependent on the steel grade,  $\eta = 1.2$  is used. If the appropriate check fails the shear buckling resistance of the section has to be calculated:

$$V_{b,Rd} = V_{bw,Rd} + V_{bf,Rd} \leq \frac{\eta f_w h_w t}{\sqrt{3} \gamma_{M1}} \quad (\text{1993-1-5: 5.1})$$

where:

- $V_{bw,Rd}$  = the shear buckling resistance of the web
- $V_{bf,Rd}$  = the shear buckling resistance of the flange

The contribution from the web is given by:

$$V_{bw,Rd} = \frac{\chi_w f_{yw} h_w t}{\sqrt{3} \gamma_{M1}} \quad (1993-1-5: 5.2)$$

and the contribution from flanges is given by:

$$V_{bf,Rd} = \frac{b_f t_f^2 f_{yf}}{c \gamma_{M1}} \left( 1 - \left( \frac{M_{Ed}}{M_{f,Rd}} \right)^2 \right) \quad (1993-1-5: 5.8)$$

# Appendix C

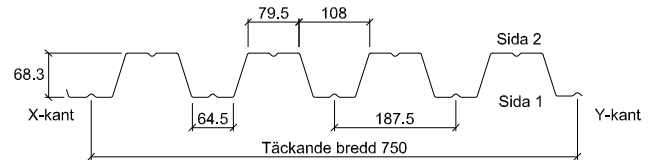
## Data sheets

Here are the data for the specific products used in the design and procedure, that includes the roofing sheets [14], post-tension jack [20] and the cable/strands used to the lifting/post-tension [19], extracted from their respective data sheets. Last there is a print from the SAP2000 steel section from the analysis of the finished structure, for element 4B7.



# Plannja 70

## Fasad



### Dimensionerande bärförmåga (kN/m<sup>2</sup>) enligt Eurokod

	t (mm)	Max rek. spännvidd		Spännvidd (m)											
				3,6	3,9	4,2	4,5	4,8	5,1	5,4	5,7	6,0	6,3	6,6	
<b>1 fack</b>	0,60	8,50	Last	2,20	1,88	1,62	1,41	1,24	1,10	0,98	0,88	0,79	0,72	0,66	
			Def=spv/200	1,11	0,88	0,70	0,57	0,47	0,39	0,33	0,28	0,24	0,21	0,18	
	0,65	8,65	Last	3,07	2,62	2,26	1,97	1,73	1,53	1,37	1,23	1,11	1,00	0,91	
			Def=spv/200	1,15	0,91	0,73	0,59	0,49	0,41	0,34	0,29	0,25	0,22	0,19	
	0,72	9,31	Last	3,83	3,26	2,81	2,45	2,15	1,91	1,70	1,53	1,38	1,25	1,14	
			Def=spv/200	1,34	1,05	0,84	0,69	0,56	0,47	0,40	0,34	0,29	0,25	0,22	
	0,85	10,18	Last	5,22	4,45	3,84	3,34	2,94	2,60	2,32	2,08	1,88	1,71	1,55	
			Def=spv/200	1,60	1,26	1,01	0,82	0,67	0,56	0,47	0,40	0,35	0,30	0,26	
	1,00	11,23	Last	6,62	5,64	4,87	4,24	3,73	3,30	2,94	2,64	2,38	2,16	1,97	
			Def=spv/200	1,95	1,53	1,23	1,00	0,82	0,68	0,58	0,49	0,42	0,36	0,32	
<b>2 fack</b>	0,60	10,03	Last	1,68	1,47	1,30	1,16	1,05	0,94	0,86	0,78	0,72	0,66	0,61	
			Def=spv/200	2,79	2,19	1,76	1,43	1,18	0,98	0,83	0,70	0,60	0,52	0,45	
	0,65	10,20	Last	2,28	2,01	1,78	1,59	1,43	1,29	1,17	1,07	0,98	0,90	0,83	
			Def=spv/200	2,91	2,29	1,83	1,49	1,23	1,02	0,86	0,73	0,63	0,54	0,47	
	0,72	10,98	Last	2,83	2,49	2,21	1,97	1,77	1,60	1,46	1,33	1,22	1,12	1,03	
			Def=spv/200	3,34	2,63	2,11	1,71	1,41	1,18	0,99	0,84	0,72	0,62	0,54	
	0,85	12,01	Last	3,88	3,41	3,02	2,70	2,43	2,19	1,99	1,82	1,67	1,53	1,41	
			Def=spv/200	4,00	3,14	2,52	2,05	1,69	1,41	1,18	1,01	0,86	0,75	0,65	
	1,00	13,25	Last	5,15	4,52	4,00	3,56	3,20	2,89	2,62	2,39	2,18	2,01	1,85	
			Def=spv/200	4,87	3,83	3,06	2,49	2,05	1,71	1,44	1,23	1,05	0,91	0,79	
<b>3 fack</b>	0,60	10,16	Last	2,02	1,77	1,57	1,41	1,27	1,14	1,04	0,95	0,87	0,80	0,74	
			Def=spv/200	2,15	1,69	1,35	1,10	0,91	0,75	0,64	0,54	0,46	0,40	0,35	
	0,65	10,34	Last	2,74	2,42	2,15	1,92	1,73	1,56	1,42	1,30	1,19	1,10	1,01	
			Def=spv/200	2,24	1,76	1,41	1,15	0,95	0,79	0,66	0,56	0,48	0,42	0,36	
	0,72	11,13	Last	3,40	3,00	2,66	2,38	2,15	1,94	1,77	1,61	1,48	1,36	1,26	
			Def=spv/200	2,57	2,02	1,62	1,32	1,09	0,90	0,76	0,65	0,56	0,48	0,42	
	0,85	12,17	Last	4,66	4,10	3,65	3,26	2,93	2,66	2,42	2,21	2,02	1,86	1,72	
			Def=spv/200	3,08	2,42	1,94	1,57	1,30	1,08	0,91	0,77	0,66	0,57	0,50	
	1,00	13,42	Last	6,20	5,45	4,83	4,31	3,87	3,50	3,18	2,90	2,66	2,44	2,26	
			Def=spv/200	3,74	2,94	2,36	1,92	1,58	1,32	1,11	0,94	0,81	0,70	0,61	

Last Bärförmåga vid last mot plåten. Upplagsbredd = 50 mm  
 Def=spv/200 Last vid deformation spv/200  
 Max rek. spv Den spännvidd(m) som ger deformationen spv/90  
 för en linjelast 1,0 kN/m ogynnsamt placerad tvärs profilen.

# THE VSL'S HEAVY LIFTING SYSTEMS

## THE VSL STRAND JACKING SYSTEM

VSL's hydraulic strand jacking system is designed for the lifting, lowering, sliding and tilting of loads.

The system's main components are a motive unit, a tension member (made up of strands and an anchorage for the load), a hydraulic pump and a monitoring and control system.

### MOTIVE UNIT

The motive unit consists of a hydraulic center-hole jack together with upper and lower anchorages.

The upper anchorage is attached to the jack's piston. When the hydraulic jack extends, the strands are gripped by the wedges in the upper anchorage and move upwards.

When the piston starts its downward movement ready for the next stroke, strands are gripped by the wedges in the bottom anchorage. The upper anchorage opens at the same time.

This sequence is repeated to move the load in a step-by-step process. For lowering operations, VSL motive units are equipped with a device that automatically controls the opening and closing of the anchorages.

### TENSION MEMBER

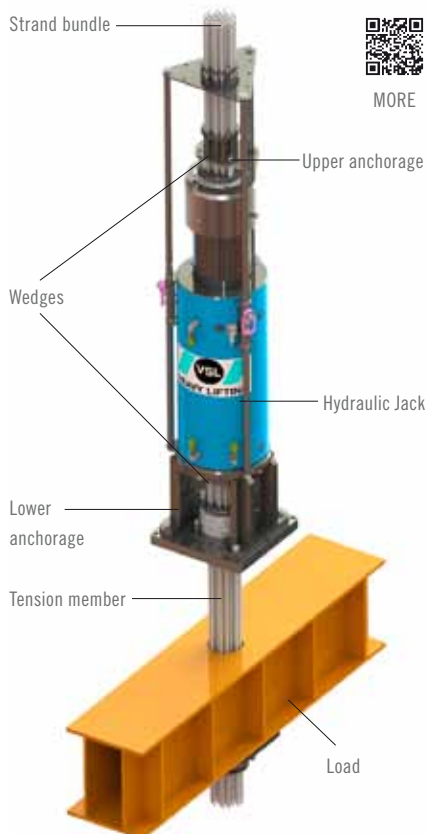
The tension member consists of 7-wire steel prestressing strands of 15.24 mm nominal diameter. It is anchored to the load by a specially designed end anchorage.

### HYDRAULIC PUMP

The oil flow for the motive units is provided by electro-hydraulic pumps with either single or multiple outlets.

The characteristics of these pumps guarantee synchronised jacking, even under variable loads. Built-in pressure gauges or remote pressure control devices allow monitoring at all times.

The size of the pump is chosen to suit the load being moved. The movement speed depends on the project requirements and can exceed 20 m/hour, if required.



To lift the cable-net roof of a major stadium, two strand jacking units were installed at each lifting point on the compression ring. Each pump served up to seven lifting points.  
Maracanã Stadium, Rio de Janeiro - Brazil (2013)



MORE



#### CONTROL AND MONITORING

The VSL jacking system enables precision-controlled movement to within millimetres, whether operated manually or by remote control.

This precise coordination of all movements across every part of the system is achieved by using specially designed, computer-based multi-point monitoring systems.

#### SPECIAL FEATURES

- / The VSL strand jacking system is lightweight and easy to handle
- / The load is secured at every step of the operation
- / The efficient, compact modular system is easily adaptable to client and project requirements

#### KEY DATA FOR VSL STRAND LIFTING UNITS

TYPE	CAPACITY <sup>1</sup>	MAX. NUMBERS OF STRANDS	CABLE DIAMETER	BODY DIMENSIONS		WEIGHT <sup>2</sup>
				Height mm	Width/Depth mm	
SLU-10 SMU-10	kN 104	1	mm 16	1536	270/270	95
SLU-40 SMU-40	416	4	67	1952	360/360	280
SLU-70 SMU-70	728	7	82	2517	460/460	530
SLU-120 SMU-120	1248	12	117	2657	520/520	750
SLU-220 SMU-220	2288	22	167	3064	520/520	1790
SLU-330 SMU-330	3224	31	191	3074	650/650	2080
SLU-580 SMU-580	5720	55	254	3280	790/790	4500

All technical data are based on VSL standard equipment.

Piston strokes vary between 160 mm and 550 mm, depending on the type of unit.

<sup>1</sup> Capacity is based on Y1860S7.15.2 strands in accordance with the requirements of EN 10138:2009; or grade 1860 [270] -15 strands meeting ASTM A416/416M-10 with a safety factor of  $s=2,5$  with respect to the minimum breaking force of the strands.

<sup>2</sup> Body dimensions and weight listed are for the basic version of the SLU lifting units with the maximum piston stroke.



# Data sheet

## Strand T15.7

### Y 1860 S7 15.7

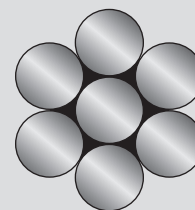
#### Specifications (according to EN 10138-3)

▶ Diameter (mm)	15.7
▶ Tensile strength (MPa)	1860
▶ Cross sectional area (mm <sup>2</sup> )	150
▶ Mass per meter (g/m)	1172
▶ Characteristic value of maximum force (kN - min)	279
▶ Maximum value of maximum force (kN)	321
▶ Characteristic value of 0.1% (kN - min)	246
▶ Modulus of elasticity (kN/mm <sup>2</sup> )	195
▶ Minimum total elongation (%)	3.5

#### Main application

- ▶ Beams

#### 7 wires



#### Agreements

- ▶ ASQPE (France), BENOR (Belgium), DIBt (Germany), ITB-IBDIM (Poland)
- ▶ Italian, Russian and Spanish approval

#### Packaging: coil

Inside diameter	Width	Indicative weight
800 or 950 mm	700 or 750 mm	2500 to 4000 kg

#### Some references

- ▶ KP1, Rector Lesage, SEAC, CRH, Consolis

#### Also available

- ▶ T9.3, T12.5, T15.2, T 15.5
- ▶ 7 wires strands unbonded (T15.2, T15.7)





# SAP2000

Minor (y)	0,009	356,278	2,437E-05	1,	
SHEAR DESIGN					
	Ved Force	Ted Torsion	Vc,Rd Capacity	Stress Ratio	Status Check
Major (z)	0,451	1,275	273,591	0,002	OK
Minor (y)	0,009	1,275	356,278	2,437E-05	OK
	Vpl,Rd Capacity	Eta Factor	Lambdabar Ratio	Chi Factor	
Minor (y)	273,591	1,2	0,465	1,2	
Major (y)	356,278	1,2	0,	1,	